

KWAME NKURUMAH UNIVERSITY OF SCIENCE AND TECHNOLOGY,

KUMASI

COLLEGE OF SCIENCE

DEPARTMENT OF CHEMISTRY

KNUST

**PREPARATION AND CHARACTERIZATION OF FAT PARTICLES-IN-
WATER EMULSIONS FOR THE ENCAPSULATION OF BIOACTIVE
COMPOUNDS USING ALLANBLACKIA SEED FAT AND TWEEN 20 AND
SODIUM ALGINATE AS EMULSIFYING AGENTS**

**A THESIS PRESENTED TO THE DEPARTMENT OF CHEMISTRY, COLLEGE
OF SCIENCE, KWAME NKURUMAH UNIVERSITY OF SCIENCE AND
TECHNOLOGY, IN PARTIAL FULFILMENT FOR THE AWARD OF THE
DEGREE OF DOCTOR OF PHILOSOPHY IN CHEMISTRY**

BY

MERCY BADU

(MSc ORGANIC CHEMISTRY)

AUGUST, 2015

DECLARATION

This thesis is submitted to KNUST, School of Graduate Studies through College of Science, Department of Chemistry. I declare hereby that this thesis has been composed by myself and has not been accepted in any previous applications for a degree here or elsewhere. Information taken from other works has been duly acknowledged.

..... **KNUST** Date.....

Mercy Badu (PG6149311)

(PhD Candidate)

Certified by:

..... **Date**.....

Dr. Johannes A. M. Awudza

(Supervisor)

..... **Date**.....

Prof. Stephen Yeates

(Supervisor)

..... **Date**.....

Dr. Godfred Darko

(Head of Department)

DEDICATION

To my father James Owusu Sekyere, my husband Kingsley Badu and our children,
Kingsley Jnr., Jeremy and Joy.

KNUST



ACKNOWLEDGEMENT

I am very grateful to the Almighty God for life, wisdom, and knowledge to understand this work. I wish to express my profound gratitude to the University of Michigan Africa Presidential Scholars Programme, the Commonwealth Split-site Scholarship Programme and the L’Oreal UNESCO for Women in Science Awards Programme for providing financial support for this research work. My sincere thanks go to my supervisors, Prof. Stephen Yeates and Dr. Johannes A.M. Awudza for their excellent supervision and support during the course of this study. I am also sincerely grateful to Prof. Peter Budd, the School of Chemistry University of Manchester and Dr. Nagila M.P.S Ricardo, Universidade Federal do Ceara Fortaleza, Brazil. I specially appreciate my dad, Mr. James Owusu Sekyere, my siblings, my husband; Dr. Kingsley Badu, and children, I say a big thank you for their support, advice and encouragement during the period of this study.

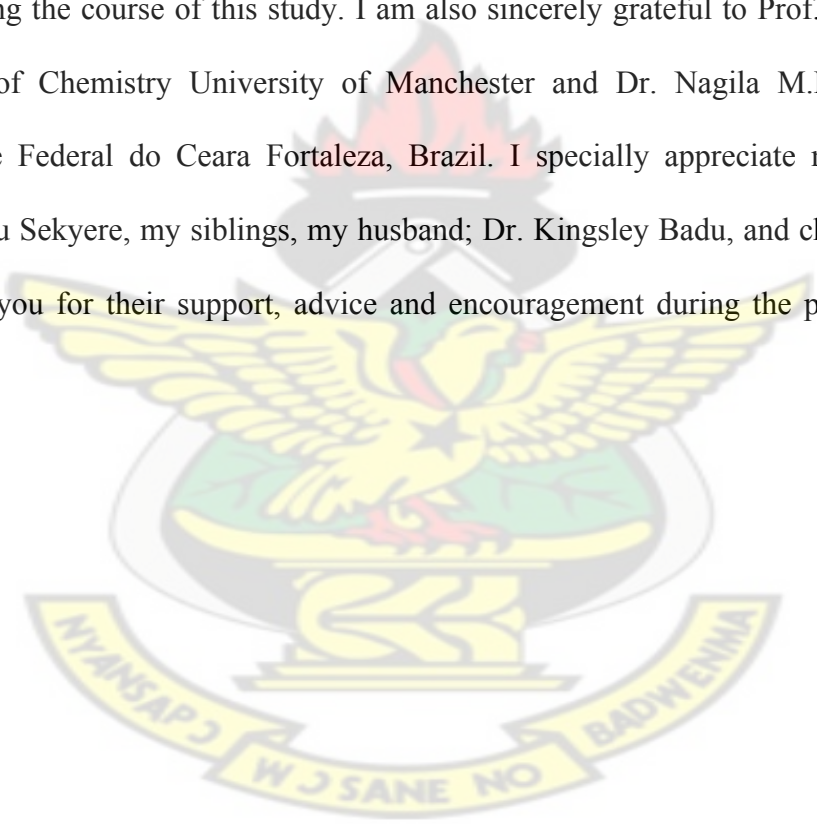


TABLE OF CONTENTS

DECLARATION	II
DEDICATION	III
ACKNOWLEDGEMENT.....	IV
TABLE OF CONTENTS	V
LIST OF FIGURES	XII
LIST OF TABLES.....	XVII
LIST OF ABBREVIATIONS	XIX
ABSTRACT.....	XX
CHAPTER 1	1
Introduction.....	1
1.1 Background.....	1
1.2 Statement of Problem.....	3
1.3 Rationale	6
1.4 Research Hypothesis.....	9
1.5 Aim and Objectives.....	9
1.5.1 Specific Objectives	10
1.6 Thesis Layout.....	10

CHAPTER 2	12
Literature Review	12
2.1 Fats as Biomaterials	12
2.1.1 Industrial Importance of Fats and Oils.....	12
2.1.2 Chemical Structure of Fats and Oils	13
2.1.3 Vegetable Fats and Oils in Polymerization Processes	15
2.1.4 Vegetable Fats and Oils in Food and Pharmaceutical Products	16
2.1.5 Physical Properties of Vegetable Fats.....	17
2.1.5.1 Thermal Behaviour of Vegetable Fats	17
2.1.5.1.1 Thermogravimetric Analysis (TGA).....	18
2.1.5.1.2 Differential Scanning Calorimetry (DSC)	19
2.1.5.2 Crystallisation Processes in Fats and Oils	22
2.1.5.3 Nucleation.....	23
2.1.5.4 Crystal Growth.....	25
2.1.5.5 Polymorphism.....	26
2.1.5 Shea Butter Fat As Industrial Feedstock.....	28
2.1.6 Allanblackia Seed Fat as Industrial Feedstock	29
2.2 Emulsions.....	30
2.2.1 Emulsion Stability.....	33
2.2.1.1 Phase Split-up (separation)	35
2.2.4 Aggregation of the Droplet	37
2.2.4.1 Flocculation.....	38
2.2.4.2 Coalescence.....	40

2.2.5 Disproportionation (Ostwald Ripening)	42
2.3 Characterization of Emulsion Instability Phenomena.....	44
2.3.1 Estimation or measurement of Droplet size.....	44
2.3.2 Flocculation Characterization	45
2.3.3 Coalescence and Ostwald Ripening Characterisation.....	45
2.3.4 Creaming/Sedimentation Characterization	46
2.4 Emulsions stabilized by Surfactants	47
2.4.1 Surfactants: Definition;.....	47
2.4.2 Surfactants as Emulsifying Agents	50
2.4.3 Alginate as a non-surfactant emulsifier	54
2.4.4 Tween Surfactants –for the Stabilisation of Oil-in-Water Emulsions	57
2.5 Encapsulation of Active Compounds in Oil-in-Water Emulsions.....	59
2.5.1 Encapsulation Techniques	63
2.5.2 Encapsulation Efficiency of Emulsion-Based Delivery Systems	67
CHAPTER 3	69
Materials and Experimental Methods	69
3.1 Materials	69
3.1.1 Vegetable Fat Samples.....	69
3.1.2 Chemicals.....	69
3.1.3 Concentration Units	70
3.2 Experimental Methods	70
3.2.1 Fatty Acid Constituents Determination	70
3.2.1.1 Preparation and Detremination of Fatty Acids Methyl Esters	70

3.2.1.2 Determination of the Saturated and Unsaturated Fatty Acid Composition ..	71
3.2.2 Thermal Studies of Fats	72
3.2.2.1 Thermal Decomposition of Fats.....	72
3.2.2.2 Thermal Properties and Crystallisation Behaviour	73
3.2.2.2.1 Melting and Cooling Profile the Fat Samples.....	75
3.2.2.2.2 Crystallisation at Different Cooling Rates	76
3.2.2.2.3 Isothermal Crystallisation by the DSC Method.....	76
3.2.2.2.4 Isothermal Crystallisation Kinetics by the DSC Stop-and-Return Technique.....	76
3.2.3 X-ray Diffraction (XRD) Analysis	78
3.2.4 Microscopic Analysis.....	79
3.2.5 Preparations and Characterization of Colloidal Dispersions	80
3.2.5.1 Emulsion Preparation.....	80
3.2.5.2 Allanblackia Seed Fat/Water Emulsion	81
3.2.5.3 Surfactant Stabilised Emulsion	81
3.2.5.4 Combined Surfactant/Biopolymer Emulsifier Mixture Stabilised Emulsion	81
3.2.5.4 Emulsion Characterizations	82
3.2.5.4.2 Crystal Morphology and Microstructure of the Dispersed Fat Particles ...	83
3.2.5.4.3 Particle Size Measurements	85
3.2.5.5 Determination of the Rheological Parameters of the Emulsions	87
3.2.6 Preparation and Efficiency of Encapsulated Particles	90
3.2.6.1 Preparation of the Encapsulated Particles.....	90
3.2.6.2 Encapsulation Efficiency	90

3.2.6.2.1 Determination of Amount of Dye Encapsulated.....	90
3.2.6.2.2 Leaching Studies.....	91
3.2.6.2.3 Swelling Studies	92
3.2.6.3. Characterization of the Solid Fat Encapsulated Sudan Orange Particles	92
3.2.6.3.1 Particle Size and Size Distribution	92
3.2.6.3.2 XRD Analysis	93
3.2.6.3.3. Thermal Behaviour of Encapsulated Particles.....	93
CHAPTER 4.....	94
Chemical Constituents and Thermal Behaviour of Allanblackia Seed Fat and Shea	
Butter	94
4.1 Determination of the Fatty Acid Constituents of Allanblackia Seed Fat (AB-GH)	
and Shea Butter (SB-GH)	95
4.1.1 GC/MS Analysis of AB-GH and SB-GH	95
4.1.2 ¹ HNMR Analysis of AB-GH and SB-GH	97
4.2 Thermal Decomposition of AB-GH and SB-GH by Thermogravimetric Analysis	
(TGA).....	99
4.3 Crystallisation and Melting Behaviour by the DSC Method.....	101
4.4 Thermal Behaviour with Increasing Cooling Rates.....	105
4.6 Studies of Crystallisation Kinetics by DSC Stop-and-Return Method.....	112
4.7 X-ray Diffraction (XRD) Studies of Fat crystals at Room Temperature.....	123
4.8 Crystal Morphology	125
4.9 Conclusion	127

CHAPTER 5..... 129

Formulation, Stabilisation and Characterisation of Fat Particles-in-Water

Emulsions – Effect of Tween 20 and Sodium Alginate Mixtures 129

5.1 Formulation of Fat Particles-in-Water Emulsions 130

5.2 Surfactant Stabilised Fat Particles-in-Water Emulsions 131

5.3 Mixed Surfactant/Biopolymer Emulsifier System in Stabilised Fat-in-Water Emulsions..... 133

5.4 Characterisation of the Dispersed Fat Particles-in-Water Emulsions..... 133

5.4.1 Effects of Fat Content on emulsion Stabilisation 134

5.4.2 Effects of Tween 20 and Sodium Alginate Concentrations on the Emulsion Particle Size 142

5.5 Rheological Characterization for the Long-term Physical Stability of the Emulsions..... 147

5.5.1 Effect of Stress on the Stability of Emulsion Against Creaming..... 147

5.5.2 The Viscous and Elastic Responses of the Emulsion-Oscillatory Measurements 151

5.6 Conclusion 159

CHAPTER 6..... 161

Encapsulation of Sudan Orange Dye in Fat Particles in the Fat-in-Water

Emulsions..... 161

6.1 Formulation of Encapsulated Fat-in-Water Emulsion Product..... 162

6.1.1 Extraction and Characterisation of the Vegetable Fat used as Matrix in the Encapsulation Process..... 162

6.1.2 Preparation of the Encapsulated Particles.....	163
6.2 Characterization of the Encapsulated Sudan Orange Dye Particles (ESODP).....	164
6.2.1 Particle Size and Size Distribution	164
6.2.3 Thermal Properties for Encapsulated Particles	168
6.3 Encapsulation Efficiency	171
6.4 Conclusion	174
CHAPTER 7	176
Conclusions and Recommendations.....	176
7.1.1 Chemical Constituents and Thermal Properties of Shea Butter and Allanblackia Seed Fat	176
7.1.2 Formulation and Stabilisation of Fat Particles-in-Water Emulsions	177
7.1.3 Encapsulation of Sudan Orange Dye in the Fat particles-in-Water Emulsion...	178
7.1.4 General Conclusions	179
7.2 Recommendations.....	180
References.....	181
APPENDICES.....	199
PUBLICATIONS ARISING.....	200

LIST OF FIGURES

Figure 2-1: Structural composition of triacylglycerols of fats and oils R_1, R_2 and R_3 are alkyl chains of fatty acid.	14
Figure 2-2: A TGA decomposition curve of soybean oil at different heating rates [52].	19
Figure 2-3: DSC thermograph showing the crystallisation profiles of palm oil fractions. Curve (a) represents palm stearin and (b) represents palm olein fractions [47]	20
Figure 2-4: (a) A triacylglycerol molecule, (b) polymorphism and subcell structures, (c) chain length structure of a typical fat composition [44].	26
Figure 2-5: Dispersed droplets in a continuous phase forming an emulsion system.....	31
Figure 2-6: Schematic representation of different emulsion systems.....	32
Figure 2-7: Sketches representing (a) the hydrophilic head and hydrophobic tail surfactant structure (b) surfactant action at the oil and water interface.	48
Figure 3-1: Schematic diagram of a Differential Scanning Colorimetric device, as the Diamond DSC from Perkin Elmer Instruments.	75
Figure 3-2: Schematic representation of the Braggs Law in X-ray diffraction instruments.	79
Figure 3-3: Sketch representing an emulsion structure: showing creaming and the particle distribution in the cream layer as adopted from Pichot (2010) [187].	83
Figure 3-4: A Scheme representing operations scanning electron microscope [188]	84
Figure 3-5: Schematic representation of the Zetasizer Dynamic Light Scattering (DLS) device, from Malvern Instruments.	86
Figure 3-6: A Sketch of the ARES Viscometer [190]	89

Figure 4-1: ¹ HNMR spectra showing the saturated and unsaturated fatty acids of: (A) AB-GH and (B) SB-GH.....	99
Figure 4-2: Thermal decomposition profile of AB-GH and SB-GH obtained from the TGA starting at 25 °C to 800 °C at 10 °C/min	101
Figure 4-3: Melting and cooling profile of fat samples obtained at temperatures between -30 °C to 70 °C at 2 °C per minute from DSC: (A) melting and cooling curves of AB-GH and (B) melting and cooling curves of SB-GH.....	102
Figure 4-4: DSC crystallisation profile of AB-GH and SB-GH from -30 °C to 70 °C at different cooling rates: (A) crystallisation profiles of AB-GH with change in cooling rates from 5 °C/min to 20 °C/min and (B) crystallisation profile of SB-GH with change in cooling rates from 5 °C/min to 20 °C/min	106
Figure 4-5: Crystallisation profiles of AB-GH and SB-GH at isothermal time of 60 minutes for the DSC experiments: (A) crystallisation profile of AB-GH at 20 °C, (B) crystallisation profile of AB-GH at 16 °C, (C) crystallisation profile of AB-GH at -10 °C, (D) crystallisation profile of SB-GH at 20 °C, (E) crystallisation profile of SB-GH at 16 °C and (F) crystallisation profile of SB-GH at -10 °C	110
Figure 4-6: Melting profile at every minute during the isothermal period where crystal fractions are melted under the DSC stop-and-return method (A) melting curves of AB-GH at 20 °C (B) melting curves of AB-GH at 16 °C (C) melting curves of AB-GH at -10 °C (D) melting curves of SB-GH at 20 °C (E) melting curves of SB-GH at 16 °C (F) melting curves of SB-GH at -10 °C isothermal crystallisation temperatures	114
Figure 4-7: Comparison of the appearance of the melting peaks at different time recorded from the stop-and-return DSC experiments: (A) peaks maxima profile of AB-GH and SB-	

GH at 20 °C (B) peaks maxima profile of AB-GH and SB-GH at 16 °C and (C) peaks maxima profile of AB-GH and SB-GH at -10 °C crystallisation temperatures	116
Figure 4-8: Formation of crystal fractions as a function with time: (A) Fractions of crystals formed for AB-GH at 20 and 16 °C crystallisation temperatures and (B) Fractions of crystals formed for SB-GH at 20 and 16 °C crystallisation temperatures	120
Figure 4-9: Diffractions obtained from the powder XRD analysis for fat kept at room temperature for six months: (A) XRD profile for AB-GH and (B) XRD profile for SB-GH.....	124
Figure 4-10: Visual images of AB-GH and SB-GH as obtained from the optical microscope at (A) 70 °C, (B) 20 °C, (C)16 °C and (D) -10 °C	126
Figure 5-1: Visual observation of emulsions after 1 hour of homogenisation (A) dispersed fat particles in water without any emulsifier (B) dispersed fat particles in water with Tween 20 surfactant (C) dispersed fat particles in water with Tween 20 and sodium alginate mixture	131
Figure 5-2: Light microscopic images of fat particles in water in the presence of both Tween 20 and sodium alginate at (A) 5/95 % fat/water (B) 10/90 % fat/water (C) 15/85 % fat/water (D) 20/80 % fat/water ratios	141
Figure 5-3: SEM images of the dispersed fat particles in the emulsion system of 18/85 fat/water composition at 3 % sodium alginate and Tween 20 content	142
Figure 5-4: Average particle size distribution (PSD) of the 15/85 fat/water particles in the emulsions (after homogenization) with respect to increasing (A) Tween 20 content at different amounts of sodium alginate (B) Sodium alginate at different amounts of Tween 20.....	143

Figure 5-5: Particle size distributions of emulsions prepared at different contents of (A) Tween 20 at 3% sodium alginate (B) Sodium alginate at 3% Tween 20 144

Figure 5-6: Visual photographs of emulsions prepared at fat/water ratio 15/85 after 30 days (A) at 3% sodium alginate with increasing concentration of Tween 20 (B) at 3% Tween 20 with increasing concentration of sodium alginate..... 146

Figure 5-7: Shear-rate dependence of viscosity for A) stabilised fat particles in water emulsions with different fat concentrations at 3% Tween 20 and 3% sodium alginate and B) stabilised 15/85 fat/water particles in water emulsions with different sodium alginate concentrations 149

Figure 5-8: A graph of frequency sweep test of emulsions, which shows viscoelastic responses to shear of emulsions prepared from 5/95, 10/90, 15/85 and 20/80 fat/water content in 3% Tween 20 and sodium alginate. The diagram gives the storage (G') and loss (G'') moduli, complex viscosity (Eta^*) and $\tan \delta$ for emulsion with increasing fat content. 153

Figure 5-9: A graph of frequency sweep test of emulsions, which shows viscoelastic responses to shear shear of emulsions prepared from 15/85 fat/water content in 3% Tween 20 with increasing sodium alginate. The diagram gives the storage (G') and loss (G'') moduli, complex viscosity (Eta^*) and $\tan \delta$ for emulsion with increasing sodium alginate content. 156

Figure 5-10: The change in phase angle with the frequency sweep at (A) increasing fat content at 3% Tween 20 and sodium alginate content (B) increasing sodium alginate concentration at 3% Tween 20 in 15/85 fat/water content (C) increasing Tween 20 concentration at 3% sodium alginate in 15/85 fat/water content..... 158

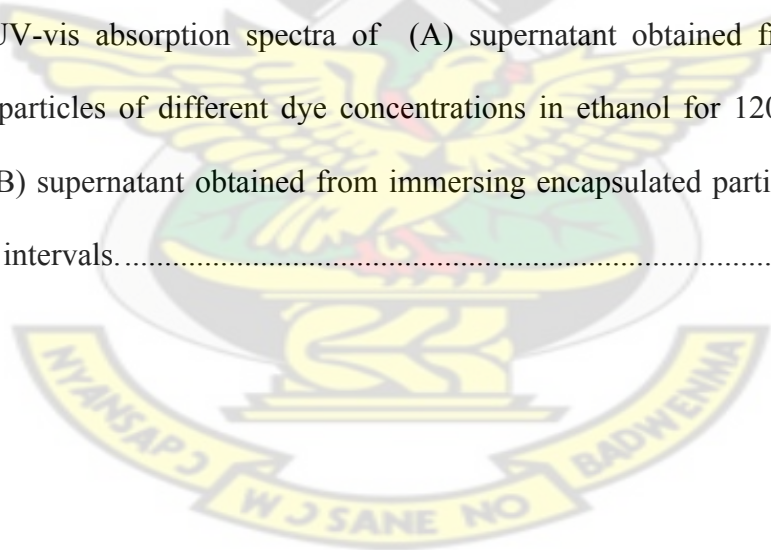
Figure 6-1: Encapsulated Sudan Orange Dye Particles (ESODP) in the crystallized fat particles-in-water emulsion system prepared from 15/85 Fat/water content with 3% Tween 20 and 3% sodium alginate. 163

Figure 6-2: Light microscope images of (A) Encapsulated emulsion particles (B) fat-in-water emulsion particles (C) Magnified encapsulated dye particles in the fat matrix (D) particle size distribution from the DLS..... 166

Figure 6-3: Diffraction patterns of (A) Encapsulated particles (B) Raw sudan orange dye particles and (C) Allanblackia fat crystals 168

Figure 6-4: (A) Thermal decomposition curves of the encapsulated particles obtained from the thermogravimetric Analysis (TGA) and (B) Melting and Cooling profile of the encapsulated particles obtained from the differential scanning calorimetry (DSC). 169

Figure 6-5: UV-vis absorption spectra of (A) supernatant obtained from immersing encapsulated particles of different dye concentrations in ethanol for 120 mins at room temperature (B) supernatant obtained from immersing encapsulated particles in water at different time intervals..... 172



LIST OF TABLES

Table 2-1: Fatty acid constituents of commonly found in some vegetable fats and oils ..	15
Table 4-1: Levels of fatty acid composition in shea butter and Allanblackia fat determined by the GC/MS	95
Table 4-2: Chemical shifts obtained from the AB-GH and SB-GH fats corresponding functional groups of saturated and unsaturated fatty acids.....	98
Table 4-3: Temperature (T_p) and the enthalpy change (ΔH_c) recorded for AB-GH and SB-GH at increasing cooling rates.....	107
Table 4-4: Isothermal crystallisation kinetics parameters; Avrami exponent (n), the crystallisation rate constant (K) and the half-time of crystallisation ($t_{1/2}$) obtained from fitting the isothermal crystallisation curve at 16 and 20 °C temperature for AB-GH and SB-GH	123
Table 4-5: Signals and their corresponding d-spacing (Å) obtained from the X-ray diffraction patterns for AB-GH and SB-GH fat samples.....	124
Table 5-1: Average size of particles (PSD) with their standard of deviations of emulsion (5/95) mixed-emulsifier stabilized emulsions and the volume fractions of creaming layer ($V_{f_{cr}}$) with change in sodium alginate and Tween 20 concentrations.....	135
Table 5-2: Average size of particles (PSD) with their standard of deviations of emulsion (10/90) mixed-emulsifier stabilized emulsions and the volume fractions of creaming layer ($V_{f_{cr}}$) with change in sodium alginate and Tween 20 concentrations.....	136
Table 5-3: Average size of particles (PSD) with their standard of deviations of emulsion (15/85) mixed-emulsifier stabilized emulsions and the volume fractions of creaming layer ($V_{f_{cr}}$) with change in sodium alginate and Tween 20 concentrations.....	137

Table 5-4: Average size of particles (PSD) with their standard of deviations of emulsion (20/80) mixed-emulsifier stabilized emulsions and the volume fractions of creaming layer (V_{fcr}) with change in sodium alginate and Tween 20 concentrations..... 138

Table 5-5: Data obtained after fitting the Power Law model on the viscosity/shear rate plot 150

KNUST



LIST OF ABBREVIATIONS

HLB	Hydrophilic-lipophilic balance
3-D	Three dimensions
O/W	Oil-in-water
NaAl	Sodium alginate
AB-GH	Allanblackia seed fat Ghana
SB-GH	Shea butter Ghana
TAG	Triacylglycerides
FAME	Fatty acids methyl esters
SEM	Scanning electron microscope
TGA	Thermogravimetric analysis
XRD	X-ray diffractions
UV-vis	Ultra Violet-visible
PSD	Particle size distribution
V_{cr}	Volume fraction of creaming
GC/MS	Gas chromatography/Mass spectroscopy

ABSTRACT

Effective delivery of poorly water-soluble bioactive ingredients has been considered a great challenge in the pharmaceutical, food and cosmetic industries. The compartmentalized hydrophobic and hydrophilic regions of emulsion systems give them the advantage to encapsulate polar and non-polar compounds for effective delivery. However, the challenge associated with emulsions is their thermodynamic instability. This study investigated the stabilisation process of fully crystallised fat globules as a dispersed phase in an oil-in-water emulsion system prepared from a naturally occurring vegetable fat, a nonionic surfactant and a polysaccharide biopolymer. The crystallisation profiles of the fats from *Allanblackia* seed and shea nuts were determined. Based on the results *Allanblackia* seed fat was selected and used as the dispersed phase in the oil-in-water emulsion system. The emulsion was formulated in the presence of Tween 20 and sodium alginate. The mixed emulsifier system gave stability against aggregation of the fat particles hence preventing coalescing, creaming and flocculation and this was more significant at 2 % to 4 % sodium alginate content. The emulsion particle size and microstructure were dependent on the fat/water ratio and a viscoelastic system with $G' > G''$ at the lower frequencies and $G'' > G'$ at higher frequencies (where G and G are....). The dispersed fat particles emulsion system was used to encapsulate sudan orange dye (a water insoluble dye) and the efficiency of the encapsulation was characterized by an increase in particle size (ranging from 246 to 250 nm) and varying size distribution. UV-Vis spectrophotometric analysis of the dye loading capacity, release rate and leaching capacity showed a successful entrapment of the dye in the fat matrix. This confirms *Allanblackia* seed fat as a potential solid fat for its application in the formulation of oil-in-water emulsions.

CHAPTER 1

Introduction

1.1 Background

The continuous formulation of new delivery systems to meet the demands of today's fast and hectic life has led to the emergence of an important area in colloid and interface science where essential bioactive ingredients are incorporated in food, pharmaceuticals, cosmetics and other products to improve their quality and health benefits. Several colloidal systems have been studied and are now being used for the encapsulation of essential compounds, especially in the area of drug delivery to maximize their therapeutic activity while minimizing any possible side effects. Emulsion technology, which is an application of colloidal science, has become interesting in recent times as a result of the numerous advantages they possess such as flexibility in formulating functional products of specific structures, compartmentalization which provides them with the ability to simultaneously carry both hydrophobic and hydrophilic bioactive ingredients in one system, ease of application and ability to impart properties for consumer acceptance.

It is estimated that over 60 % of new drug compounds produced suffer from poor water solubility with only 8 % exhibiting high water solubility and subsequent permeability [1]. Since the major route for the delivery of many drug compounds used in treating many chronic diseases is oral, the poor water solubility of these drugs often leads to insufficient bioavailability, deficiencies in dose proportionality leading to incomplete absorption that may cause toxicity during and after administration [2]. Effective delivery of poor water-

soluble (hydrophobic) bioactive compounds has therefore been considered a challenge especially in the pharmaceutical and food industries. These limitations have led to the recent increase in research interest in the development and use of colloidal systems through emulsification techniques in order to explore their potentials for the delivery of poorly water soluble bioactive components for effective oral consumption [3, 4].

Emulsions are fine dispersions of minute droplets of one liquid dispersed in another. The two liquids are immiscible [5]. They are categorized based on the nature of the dispersed and the continuous phases. Emulsion systems; due to their compartmentalized hydrophobic and hydrophilic regions gives them the benefit to encapsulate water-soluble, non-water soluble compounds or both, for an effective delivery system. They also possess the ability to control the chemical stability of the encapsulated active compound, their rheological properties to suit their specific application and protect the active component against any form of degradation. The biggest challenge associated with oil and water emulsions in delivery systems is the fact that they are thermodynamically unstable [5]. The instability phenomenon is as a result of the fact that the free energy of the oil and the water phase as separate entities is lower as compared to that of the emulsion system. Emulsions prepared under such conditions tend to break down over a period of time as the dispersed phase forms flocks or coalesce [6]. The rate of break down of emulsions is strongly affected by the composition of the formulation, production conditions including concentration and temperature as well as environmental factors.

A lot of work has gone into the enhancement of the stabilisation of emulsions by the application of emulsifiers and thickeners. The emulsifiers, which are surface-active molecules, are adsorbed to the surface of the newly dispersed droplets at the processing

stage and form a protective layer to protect and prevent the droplets from aggregating [7]. The presence of the emulsifiers enhance the stabilisation process of the emulsion in two ways; they lower the interfacial tension between the dispersed phase and the continuous aqueous phase and also form a mechanically cohesive interfacial film around the droplets which is able to prevent the oil droplets from coalescing [8]. Another important component used to improve the stabilisation of emulsions is the application of thickeners or texture modifying agents. These compounds are usually applied to increase the thickness of the continuous phase of the emulsion system, this delays and hence inhibits droplet movement in the continuous phase to reduce the rate of droplet aggregation and so improving the stabilisation process of the emulsion [9]. The selection of the suitable stabiliser(s) is very important in controlling the physicochemical properties of emulsions and the shelf life of their products. The extent of stability of the emulsion system provided by the emulsifier depends on the nature and amount used [10]. Even though the use of food grade emulsifier systems such as the polysorbates, sorbitan esters and polyethylene glycols used in food and other pharmaceutical products have not recorded any associated negative health effects, it is known that high levels of emulsifier concentration affects the texture, appearance and taste of their end products. Hence a lot of research is on going to find effective means of improving emulsion stability with minimal use of emulsifiers.

1.2 Statement of Problem

An emulsion-based delivery system for the food and pharmaceutical industry must contain solely permitted food grade components and also using approved processing techniques [11]. The occurrence of poor and variable absorption of water insoluble

bioactive drug compounds may result in sudden toxicity, making their production expensive and difficult. The solubility of many bioactive drug compounds in the gastrointestinal tract has been associated with the presence of food, lipid-based formulations that are employed to improve drug absorption. Strickley [12] in his recent survey, published that about 2-4 % of commercially available drugs are made of oral lipid-based formulations, of which the most frequently chosen excipients for their preparation were dietary oils. Although the uses of oral lipid-based formulations have enormous health benefits such as easy digestibility, it has not been used as expected probably due to the high chemical and physical instability issues associated with these dietary oils. Most of the products found on the market can endure stability at room temperature during storage for a short time and therefore require storage at much lower temperature conditions to ensure their long-term stability. However, the stability of lipid-based emulsions against temperature variation may be improved in a crystallised system [13, 14]

The flow, physical appearance and the overall stability of an emulsion system are critical issues in the successful application of emulsion technology in the development of food-grade delivery systems. The flow, physical appearance and the overall stability have direct influence on the quality and life of an emulsion product. However, the achievement of a stable product is dependent on the ingredients for the formulation, methods employed for preparation and the environmental factors that influence the formulation processes. The use of stabilisers (emulsifiers) has been an area of interest in many research works over the years due to their ability to promote improved flow, physical appearance and stability of an emulsion system [9]. The emulsifier may be synthetic, or

naturally occurring compounds that have the ability to improve the interfacial tension generated within the emulsion system, and lead to reduction or prevention of emulsion breakdown. It is estimated that about 500,000 tons of emulsifying agents are produced and sold all over the world [15] but the choice of the emulsifiers in edible emulsions is limited by the regulations of the Food and Drugs Administration of a particular country and that the approved emulsifying agent should be affirmed as generally recognised as safe (GRAS) compounds [16]. Therefore, the choice of the emulsifying agent is an important step in the emulsification process.

Apart from the instability issues associated with the emulsion system of dietary lipid-based emulsion, there is also the possibility of occurrence of leakage of the encapsulated compounds from one compartment to another within the emulsion system and this may lead to undesirable distribution of the encapsulated component hence a poor formulation. Also the choice of lipid as an excipient has become critical as these oils are made of mixtures of triglycerides with different molecular characteristics. The lipids are made up of fatty acids of different chain lengths and unsaturation that may have a major impact on the lipid digestibility and hence its associated health effects. The melting point of a lipid oil increases as the carbon chain length of the constituent fatty acids increases and decreases with increasing unsaturation [17]. An increase in the unsaturation may also increase their susceptibility to oxidation in the emulsion system, which affects the taste and quality of the product. The selected lipid oils used so far are composed of medium to long-chain saturated triglycerides or hydrogenated unsaturated triacylglycerides but this strict selection procedure is affected by the high market demand on some particular lipid oils, and this may lead to an increase in cost of production of the delivery system.

In view of the mentioned problems associated with emulsion formulation, ingredients and stability, this study sought to use solid fat particles, which crystallise at room temperature to improve the stability of the emulsion against change in environmental conditions. Additionally, the presence of the crystallised fat will prevent the movement and leakage of any encapsulated compound from one compartment to the other within the emulsion system. Again since the fats are made of saturated fatty acids their presence in the emulsions was expected to improve the stability of the emulsion against oxidation. The study also sought to combine Tween 20 surfactant and sodium alginate thickener as a mixed emulsifier system to improve the flow, physical appearance and the overall stability of the emulsions.

1.3 Rationale

Ideally, an emulsion for a good delivery system must have the ability to protect the encapsulated compound from any kind of degradation. This can be achieved by reducing the ability of the core material to react to its immediate environment, ensuring a decrease in undesirable leakage of the core material, modifying the physical properties of the regular compound to allow easy handling and finally modifying the release of the bioactive material at a slow rate with time. The use of the vegetable fats as starting materials presents several advantages such as increased solubilisation capacity, low toxicity, inherent biodegradability and bioavailability and high purity.

The presence of solid fat globules gives a positive impact to the rheology of the bulk emulsion properties, such as the emulsion viscosity, elasticity and viscoelastic properties [18]. Since the ability of the emulsion to resist a breakdown and the subsequent instability phenomenon is largely dependent on their interfacial characteristics, the

presence of a favourably viscous and inelastic interfacial film may stop or reduce the time at which the interfacial film breakage may occur thereby minimizing or resisting globule rapture and hence promoting emulsion stability. The solid fat particles also provide a network structure, which entraps the encapsulated bioactive compound thereby providing a stable and effective encapsulation for the core material within the emulsion system. The formation of a rigid network structure gives the advantage of improving the mechanical properties, physical properties, functionality and texture of the emulsion product. Additionally, the fully crystallized fat globule presents discrete and smaller particle sizes, since the crystal network prevents the possible occurrence of coalescence. Solid fat crystals have been used as rheological modifiers for a variety of emulsion product [19]. The presence of high amounts of saturated fatty acids leads to the high melting properties exhibited by the vegetable fats and also their resistance to oxidative degradation. Several researches have shown the importance of fat crystallisation for improved functionality in oil-in-water emulsions [18]. However the presence of the solid fat particles as the dispersed phase may lead to increased aggregation, which eventually leads to emulsion instability [14].

The emulsion kinetic stability is improved by the addition of a nonionic surface-active agent, Tween 20. Addition of Tween 20 lowers the interfacial tension between the dispersed fat globules and the aqueous phase and this produce a film around the fat particles thereby preventing globule-globule collision. The Tween-20 molecule with a high hydrophilic-lipophilic balance (HLB 16.7) will curve towards the fat globules and also promote stabilisation as a result of the formation of strong hydrogen bonds with the water molecules in the continuous aqueous phase [7]. Additionally, an alginate polymer,

which is a natural polysaccharide, added to facilitate and promote the formation, stabilisation and the possible occurrence of controlled-fat destabilisation. The alginate, which is a rheological additive or thickening agent, further increases the viscosity of the continuous water phase. The increase in thickness of the continuous phase increases its viscosity, thereby impeding the rapid and random movement of the fat globules in the emulsion system, hence a reduction in aggregation. The alginate, has low toxicity and is able to form a network structure, which leads to immobilization of the fat globules. The alginate is also inexpensive, biocompatible and usually available and used as food or pharmaceutical material. Alginate also present numerous exceptional characteristics that gives it an advantage to be used as a matrix for entrapment of bioactive compounds for controlled and targeted delivery systems [9, 20–23]. The addition of the alginate also gives the opportunity to reduce the addition of the surfactant molecules in the emulsion system hence promoting low-fat emulsions. The stabilisation capacity of the mixed emulsifier system is greatly improved by synergistic mechanisms to reduce the surface tension, establishment of rigid interfacial films and increased viscosity of the continuous aqueous phase.

A success in the utilization of solid fat particles in the production of stable emulsion system will provide the advantage of the possibility to formulate poorly water soluble bioactive compounds in aqueous systems while protecting the compound against degradation or alteration of their biodistribution after administration, therefore enhancing controlled delivery. The presence of the mixed surfactant-biopolymer emulsifier system will lead to the production of emulsions for their application in the food and pharmaceutical industries since the emulsion ingredients can be certified as GRAS

materials. For a food-grade emulsion, it should contain reduced surfactant molecules and since the fat is typically composed of saturated fatty acids, the emulsion products are expected to exhibit improved stabilisation against oxidative degradation.

1.4 Research Hypothesis

The study was based on the fundamental hypothesis that, the use of dispersed solid fat particles, a surfactant molecule and a thickening agent will synergistically produce an improved stabilised emulsion system. The use of the solid fat particles will provide a rigid 3-dimensional network structure, which gives the advantage of improving the mechanical properties, physical properties, functionality and texture of the emulsion product. The presence of the surfactant and thickening agent reduces the interfacial tension and the velocity of the dispersed phase and hence improves the stability of the emulsion system.

1.5 Aim and Objectives

The overall aim of this work was to investigate the stabilisation process of fully crystallized fat globules as a dispersed phase in an oil-in-water emulsion system prepared from a naturally occurring vegetable fat, a nonionic surfactant and a polysaccharide biopolymer. The study also sought to use the successfully stabilised emulsion system for the encapsulation of a water insoluble dye for its application in delivery systems.

1.5.1 Specific Objectives

The specific objectives of the study were to

1. determine the effect of the fatty acids constituents on the thermal behaviour of two tropical vegetable fats namely Allanblackia seed fat and shea nut fat.
2. investigate the stabilisation process of a fully crystallized fat particles-in-water emulsion system.
3. evaluate the efficiency of encapsulation of the dispersed fat particles in the aqueous phase for a poorly water soluble component.

1.6 Thesis Layout

This thesis is made up of seven chapters: introduction, review of relevant literature, experimental methods chapter, three result chapters and finally a conclusion and recommendation chapter.

1. Chapter 1 gives the background to the underlining relevance of the study and the aims and objectives of the research.
2. Chapter 2 reviews the relevant literature that summarises the technical information and knowledge in relation to the subjects stated in the thesis; it also gives definitions to the terms used in this study.
3. Chapter 3 covers the experimental procedures performed in this work.
4. Chapter 4 is the first results chapter and it covers the comparative study of the fatty acids compositions of Allanblackia seed fats and shea nut fats and their thermal behavior.

5. Chapter 5 is the second results chapter regarding the formulation and characterization of solid fat particles dispersed in an aqueous phase containing varying concentrations of surfactant/biopolymer compounds.
6. Chapter 6 is the third and final results chapter, which features the encapsulation efficiency of the stabilised emulsion system for a non-water soluble component.
7. Chapter 7 summarizes all the conclusions made in this research work and provides subsequent suggestions and recommendations for future work.

Publications arising from this research work are presented in the appendix.



CHAPTER 2

Literature Review

2.1 Fat as Biomaterials

Biomaterials are raw materials from renewable resources used as industrial feedstock for monomers and polymer materials. Vegetable fats and oils are one of the most commonly used renewable resources in many industrial processes for non-fuel applications. The fatty acid compounds in fats and oils undergo functionalization of the C – H bonds in the alkyl chain, radical, electrophilic and nucleophilic reactions at the C – C double bond which may lead to a wide range of innovative compounds with stimulating characteristics useful for their applications in the chemical industry.

2.1.1 Industrial Importance of Fats and Oils

In this age of fossil oil reserve depletion and with the increase in emission of green house gases, the exploitation of renewable resources such as fats and oils is an essential step that may lead to ensuring sustainable development. Fats and oils as renewable raw resources has contributed appreciably to a viable development for their non-fuel applications [24]. They are greatly used as resources for the production of surfactants, cosmetic products, and lubricants [25]. Additionally, they have been used in the production of paints, floor polish and for the production of coatings and resins [26]. Vegetable oils and fats have become important renewable feedstocks in the chemical industry, since they provide raw materials on the regular bases for our day-to-day products and this may prevent or minimize emission of green house gases. Vegetable fats and oils have been discussed as important renewable feedstocks for the growing chemical industry in the promotion of green and sustainable development. This is due to their

ability to undergo oleochemical transformations such as the hydrolysis and the transesterification at the ester functionality of the native triglycerides. The transformational products may be used in the production of important industrial chemicals such as surfactants, lubricants and coatings. They also give advantage of their application in green chemistry, in that the raw materials show built-in design for degradation or lead to the production of low toxicity products.

The importance of fats and oils as raw materials for the home, personal care and many other industrial applications is also due to their exhibited excellent properties such as high productivity, low price, high stability to thermal oxidation and their plasticity at room temperature [27, 28]

2.1.2 Chemical Structure of Fats and Oils

Fats and oils are naturally occurring compounds that are obtained from either plant or animal sources. Fats are solid, brittle at room temperature and melt at elevated temperatures while at room temperature oils are liquid. Fats and oils are categorized as vegetable fat or oil when obtained from a plant source and animal fat or oil from an animal source [29]. Vegetable fats and oils can be obtained from different plants and are usually identified by their plant source, examples are soybean oil and palm oil, shea butter fat cocoa butter fat and Allantropa seed fat. They are made up of saturated and unsaturated fatty acids as the major chemical constituents. The fatty acids can exist as long chain or short chain carbon compounds. The length of the carbon chain determines the nature of the fatty acid and hence their characteristic physico-chemical properties and the subsequent physiological behavior [30]. The variations in the chemical structure of fatty acids affect the molecular structure of their triacylglycerol (TAG) compounds,

which constitute about 95-98 % of the whole fat or oil composition [31, 32]. The triacylglycerols are formed from a trimer of a glycerol and various fatty acids as shown in Figure 2-1.

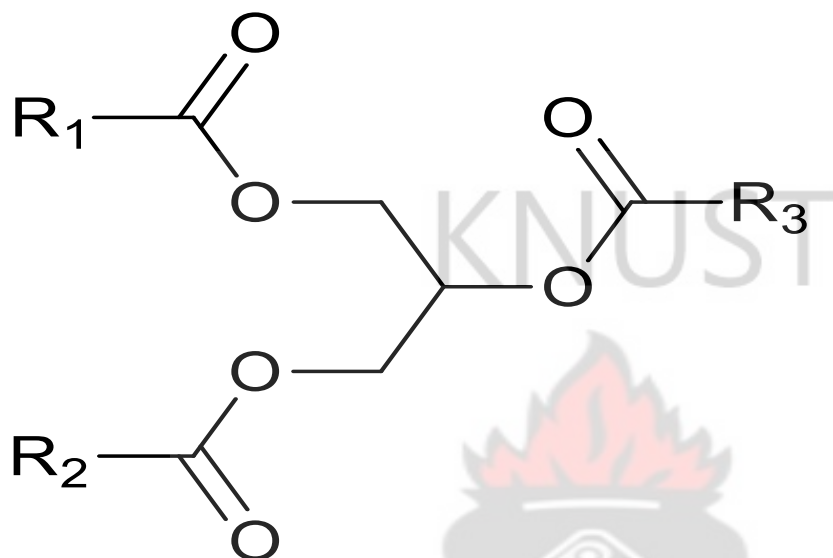


Figure 2-1:Structural composition of triacylglycerols of fats and oils R₁,R₂ and R₃ are alkyl chains of fatty acid.

Distinctive vegetable fats and oils are made up of different constituent fatty acids and this depends on the plants source and the environment they grow in [33]. The physicochemical properties of fats and oils are dependent on the degree of saturation or unsaturation in their molecular structure. The number of double bonds present in the fat or oil molecule characterizes the level of unsaturation and this is usually determined by calculating the iodine value (IV) [26]. The iodine value is a measure of the total iodine (mg) reacting with the carbon–carbon double bonds in a 100 g of the fat or oil. A high iodine value indicates the presence of large number of carbon–carbon double bonds in the triglyceride structure. Based on the iodine value the vegetable fats or oils may be categorised as drying oils (IV > 130), semi-drying oils (100 < IV < 130), and non-drying

oils ($IV < 100$) [34, 35]. Table 2-1, reviews the common fatty acids found in most vegetable fats and oils.

Table 2-1: Fatty acid constituents of some commonly found in vegetable fats and oils

Fatty acid	Molecular formula	Carbon-double bond ratio
Capric acid	$C_{10}H_{20}O_2$	$C_{10}:0$
Lauric acid	$C_{12}H_{24}O_2$	$C_{12}:0$
Myristic acid	$C_{14}H_{28}O_2$	$C_{14}:0$
Palmitic acid	$C_{16}H_{32}O_2$	$C_{16}:0$
Stearic acid	$C_{18}H_{38}O_2$	$C_{18}:0$
Oleic acid	$C_{18}H_{34}O_2$	$C_{18}:1$
Linoleic acid	$C_{18}H_{32}O_2$	$C_{18}:2$
Linolenic acid	$C_{18}H_{30}O_2$	$C_{18}:3$
Arachidic acid	$C_{20}H_{40}O_2$	$C_{20}:0$

2.1.3 Vegetable Fats and Oils in Polymerization Processes

Another important application of fats and oils is their utilization in the production of polymeric materials. The presence of multiple carbon-carbon double ($C=C$) bonds makes the fat or oil an ideal and important building units for the production of different kinds of useful polymeric materials [36, 37]. The transformation of the fats and oils into industrially beneficial materials is through the functionalization and reacting the $C=C$ bond to produce polymer materials or through direct reactions of the fatty acid component with different hydrocarbon monomers [38]. Several works have been reported

on the conversion of C=C bonds of several fats and oils into polyols by epoxidizing the C=C bonds of the triglyceride oil [39]. These synthesized polyols are made to undergo several reactions, which lead to the production of polyurethanes [40]. Other workers have also produced a variety of many useful different industrial biopolymers from numerous vegetable oils exclusive of any initial chemical modification of the starting fatty acids. They have successfully copolymerized vegetable oils such as soybean oils with divinylbenzene (DVB), resulting in rigid and brittle plastics with glass transition temperatures (T_g) of about 60–80 °C [38]. The resulting biomaterials produced from these fats and oils have outstanding thermal and mechanical characteristics, such as damping [39] and shape memory [37] profiles, and this gives it the potential to replace petroleum-based rubbers and other synthetic plastics.

2.1.4 Vegetable Fats and Oils in Food and Pharmaceutical Products

Apart from using vegetable fats and oils in cooking and their use in the production of spreads, creams and chocolates, more recently vegetable fats and oils have been introduced into the delivery of essential compounds in the food and pharmaceutical industries. To be applied in delivery systems, the fat or oil is treated to eliminate all kind impurities or sometimes their different fractions isolated from their original state, and used in the encapsulation of oral formulations. One of the disadvantages of using vegetable fats or oils in food and pharmaceuticals is the issue of oxidation of the highly unsaturated fatty acids. In order to reduce the occurrence of the oxidation process, unsaturated triacylglycerols are sometimes hydrogenated to produce fatty acids of reduced degree of unsaturation. The fractionation of these naturally occurring compounds into their various glyceride fractions or the utilization of the unmodified saturated fatty

acids has also been widely introduced and utilised in the preparation of pharmaceutical excipients that employs the needed physical and drug absorption-promoting properties, as well as reducing the issues of oxidation [41, 42]. The triglycerides have several benefits when used in self-emulsifying drug delivery systems. They usually are ingested into the food or food product, after which they are digested and subsequently absorbed, hence they are regarded as generally regarded as safe.

2.1.5 Physical Properties of Vegetable Fats

2.1.5.1 Thermal Behaviour of Vegetable Fats

The study of thermal behavior in polymeric materials is basically following the characteristic change in their physical properties with temperature change [43]. Heat transfer and its related phenomena in fats and oils is fundamental and are used to elucidate the chemical and physical properties as biomaterials. Fats and oils show complexity in their thermal profiles and this is essentially due to the existence of great variety in their triacylglycerol structure, which is the principal constituent [44, 45]. Due to the complex nature of the TAG structure, it is challenging to define the thermal profile of fat and oil systems; therefore they are usually described in a range of their specific thermal properties (melting or crystallisation temperature). Nonetheless, the thermal profiles of vegetable fats and oils give extensive information concerning the type transition occurring at their various states and this can be used as valuable tool to investigate probe a given oil or fat [46]. Many different methodologies have been proposed for the evaluation of the quality of many commercial oils. Most of these methods subject their samples to conditions that accelerate oxidation normal process. But for the precise evaluation of the quality of fats and oils, thermoanalytical methods such as

differential scanning calorimetry (DSC) and thermogravimetry (TG) have received a lot of attention in recent times [47–50]. These methods present several advantages over many other conventional methods because they are able to use smaller amount of samples, and they present higher precision and sensitivity as well as give results in a faster way.

2.1.5.1.1 Thermogravimetric Analysis (TGA)

Thermogravimetric Analysis (TGA) is a thermoanalytical method in which the weight lost of a given material is observed with change in temperature or time. In this technique the material is heated under a controlled temperature and controlled atmosphere program which results in weight increase or decrease. So the thermogravimetric analyzer determines the weight of a material during its heating or cooling in a furnace. The thermogravimetric analyzer is made up of the sample pan, which is reinforced by a precision balance; the pan is placed in the furnace, and this is heated during the experimental procedure and the sample weight loss or gain observed. A sample purge gas is used to control the environmental conditions of the sample during the experiment and this gas may be a reactive or a nonreactive gas, which, moves throughout the sample until it, is exited through an outlet in the setup. The instrument is able to quantify the loss of water, loss of solvent, loss of plasticizer, decarboxylation, pyrolysis, oxidation, decomposition, weight % filler, amount of metallic catalytic residue remaining on carbon nanotubes, and weight % ash. All these applications, which are also quantifiable, are usually done upon heating, but some experimental results and information may also be obtained upon cooling.

Information obtained from a particular sample is displayed as a TGA thermal curve, which moves from left to right as indicated in Figure 2-2. The descending TGA thermal curve indicates the occurrence of a weight loss [51].

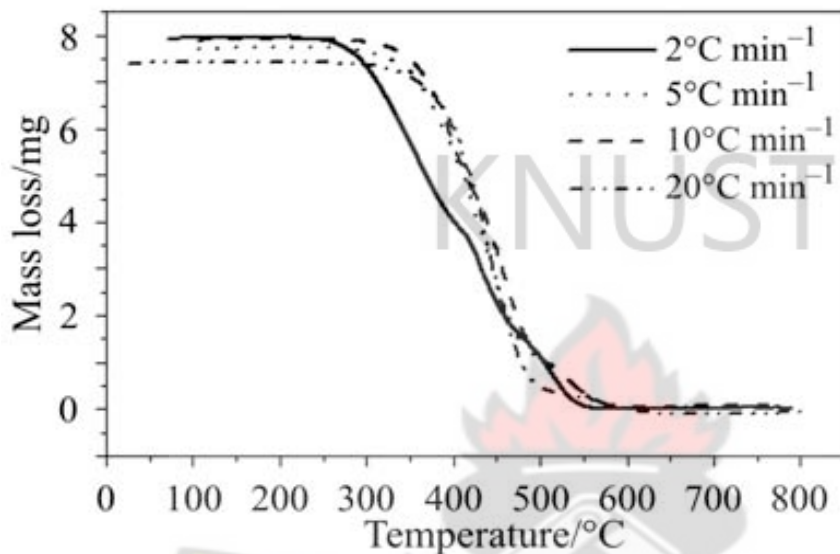


Figure 2-2: A TGA decomposition curve of soybean oil at different heating rates [52].

2.1.5.1.2 Differential Scanning Calorimetry (DSC)

Differential Scanning Calorimetry (DSC) is a technique used to determine properties of materials associated with temperature change. This measurement is based on the time at which the material absorbs the heat energy and compared to a reference material. This method is based on a forced thermal denaturation of the polymers and other material. It uses the energy changes occurring in the different transformations at the molecular level of the materials [53]. From the energy changes, several properties of a material including their melting profiles, enthalpy change of melting, crystallisation profile, glass transition temperatures and degradation temperatures are measured. It is extensively used to compare native and mutant variants of proteins, for optimisation of buffer conditions, and

for confirmation of molecular interactions including quantitative determinations of affinities. The key benefit with the DSC is the fact that its data acquisition is based on the measurements of heat change and therefore allows the characterisation of native biomolecules without the use of any spectroscopic readings [46].

The fact that the application of the DSC does not depend on any spectroscopic measurements, means samples do not have to be optically clear before their molecular properties can be measured. The DSC characterises both the melting and crystallisation profile of materials and these are usually detected as thermographs as shown in Figure 2-3. It also provides data on the forces involved in folding of biomolecules and the mechanism by which they unfold.

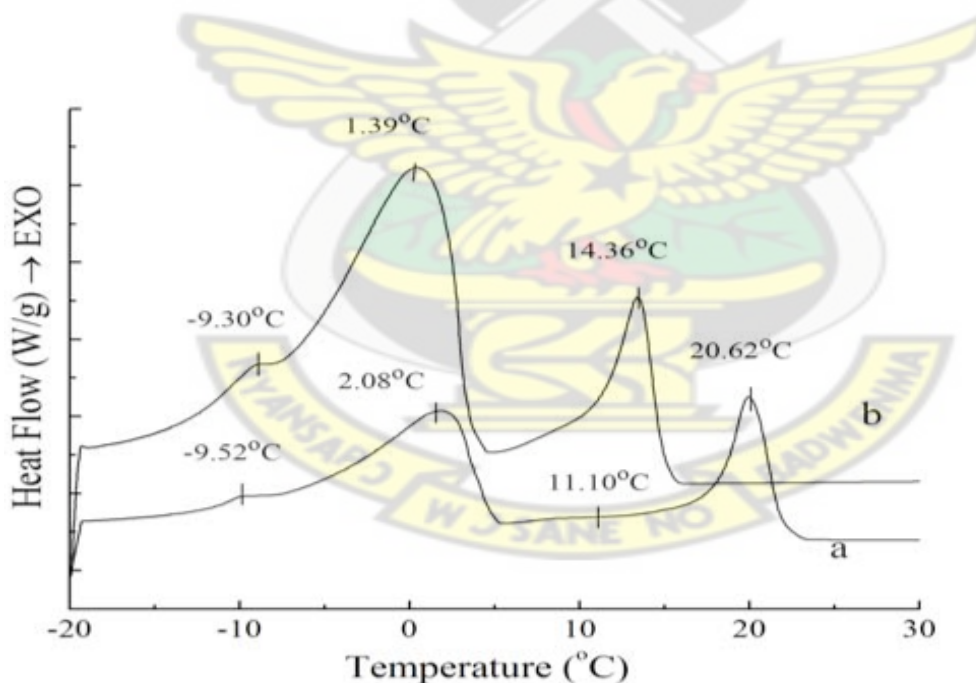


Figure 2-3: DSC thermograph showing the crystallisation profiles of palm oil fractions. Curve (a) represents palm stearin and (b) represents palm olein fractions [47]

Since the development of the first power controlled DSC in the 1960s by Mike O'Neill and co-workers, several research work have used the DSC to determine the consequence of heat flow on the stability of polymers [54]. The thermodynamics of the TAG content of fat in the bulk phase behaviour and their complex crystallisation and melting behaviour, has been studied by DSC [55–57]. The differential scanning calorimetry screens the changes in the physical and chemical properties of a substance with change in temperature. The technique detects the change in heat related to phase transformations leading to crystallisation and glass transition. This observation was reported by Kong and Hay, (2002) [58]. The instrument compares the heat flow rate of the sample with an inert reference material as both are heated or cooled. The study of lipid chemistry has also taken the versatility of the DSC instrument. In profiling the melting and crystallisation properties of edible oils, the instrument measures the heat of fusion, the temperature of crystallisation, the fat liquid/solid ratio, their polymorphic transformations [59]. Tan and Che Man (2000) have also reported on the use of the DSC to investigate systematically the quality of some selected vegetable oils. They also studied and associated the use of the DSC with other standard chemical methods. This includes the determination of the total polar compounds, iodine value and free fatty acids for the oxidation of fat. They found that the DSC measurements compare very well with the various standard chemical methods [45, 46]

Even though DSC has been reported as having high sensitivity and resolution, it is sometimes an inconvenient method as its signals become difficult to be integrated especially during the use of DSC in the study of isothermal crystallisation, when there is the possible occurrence of a polymorphic transformation simultaneously

with the crystallisation process [60, 61]. In the light of such a disadvantage associated with the utilization of phase transition based on the heat flow, another method termed the stop-and-return DSC technique is reported to overcome such problems [62, 63]. In this method the isothermal crystallisation process is interrupted at distinctive times and the sample re-melted. The melting thermographs thus obtained are then integrated to describe the advanced cooling process. At the different polymorphic transitions, different melting points and enthalpies are recorded and their peak areas and temperatures are interpreted to give insight into the different proportions of the fat or oil crystallized at the particular time [62, 64]. This also provides information on polymorphic transitions of the particular fat or oil. The stop-and-return DSC technique is described as a valuable and inexpensive tool for elucidation of the crystallisation mechanisms in fats [46].

2.1.5.2 Crystallisation Processes in Fats and Oils

Vegetable fats are one of the major food ingredients commonly used as a lipophilic substance in the food industry as well as the pharmaceutical and cosmetic industries. They are complex mixtures of triacylglycerol (TAGs), as the major component [65], diacylglycerols (DAGs), monoacylglycerols (MAGs), free fatty acids (FFAs), phospholipids, glycolipids, sterols and many other minor components [66]. The triacylglycerols during the cooling process, from the melt at a temperature above its melting point to a temperature less than the melting temperature, they experience supercooling and hence experience a liquid–solid transition leading to the crystallisation of the fat [67, 68]. Crystallisation is defined as a supramolecular activity whereby arbitrarily prearranged molecules in a melted state come together leading to the formation of well arranged three-dimensional molecular structure called crystals [69].

Crystallisation of fat accounts for several effects on properties such as consistency and the mouth feel in food products; and stability in an emulsion. Crystallisation of vegetable fat plays a significant role in the separation of fat fractions in a fat material into their individual components. This is significant because the fractionation process may lead to different products of varying melting and physical properties. The driving force of the crystallisation process is attributed to the change in chemical potential ($\Delta\mu$) measured in joules per mole (J mole^{-1}) between the liquid and the solid phases. The higher the chemical potential difference, leads to high driving force for the crystallisation process. The mechanism of fat crystallisation is grouped into two different steps. In the first step, a thermodynamic force is generated which is sufficient enough to initiate the occurrence of a nucleation process. Nucleation is the process during which fat particles are produced by transporting growing units, which are collected to form a crystal lattice. Once the nuclei are produced, they develop to incorporate triacylglycerol compounds in the liquid leading to crystal growth. The molecules in fats and oils experience two fundamental phenomena: they experience nucleation and subsequent crystal growth and the occurrence of polymorphic transition.

2.1.5.3 Nucleation

Nucleation is defined as the process of forming the initial stable crystal in a supercooled mix of melted triacylglycerides [70]. The nucleation process is the formation of a nucleus of fat upon which several crystals grow. The nucleation process occurs in different ways. It can be a primary nucleation, which occurs either as homogeneous or heterogeneous. It can also be a secondary nucleation, which usually occurs only after the primary nucleation process. Upon forming the nucleus, the crystal propagates by combining other

triacylglycerol compounds in the liquid phase onto the crystal network. The pattern and rate of the crystallisation progress change on conditions including the degree of supercooling and the change of diffusion with time of the growing crystal particles from the liquid phase.

When the nucleation occurs without the process being catalyzed by fat crystals present or by the presence of any foreign solid surfaces, the process is termed a primary nucleation and this occurs through a homogeneous mechanism. Such a process occurs in a highly supercooled melted fat system before the crystallisation begins. But in a situation where the presence of a foreign surface catalyses the nucleation process in a primary nucleation, the process is termed as a heterogeneous nucleation mechanism. The heterogeneous nucleation is as a result of a molecular orientation, which is usually enhanced by the presence of other foreign surfaces, such as dust particle or any other microscopic impurities on the walls of the containers. The presence of these impurities causes the molecules to orient themselves to form a more definite crystal lattice. The heterogeneous process occurs at a much lower level of supersaturation as compared to that of the homogeneous nucleation. The secondary nucleation occurs once primary homogeneous or heterogeneous nucleation and fat crystals have already been formed. During the nucleation process tiny crystal particles produced goes beyond the “critical size”. These tiny crystal particles are taken from the top of the already formed crystals and are used as the secondary nuclei upon which new crystals are formed. The secondary nucleation is more prominent if there is crystallisation in a solution or industrial crystallizers.

2.1.5.4 Crystal Growth

After the nucleus is formed and exceeds the critical size, it becomes crystallites upon which the growth occurs. The growth occurs by adding additional TAG compounds formed in the liquid phase on top of the crystal structure. As the nucleus grows, molecules migrate by diffusion to the top of the crystallized particles and arrange themselves to a suitable site during deposition [71, 72]. During the formation of the crystals, latent heat is discharged; energy moved from the surface of the fat particles in order to reduce any rise in temperature, or the termination of further growth. The crystal microstructure is estimated from the various constituents in the mixture, and the change in growth with time. The steps through which the crystal surface increase, is defined by the interfacial properties of the crystal and liquid phase.

Three types of crystal faces exist: kinked (**K**), stepped (**S**) and flat (**F**) faces. The kinked (**K**) face is an countless number of kink sites. The kink sites possess no thermodynamic barriers which could prevent the growth process and therefore promotes the continuous growth of the crystals. As the crystals grow from the melted liquid, the free energy is activated free for the dispersal of the TAG compounds in the molten stage has important effect on the growth kinetics and therefore the rate at which the crystals grow rate is inversely proportional to the viscosity of melted fat. The stepped (**S**) face has similar kinetic properties as that of the kink face. The number of stepped points per unit area is lesser in comparison with the **K** face. The occurrence of growth rate for the **S** face is proportional to the relative supersaturation of the melted fat. The flat (**F**) face grows layer after layer, and this can either by a two-dimensional nucleation pathway when the crystal surface is without defect or be a spiral growth mechanism. The spiral mechanism occurs

much more frequently than the two-dimensional nucleation mechanism [44, 64, 69].

2.1.5.5 Polymorphism

Fat crystal polymorphism may be described as the power of solid TAGs to produce distinctive crystals with identical chemical constituents, which mutually vary in structure nonetheless gives indistinguishable liquid in its molten stage [73]. Polymorphism of fats and oils is characterized by three main forms: α , β' , and β , a nomenclature based on the Larsson theory in 1966 [44] which has also been discussed by several other authors in the literature [74].

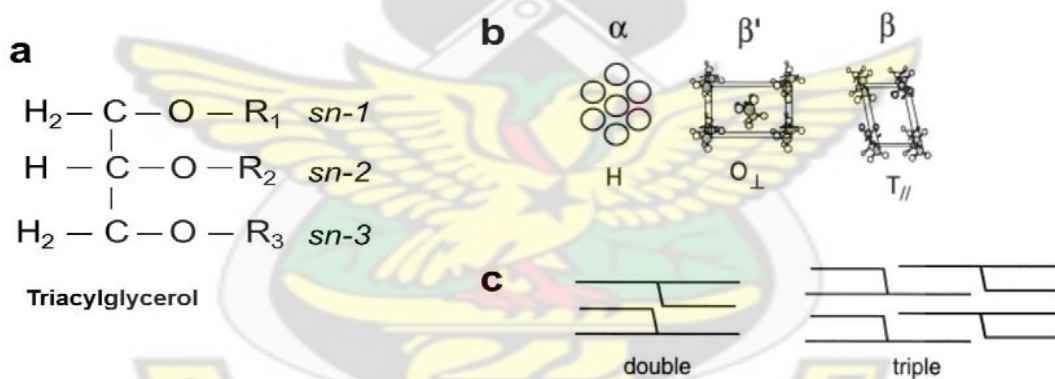


Figure 2-4: (a) A triacylglycerol molecule, (b) polymorphism and subcell structures, (c) chain length structure of a typical fat composition [44].

The various polymorphs are designated by their crystal subcell structure, that is a characteristic of the packing modes of the zigzag hydrocarbon chain. The α form corresponds to a hexagonal subcell structure (H), that is the acyl chains do not form an angle of tilt; β' corresponds to an orthorhombic perpendicular subcell structure (O_{\perp}),

where the chains are perpendicular, and they form an angle of tilt between 50° and 70°; and the β form corresponds to a triclinic parallel subcell structure (T//) with the same angle of tilt as β' but with a parallel chain orientation (Figure 2-4) [64].

The polymorphs vary in their melting profile, the stability of the melting enthalpy and density. These parameters are classified according to their stability. The polymorphs as arranged in their order of increasing stability is $\alpha < \beta' < \beta$. The α form which has the lowest stability and shows the least melting temperature, melting enthalpy and density can be transformed into a β' or β during temperature change treatment. The metastable β' , gives an intermediate character. The β' polymorph is that which is much desired in production of many food products for their optimal morphology and crystal network for a desired textural properties. The β polymorph gives the highest stability and hence shows the highest melting temperature, melting enthalpy and density. They form a characteristic plate-like crystals, which are usually large and give a resulting poor crystal network which is brittle in nature [74]. Due to the presence of the subcell packings the various polymorphic structures can be identified and characterized by powder X-ray diffraction patterns. The α polymorph, which occurs through hexagonal subcell packing, is identified by the occurrence of one intense diffraction pattern around 4.15 Å. Two intense diffraction patterns shown around the 3.7 and 4.2 Å corresponds to the orthorhombic subcell packing of the β' polymorph. The triclinic subcell packing of the β polymorph is characterized by a series of diffractions consisting of a more intense pattern at 4.6 Å and two less prominent patterns in the region of 3.6 and 3.8 Å [75]. Two polymorphic crystalline forms exist, and they are monotropic and enantiotropic. The monotropic form occurs through an irreversible pathway. In this process one polymorph appears all the

time and is very stable and by changing the environmental conditions such as the temperature and pressure forms it. In the monotropic polymorphism, the crystal with highest stability are modified successively from α to β' and then to β , at an adequate time interval and their transformation only occurs in way of which the most stable form can be formed. On the other hand enantiotropic polymorphism is a reversible process and for two crystalline forms to be enantiotropic, each one of them should occur in a definite stability range. This is usually linked to a precise choice of temperature and pressure within which every one of the polymorphs exist in its highest thermodynamically stable state.

The polymorphs usually are discussed in the contest of crystallisation from the melt, which usually is said to be nucleation dependent. However, the formation of a polymorph can also be melt-mediated, that is it is observed directly from the melt solution [64, 76].

The rate of crystallisation decreases from α to β , and applying the optimal cooling rate for each polymorphic form this can be achieved. At low supercooling, the particles will integrate into the energetically most favorable sites, which lead to the formation of a more stable polymorph; although at high supercooling integration favors the least energetically favorable sites. Prediction of the rate of cooling for each polymorph as a simultaneous crystallisation process of more polymorph may occur is not an easy task.

2.1.5 Shea Butter Fat As Industrial Feedstock

Shea butter is a vegetable fat extracted from the kernels of the fruit of the shea tree (*Vitellaria paradoxa*), a deciduous tree that grows in the wild, in the savannah belt of Africa. Shea butter is widely used as cooking oil, for producing soap, and used in

pharmacological and cosmetic products locally [77]. In recent times shea butter has gained increasing international demand. It is classified as an oleaginous product based on its physicochemical properties, which has been used in its application as industrial feedstock. It has also been used extensively world wide in the cosmetics industry and in pharmaceuticals. Shea butter is a semi-solid fat composed of triglycerides and fatty acids including oleic acid (60 to 70%); stearic acid (15 to 25%); linolenic acid (5 to 15%); palmitic acid (2 to 6%); linoleic acid (<1%) [78]. Shea butter has also been reported to contain about 10 % trioleic (OOO), 35 % stearic-oleic-oleic (SOO), 40 % stearic-oleic-stearic (SOS) and 8 % palmitic-oleic-stearic (POS) triacylglycerol compounds. It also contains other TAGs made up of linoleic acid and arachidic acid in minor quantities [78]. Based on the triacylglycerol composition, shea butter exhibit excellent physico-chemical properties hence their broad industrial and domestic applications. Additionally, high unsaponifiable matter levels as compared to different vegetable fats and oils has been reported, and this gives information about the potential to develop shea butter into medicinal products [79]. The high moisturizing properties of shea butter, its buttery consistency and spreadability gives it the advantage to be considered in emulsion technology.

2.1.6 Allanblackia Seed Fat as Industrial Feedstock

The Allanblackia fat is gotten from the seeds of the Allanblackia fruit (*Allanblackia parviflora*). Allanblackia tree grows in the evergreen lowland and deciduous forests in Africa. The Allanblackia seeds contain about 72 % fat, which is solid at room temperatures. Allanblackia seed fat contains stearic acid and oleic acid as their major fatty acid content [80]. Its fatty acid composition is about 45 - 58% stearic acid and 40 -

51% oleic acid with traces of other fatty acids such as palmitic acid and arachidic acid present [81]. The fatty acid composition of the Allanblackia seed fat and their relatively high melting temperature (35°C) brands the fat a valued natural resource. This implies that it can be used without any modification to increase the uniformity of many food products. The physicochemical properties (semi-solid at room temperature) of the Allanblackia seed fat is determined by their triacylglycerol composition which is characterized by high contents of stearic-oleic-stearic (SOS) and stearic-oleic-oleic (SOO) (average values 69 % SOS; 23.0 % SOO). The simplicity and distinctive organization of the fatty acids on their glycerol backbone makes the fat suitable as a hardstock component and also provides the Allanblackia seed fat quality criteria as an edible vegetable fat. This quality gives the Allanblackia seed fat its intended use as a novel food ingredient.

2.2 Emulsions

Emulsion may be categorized as a colloidal system consisting of two liquids that are immiscible, in which one of the liquids is distributed as droplets (the internal component) and the other forms the continuous phase (which is the external component) [82, 83].

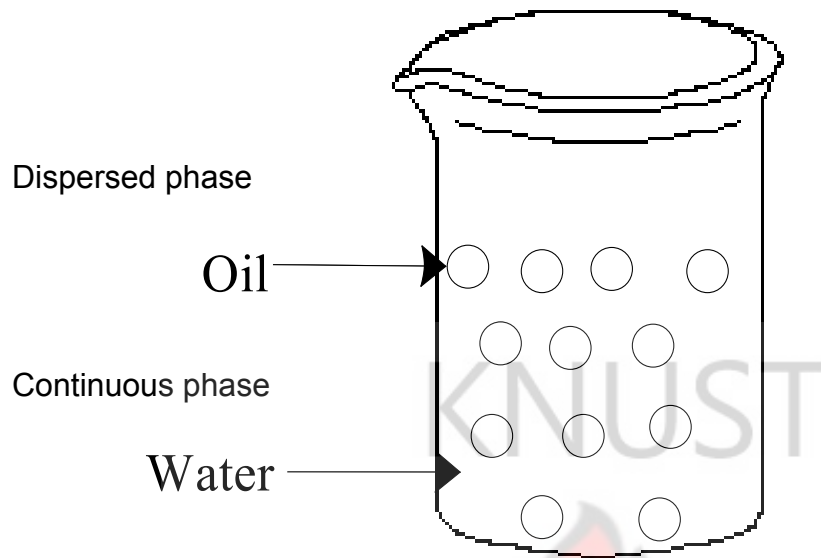


Figure 2-5: Dispersed droplets in a continuous phase forming an emulsion system

The emulsion may be classified as microemulsion with the droplet size ranging from about 0.01 to 0.1 μm and macroemulsion with droplet size of about 5 μm . When the emulsion system is made up of one internal phase, it is referred to as a primary emulsion such as oil-in-water (O/W), also, water-in-oil (W/O) and then, oil-in-oil (O/O). However, when an emulsion consists of two internal segments or phases as it is seen in oil-water-oil (O/W/O) or may be water-oil-water emulsion (W/O/W), these are referred to as secondary or multiple emulsion [5, 6].

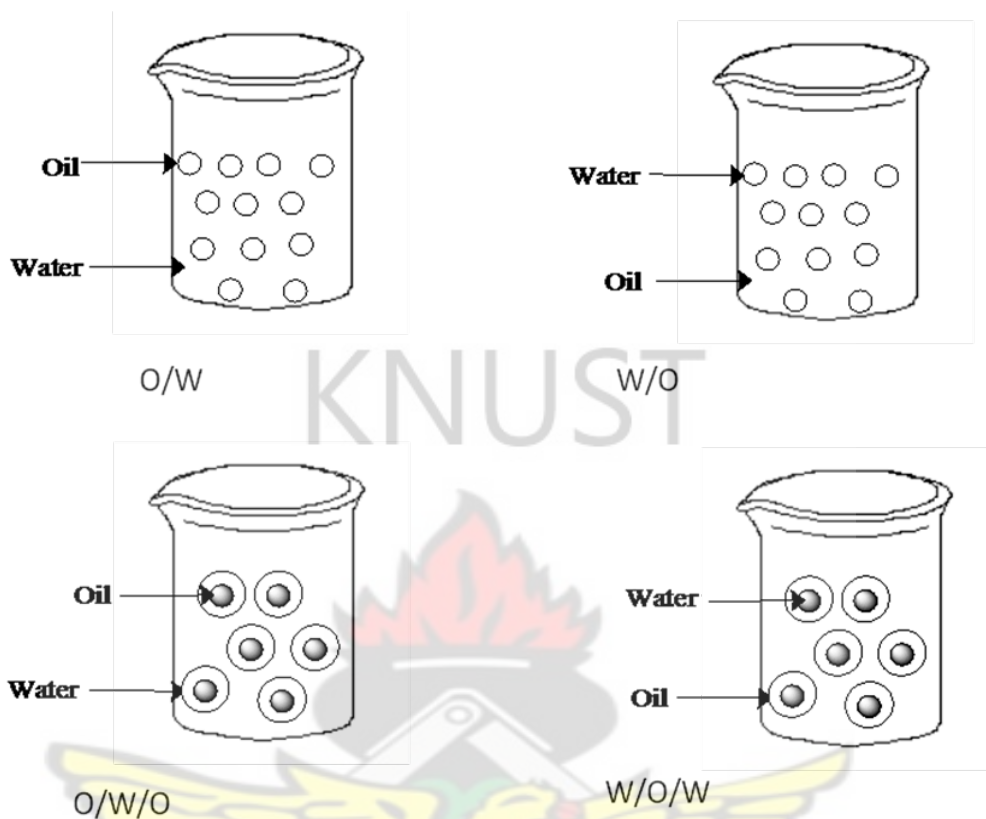


Figure 2-6: Schematic representation of different emulsion systems

Emulsions have been used in different applications as materials and products in everyday life. They are used in personal care items, foodstuffs and pharmaceuticals. The emulsion technology has seen vigorous investigations owing to its potential industrial applicability. The advantages of using an emulsion are its ability to carry multiple active components of differing solubility, its ability to improve the distribution and /or permeability of an active pharmaceutical ingredient upon application and also for aesthetics. The presence of liquid/liquid immiscibility in the emulsion system generates surface tension (force) between the two phases where they come into contact with each other. This is because at the point of contact between the two liquids, the cohesive forces between the molecules

of the two liquids virtually exceed the adhesive forces between them. As a consequence in respect of the thermodynamics, emulsions are not stable. This thus results in the separation of the two layers reducing the surface area. The extent of phase separation can be minimized from the emulsification method and also by the addition of emulsifying agents. [5, 9, 84]

2.2.1 Emulsion Stability

Information about the processes taking place during the homogenization of the emulsion is best explained by the thermodynamics of the system while the kinetics offers knowledge on the speed with which the various activities ensue. When water and also oil mixed, considering the free energies before and after the homogenisation process can monitor their thermodynamic stability. The free energies obtained can then be compared with the interfacial area to understand the extent of thermodynamic stability [85]. Several works have investigated the 'free' energy in the oil/water system prior to homogenization as well as at the end of the homogenization process in food grade emulsion. In such studies the total 'free' energy is additive and can be accounted for the upsurge in the surface area between the two segments of the emulsions hence their thermodynamic instability [86, 87]. Several breakdown processes are almost certain to occur in the emulsion system especially upon storage and this is usually attributed to their thermodynamic instability. However, during the production of an emulsion, an additional constituent is needed to decrease the interfacial tension thereby reducing the episodes of emulsion breakdown. The period at which any of the instability processes occurs is described by the kinetics of the emulsion. Even though emulsion systems may not be thermodynamically stable; they continue to be stable in terms of their kinetic energy for a

long period of time. This is because; events responsible for generating thermodynamic instability happen over a long span of time. Although, the speed at which changes occur in the characteristics of an emulsion system may be slow, it is still very critical especially when applied to the food and pharmaceutical industry.

Stability of an emulsion may be described as its ability to resist changes in its physical characteristic over a time period. This may be achieved or enhanced by adding emulsifiers. After the homogenization process, a high surface area is results to maintain the dispersion of the droplets. This phenomenon subsequently results in the upsurge of 'free energy at the surface considering here this equation below;

$$W = \gamma_{o/w} \cdot \Delta A \quad \text{eqn 2.1}$$

Where **W** is surface free energy, $\gamma_{o/w}$ is interfacial tension of the oil-in-water emulsion system and ΔA is surface area

From the equation, an increase in the surface free energy also leads to an upsurge of the force between the phases interfacial. The high interfacial force causes variation within physical characteristics of the emulsion with time. Thus, Stability of an emulsion can be described in two forms, thermodynamic stability and kinetic stability. When the two immiscible liquids (oil and water) are mixed by homogenization, the internal phase (or segment) immediately forms droplets, which disperse evenly in the uninterrupted or continuous half. The process of breaking down internal segment into dispersed droplets increases the interfacial area hence an increase in the surface free energy and this may cause an upsurge in the force between the two phases or segments. The high tension

(force) between the phases causes the dispersed particles to redistribute within the continuous phase in a direction that depends solely on the variation of density between the phases. The redistribution of the dispersed droplets causes the various instability mechanisms such as: (1) flocculation; (2) creaming a kind of blending (3) Ostwald ripening; (4) amalgamation also known as coalescence; and (5) phase transposition [88]. A couple or even multiples of these instability processes may happen simultaneously. By virtue of their utter relevance, it is crucial to decipher the processes that make emulsions unstable in order to select wisely, their constituent in order to prevent instability and improve their shelf life.

2.2.1.1 Phase Split-up (separation)

The droplets within an emulsion system are constantly in motion and their densities are almost always different from that of the uninterrupted or continuous phase. As the droplets continuously move freely in the system, external forces, which are usually gravitational or centrifugal forces act on them. When these forces surpass the kinetic energy of the droplets, a gradient of the concentration is formed. As the gradient builds up, droplets which are bigger but with lower density move faster atop to form a stratum of droplets above or to the bottom when the density is greater than the density of the medium phase [6, 82, 89].

Creaming is the main phase separation process in an oil-in-water system. The separation occurs only if the oil droplets formed is of lesser density than the continuous phase thereby moving up to form a stratum of oil droplets above in the emulsion system. On the other hand, the separation may be termed as sedimentation, which occurs when the droplets formed are heavier than the continuous water phase; this causes the droplets to

move towards the bottom of the emulsion to form a stratum at the base. Since the density of oil is lower than the density of water, droplets formed in oil-in-water emulsions usually undergo creaming, while sedimentation occurs in water-in-oil emulsions [90]. The speed with which a single droplet creams is regulated by the Stokes Law [90], which states that the rate of creaming is equal to the variation in density between the two segments (i.e. oil and water) to the square of the diameter of the droplet and to the acceleration acting on the droplet and is inversely proportionate to the thickness of the uninterrupted segment [91].

$$V_s = \frac{2a^2(\rho_o - \rho)}{9\eta_o} \quad 2.2$$

Where V_s is the velocity of separation or creaming rate, a is the droplet particle radius, ρ is density of the droplets phase, ρ_o is the density of the medium containing the droplets whilst η_o is the viscosity.

The creaming velocity is totally dependent on the density variation amongst the two liquids, the viscosity of the continuous uninterrupted phase and the droplet particle size. Several works have described different ways to reduce the occurrence of creaming in oil-in-water emulsions [92–95]. Several modification methods leading to the reduction of the variation in density among the dispersed and the uninterrupted aqueous segment are adopted [96, 97] This principle is achieved by employing similar densities for the phases. This is achieved by adding an agent, which usually would increase the density of the oil before the emulsification process or use a much denser emulsifier that is able to increase

the weight of the droplets once formed after emulsification. The reduction of the droplet size has also been considered as an effective way of reducing the rate of creaming [5, 9]. The reduction of the droplet size is critically associated with the homogenization process and the energy input during such processes. The presence of smaller droplets leads to decreasing force between the oil and water phases, which then prevents coalescence. The efficient disruption of oil droplets and its subsequent resistance against coalescence is achieved by the adoption of a more efficient homogenization process and the right choice of emulsifiers and their presence in adequate concentrations [85, 98].

The thickness of the continuous water phase may also be improved to reduce the speed of creaming in an oil-in-water emulsion system. The upsurge of the viscosity (thickness) of the liquid phase neighboring the droplet reduces the movement of the droplets in the emulsion system (velocity). The addition of thickeners in the continuous aqueous phase can be used to improve the thickness of the uninterrupted continuous phase [20, 99, 100]. Another important improvement method is the ability to increase the droplet concentration in the emulsion system [101]. When the droplets are in high concentration, they tend to get packed closely which prevents their movement freely in the system. But, it is a formidable task to increase the concentration of the droplet due to physicochemical limitations of the emulsion system.

2.2.4 Aggregation of the Droplet

The mechanical agitation, the effect of gravity and the presence of Brownian motion leads to the constant movement of the emulsion droplets and therefore triggers the droplets to come close towards one another, which subsequently results in to their frequent collision [88]. The extent of collision depends on the force (internal and

external) acting on the droplets and this informs the kind and nature of the aggregation. Two types of droplet aggregation that may occur are flocculation and coalescence. Flocculation is the type of aggregation in which the droplets maintain their physical characteristics whilst coalescence is the kind in which droplets combine after coming into contact with each other to form one big droplet. Flocculation thus may be revocable (if it is weak enough) or permanent that is irrevocable (if it is strong). Coalescence could be partial or total and they are irreversible [5, 6]. Within an emulsion system, the droplets particles are encompassed by the continuous uninterrupted phase within which the droplets are formed and distributed. When the droplets run into one another, they form a thin stratum, which is usually referred to as thin film or layer. This thin film is formed amongst the droplets by the uninterrupted phase. The advent of the thin film provides the ability to prevent contact of the droplets and this is ascribed to the occurrence of hydrodynamic resistance produced by the thin film [102–104]. The viscosity of this thin layer hangs on the kind of the colloidal and hydrodynamic forces within the emulsion [105–109]. This can also be achieved by the existence of non-adsorbing polymers in the uninterrupted phase, which can cause a reduction of the attractive force. As the thin layer forms a ‘wall’ between the dispersed droplets; the viscosity of the thin film becomes directly proportional to their collisions. The thin films tend to rupture at high energies and this also determines the extent and nature of droplet collisions. The presence of high-energy barrier implies little or no droplet aggregation while lower energy barrier leads to frequent collisions, which could lead to either flocculation or coalescence.

2.2.4.1 Flocculation

Droplet flocculation is the aggregation or collection of droplets that does not cause a

change the size of the droplets. This process is due to the presence of van der Waals attraction between the dispersed systems and may occur only if there are not enough repulsive forces to repel the droplets. Flocculation thus directly affects the stability of an emulsion system and its perceived as an important factor in speeding up creaming of the system [5, 6, 110, 111]. Flocculation can be described either in dilute emulsions or concentrated emulsions. In the emulsions, the flocs formed may have little or no interaction at all with each other and this may cause an increase in the creaming velocity. In a polydispersed emulsion, due to the presence of different droplet sizes the emulsion tend to cream at varying speeds, which may lead to a tendency for the faster moving droplets colliding and forming 'traps' for the slow moving particles. Several mathematical models take into account the collision frequency and collision efficiency and this phenomenon have been used to compute the effect of flocculation on the stability of an emulsion system.

The formation of flocs is a crucial topic within the scope of study of nutrition applications as they increase the viscosity of the emulsion and may be seen as a disadvantage to the food product. But on the other hand, the flocs may form a network structure in the emulsion system, which may present an advantage of controlling product. This therefore makes it very important to study and understand flocculation in emulsion systems. Several methods can be used to control or eliminate flocculation, however choosing an approach depends on the components of the emulsion and the expected final products. The most effective to approach to mitigate the speed and scope of flocculation is to create an energy hurdle between the droplets thereby regulating the interactions between droplets.

2.2.4.2 Coalescence

Coalescence is the amalgamation of a couple or multiples of droplets into a bigger but a single droplet which results in the formation of a stratum of the oil droplets atop an emulsion [5, 88]. This occurs when the droplets involved stay close for some time either during aggregation or during creaming where there exists only a thin stratum of the uninterrupted phase to prevent the droplet – droplet contact. As the droplets run into one another after staying together for sometime, the thin film separating the droplets may break spontaneously or rupture. The spontaneous rupture of the thin film depends on the size of the oil droplets; the larger the droplet the thinner the film diameter and vice versa. The rate of rupture of the thin film is of great importance as it helps in the prediction of the occurrence of coalescence in emulsion systems. Immediately after the film breaks, the oil in the droplets flow to sites of lower pressure and assumes a spherical shape [112, 113].

The droplets are in constant movement, which actually makes the time permitted for the collision minimal. But as the droplets stay closely to each other for longer periods, they afford the thin film enough time that is required for the film rupture and hence the coalescence. The mechanism of droplet coalescence hangs on the surface properties of the continuous segment. Therefore the addition of a surfactant (emulsifier) to improve the surface properties of the continuous phase has become a prerequisite for a successful stabilised emulsion preparation. The surfactant molecules are adsorbed at the droplet surface and form an interfacial layer that acts as a protective membrane, which provides protection for the breakage of the oil droplets. Due to the importance of droplet coalescence it has become of major concern in emulsion systems. Several methods have

been employed in the prevention and or the control of coalescence in emulsions. These methods are basically based on improving the hydrodynamic interactions occurring between the oil droplets and the various emulsion components. These methods are developed to help reduce or prevent droplet-droplet contact and the subsequent film rupture [114–116]. Coalescence has been classified under two main classes; partial coalescence and the ‘true’ or total coalescence. While true coalescence is described as a critical emulsion instability phenomenon, partial coalescence has been looked at as an important process which when carefully studied can be used to achieve good product properties.

Partial coalescence occurs when there is the presence of solid crystals in the dispersed droplets. It is a common phenomenon usually found with solid fat molecules, when the solid fat particles are formed in the emulsion system, some of the crystals are found to protrude from the solid particles into the continuous phase. In such a case, as the particles approach each other and collide, the protruding crystals pierce the adsorption layer of the other particle leading to particle-particle contact and hence the observance of partial coalescence. The event of partial coalescence within an emulsion systems has been seen as an important requirement in manufacturing food grade product to achieve desired properties such as structure development, improved physicochemical characteristics and the sensory characteristics of the food products. The mechanism of the partial coalescence is such that solid particles should exist in the dispersed phase. Partial coalescence is achieved in the presence of solid fat crystals within an oil-in-water emulsion. During the cooling process after the homogenization, the fat droplets begin to crystallize out. When two partially crystalline particles come close to each other, the

existence of projecting crystals penetrate the thin film among them leading to adsorption of the layer around the second fat droplet. The penetrating crystal at this point prefers to be doused by the oil present to the uninterrupted aqueous segment. In the presence of sufficient liquid fat in the dispersed fat particles, the liquid fat begins to stream about the crystals, which reinforces the link in-between the 2 droplets [88]. The prevention of droplet coalescence achieved quite often by the application of emulsifiers. These are surface-active molecules and 'stick' against the oil-water interface to reduce the interfacial tension thereby preventing droplet-droplet contact.

2.2.5 Disproportionation (Ostwald Ripening)

Disproportionation in an emulsion system is the gradual growth of larger droplets due to diffusion of molecules in a polydisperse phase. This occurs because of the solubility of smaller droplets within a continuous aqueous phase [6]. Even though during the emulsification process, the two phases are said to be immiscible, they often show mutual solubilities to some extent and this is often not negligible. When the emulsion is polydisperse, the smaller droplets tend to be more soluble in the continuous phase. This phenomenon is highly dependent on the rate of diffusion of the disperse phase molecules that is smaller to larger droplets through the continuous phase. The pressure of dispersed material is greater for smaller droplets than the larger droplets according to the Laplace equation:

$$P = 2\gamma/r \qquad \text{eqn 2.3}$$

Where, **P** is the Laplace pressure, γ the force of surface tension and **r** the radius of the droplet.

The force generated as a result of the differences in pressure among the smaller and larger droplets is responsible for driving the diffusion process while the speed of diffusion depends on the ability of the dispersed phase to dissolve in the continuous phase. On the other hand the rate of diffusion is also greatly affected by the kind and thickness of the continuous phase. This has been described by the Stokes-Einstein equation:

$$D = k_B T / 6\pi\eta r$$

KNUST

eqn 2.4

Where, **D** stands for diffusion coefficient of a droplet particle and η is the continuous phase (thickness) viscosity.

The occurrence of Ostwald ripening is associated with the solubility of the discontinuous phase and which is inversely proportional to the droplet size. To reduce the Ostwald ripening, emulsions of bigger droplet sizes are encouraged. In preparation emulsions with smaller droplet size distribution, it is crucial to guarantee a smaller difference between the sizes of the individual droplets. Another important factor that has been considered in controlling Ostwald ripening is the solubility of oil-in-the water segment. The ability of the oil to be miscible in the water phase is as a result of the presence and properties of emulsifier used in the emulsion system. Therefore to decrease the occurrence of Ostwald ripening, an emulsifier should be chosen such that it will reduce the possibility of oil solubility in the continuous phase. It is therefore crucial to estimate droplet size and their size dispersion in an emulsion system.

2.3 Characterization of Emulsion Instability Phenomena

Emulsions have wide ranging applications in the food, cosmetic and the pharmaceutical industries. One major advantage of the use of emulsions in delivery systems is their inherent capacity to maintain an encapsulated compound safe over a long period of time and their high level of biocompatibility [3, 117, 118]. Nonetheless, the applications of these emulsion systems suffer some challenges, which are related to their physical stability. Therefore for a successful application of emulsions in delivery systems there is the need to measure and characterize the factors and processes that make an emulsion unstable.

2.3.1 Estimation or measurement of Droplet size

The size of the droplet and their distribution within the emulsion system is the main parameter to be characterized in investigations into emulsion stability. The evolution of the droplet size has become the main character that directly affects most of the emulsion instability phenomena, except for the occurrence of flocculation, which cannot directly affect the droplet size because it does not merge droplets into larger droplets. The occurrence of Ostwald ripening and coalescence increases the average droplet size in an emulsion system as a result of the fact that they either lead to the merging of two or more droplet or the diffusion of droplets. Creaming, the speed of creaming is directly influenced by the size of the droplet and distribution of emulsion droplets. This makes the measurement of emulsion droplet size of great importance. Such measurements provide information on the properties governing the emulsion system. Some of the techniques that have been developed and employed in the measurement of droplet size distribution include the use of microscopy [119, 120], light scattering [121–123] ultrasonic methods

and nuclear magnetic resonance methods [116, 124].

2.3.2 Flocculation Characterization

The presence of flocs in an emulsion system is best observed by microscopy. The rate of occurrence of flocculation may be deduced by estimating the size of the flocs with time and this is best achieved by employing particle-sizing instruments. Image analysis technology may be utilized to deduce the droplet size of the flocs [116, 121]. It is important to be very careful when preparing the emulsions for analysis as careless handling can lead to the breaking of the flocs.

2.3.3 Coalescence and Ostwald Ripening Characterisation

Due to the critical role coalescence and Ostwald ripening play in emulsion stability, several methods have been described for their characterization. The first direct method, which has been frequently used, is optical microscopy. To investigate these phenomena with an optical microscope, an amount of the emulsion either diluted or as prepared depending on the thickness of the emulsion product, is placed on a glass slide under a microscope where the variation in the droplet shape and size are monitored as a correlate of time. The occurrence of coalescence as well as ripening could also be investigated and characterized by estimating the droplet size dispersion with particle sizing technology. Coalescence as well as ripening may all lead to an upsurge in the mean droplet size of the emulsion. To measure and distinguish the extent of occurrence of any of the two parameters at a specific time needs sophisticated microscopic tools such as the scanning electron microscope [8, 125].

2.3.4 Creaming/Sedimentation Characterization

Two other important instability phenomena, which need to be monitored and measured, are the creaming and sedimentation processes. These are frequently monitored by visual observations. Creaming is characterized by the presence of a white or yellow stratum lying atop an emulsion system and sedimentation occurs when such a layer emerges at the base of the emulsion. The speed with which creaming or sedimentation occurs is usually deduced by estimating the volume ratio of the cream layer as a correlate of time. The volume ratio is measured by placing a known volume of the emulsion in a calibrated beaker and the rate at which the creamy layer is formed either at the topmost or bottommost part of the emulsion is measured at a particular time determined by the investigator. In situations where the creaming or sedimentation occurs very fast, the use of visual observation does not give accurate results and therefore more sophisticated technology such as light scattering [121–123] or ultrasonic imaging may be employed.

The utilization of microscopic techniques in the characterization of emulsions has become an important tool. They are used to distinguish between the different instability processes. Investigating the dependence of the distribution droplet size as a correlate of time with particle sizing instruments has also been shown to provide quality information on the upsurge of the mean droplet size. But all these tools are not able to clearly show the distinction between the nature and kind of droplet increase. To really understand the physicochemical properties and to help forecast a durable stability of an emulsion system, it is crucial to know the kind of droplet size increase occurring in the emulsion. This will give information as to whether the increase in the droplet size is as a result of coalescence, Ostwald ripening or flocculation. Methods available to distinguish which

phenomenon is responsible for the droplet size increase are quite complicated. In some cases, there is the need to apply mechanical agitation to the emulsion in order to break any flocs present. In such a case the droplet size is measured before and after the mechanical agitation and the difference in the size distribution gives an indication if flocs were present or not. The use of dyes is also employed to investigate the nature of the droplets. In this case the dispersed droplets are dyed with two different colours, the occurrence of coalescence will lead to the formation of a dispersed droplet with a colour representing a combination of the two dyes. Where there is coalescence the bulk dispersed phase will be made of droplets of two different colours. So if the dispersed droplets maintain their colour but yet display an upsurge in the droplet size measurement then the increase can be associated with the occurrence of flocculation.

2.4 Emulsions stabilized by Surfactants

2.4.1 Surfactants: Definition;

Invariably, one of the most versatile and widely used products of the chemical industry is Surfactants [126]. They may be commonly used as detergents for daily applications, as templates for constructing nanoparticles delivery systems in drug delivery, as catalysts in organic synthesis and sometimes as models for obtaining basic knowledge self-assembly systems [127, 128].

A surfactant is defined as a surface-active vehicle, that which is able to adsorb onto the surface or the interface in a system even when it is in lower concentrations. It can significantly alter the 'free' energies between the surfaces of the system. It is worth noting that the term interface describes a border between any two phases that cannot mix

and the term surface is used for a boundary where one phase is a gas (air). The interfacial ‘free’ energy refers to the least total energy needed to construct that interface. The presence of the surfactant reduces the interfacial energy [7, 129, 130]. Surfactants are amphipathic compounds with a characteristic molecular structure having on one side a hydrophobic group and on the other side a hydrophilic group. The terms hydrophobic and hydrophilic are usually used to describe the molecular structures when the solvent is water. In that case the hydrophobic group will be the group with little or no attraction for the solvent while the hydrophilic group exhibits a huge attraction for solvents. In this study, the structural molecule of the surfactant is described as hydrophobic and hydrophilic. The hydrophilic and hydrophobic ends of the structural formula of the surfactant are described as the head and tail of the molecule and these groups are used to describe the type and nature of a particular surfactant. Each surfactant presents a characteristic chemical property, which is highly dependent on the kind of head and tail groups of surfactants [7]

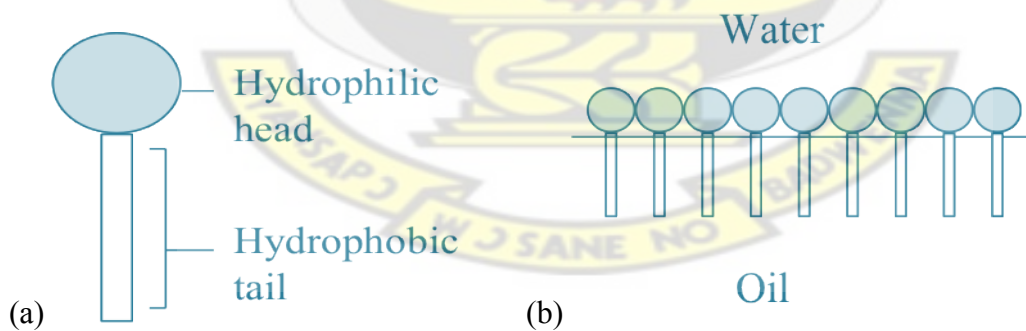


Figure 2-7: Sketches representing (a) the hydrophilic head and hydrophobic tail surfactant structure (b) surfactant action at the oil and water interface.

When a surfactant molecule is dissolved in a solvent, its reaction mechanism is such that the hydrophobic group may distort the solvent structure and the hydrophilic end precludes the surfactant from being excluded totally from the solvent as a discrete phase [5]. The chemical compositions of the structural ends, which are suitable to be used as hydrophobic and hydrophilic parts of the surfactant, may change with the kind of the solvent and the conditions of their usage. The hydrophilic end may be a charged or neutral molecule; a small compact or a polymeric chain molecule and the hydrophobic end may usually be a singly or doubly bonded, straight hydrocarbon chain or a kink. They may also consist of fluorocarbon, siloxane, or an aromatic group(s). The ability for a surfactant to solubilize in a water soluble medium is governed by the affinity of the hydrophilic part of the surfactant with the media [130, 131]. A surfactant molecule may be classified` as indicated by Rosen and his coworkers [7], primarily according to the nature of the hydrophilic end and this may be grouped as follow:

Anionic: when the surface-active moiety of the surfactant molecule possesses a minus charge. An example is Dioctyl sodium sulfosuccinate

Cationic: when the surface-active moiety carries a net positive charge such as octenidine dihydrochloride.

Nonionic: when the surface-active moiety carries no charge such as polyoxyethylene.

Zwitterionic: when the surface-active moiety carries both positive and negative charges.

With an example as cocamidopropyl betaine

When the surfactant dissolves in a liquid medium, they may form a micelle by

assembling themselves or are adsorbed between the surface of dispersed droplet and the continuous water phase as a result of the hydrophobic group [7, 128]. Adsorption of the surfactants at the interface results in the creation of a structural change of the interfacial area between the dispersed droplets and the continuous phase. This phenomenon leads to reduction in their interfacial forces. In the case of the action of a surfactant in the formation of micelles, the micelles formation is dependent on the surfactant concentration present. At significantly elevated concentrations, large amounts of micelles are formed from clusters of surfactant molecules. The micelles are formed at the concentration known as the critical micelle concentration (CMC). Above the critical micelle concentration any further increase in concentration results in the formation of the aggregates and the concentrations of the unassociated molecules remains unchanged. The nature (size and shape) of micelles formed is regulated by the geometry of hydrophobic and hydrophilic ends of the surfactant molecule and their subsequent interactions [7].

2.4.2 Surfactants as Emulsifying Agents

There are several different types of surfactants used in the chemical industry. They can be used as natural or synthetic such as detergents, wetting agents, foaming agents, and dispersants. Most of these surfactants are derived from crude oil with a larger volume of them being petrochemical-based [128, 132]. Huge amounts of these surfactants have been used extensively as emulsifiers, in personal care, food, painting and pharmaceuticals. The application and utilization of surfactants in emulsions have been investigated and significant amount of reports are found in the literature [8, 114, 133]. The fundamental characteristic of surfactants is its ability to adsorb at interfaces in an oriented fashion due to their amphiphilic nature. The surfactant is made of a hydrophilic end, which stays in

water and a hydrophobic end usually found in oil. Even as surfactant molecules adsorbed onto the interface, the molecules present take the place of the water and oil molecules originally at the interface. After the surfactant is adsorbed at the interface, the hydrophilic end now interacts with the water molecules and the hydrophobic ends also interact with the oil molecules at the interface [7, 130]. The amount of surfactant present at the interface gives a measure of the interface to be covered, and this informs its performance in a particular product. In the emulsification process the existence of surfactant molecules at the interface increases the oil/water interactions and this leads to decreasing interfacial force across the interface within the emulsion system. Apart from the concentration of the surfactant another important factor to consider is the orientation and stuffing of the surfactant molecules at the edge. The orientation of the surfactant molecules affects the positioning of the hydrophilic and hydrophobic groups [103, 134].

During the emulsification process, the bulk-dispersed phase breaks up and in the process forms the droplets. As the droplets are formed, the emulsifier molecules present in the system get adsorbed onto the droplets [101, 135]. There is also the occurrence of droplet interactions and all these processes may occur at the same time during the emulsification process. The existence of the surfactant molecules lowers the interfacial force and also assists droplet break-up and these properties work together to prevent or delay most of the instability processes in the emulsions. The occurrence of the instability processes such as aggregation and coalescence depends on the surfactant concentration. Lower concentrations form an initial layer around the droplets, but since the intensity of the layer is not strong enough, the droplets tend to coalesce or aggregate as they approach and collide with each other [136].

Consider a typical case whereby two dispersed oil droplets are covered by surfactants at lower concentration. As they move towards each other, the surfactant molecules are adsorbed between the phases of any two of the dispersed droplets. But, as the quantity of the surfactant molecules accessible for adsorption is reduced as a result of their low concentrations, the thin film separating the droplets becomes smaller. The thinner the film between the approaching droplets the more an interfacial force gradient is observed. The gradient of interfacial force leads to non-uniform surfactant molecules coverage in the entire emulsion system. This gradient causes surfactant molecules to move to interfaces or sites with low surfactant molecules coverage resulting in less surfactant molecules at regions of the interface where the droplets are the closest. As the interfacial tension increases the water molecules, which are present as the continuous aqueous phase moves in the orientation towards the highest interfacial force. This streams the droplets further from one another [124].

The classification of a mixture of two immiscible pure liquids as an emulsion (usually oil and water) is always difficult, as the mixture cannot stay stable to be classified. When there are no emulsifiers added to clean oil and aqueous systems, the kind of emulsion formed is always reliant on the volume fraction of every single phase present. For a mixture of one liquid in another to be stable to be classified as an emulsion, there is the need to add a third component. The third constituent, also referred to as emulsifying agent and routinely a surface-active agent, introduces stability to the system [97, 137]. The surfactant could be dissolved in either the oil, or water and this is dependent on the magnitude of the head and tail groups. When tension between the oil- hydrophobic ends is greater than the tension at the water- hydrophilic end, the film turns concave to the oil;

this results in closure of the oil by the water hence creating an oil-in-water emulsion. If the tension at the water-hydrophilic ends becomes larger, as compared with the tension at the oil-hydrophobic ends, the film becomes concave towards the water, forming a water-in-oil emulsion. The theory explaining the stabilisation of oil in water emulsion and water-in-oil emulsions is usually based on empirical Bancroft rule. Bancroft has associated the capacity of the surfactant to stabilise an emulsion to its capability to dissolve in the oil or water medium. According to the Bancroft rule, oil-soluble surfactant can stabilise water in oil emulsions, and water-soluble surfactant can also stabilise oil-in-water emulsions [5, 7]. Several investigators in this field have also explained that the interfacial region produced as a result of the adsorption and alignment of the surfactant molecules between the phases can have diverse interfacial forces between the hydrophilic ends of the surfactant and the aqueous phase from that between the hydrophobic ends of the surfactant and the oil phase [128].

Due to the important role surfactants play in the production of well-developed and stabilised emulsions, and the fact that the use of a particular surfactant is based on the constituent of the water and oil phases, your choice of a specific surfactant for an emulsion is a complicated one. Some investigators use experimental procedures to determine to choose a surfactant in a particular emulsion. In theory, the very common and frequently used approach for selecting a surfactant in emulsification is the Hydrophilic-Lipophilic Balance (HLB) technique. In this approach a numerical figure ranging between 0 to 40 is assigned to the surfactant in relation to the equilibrium between hydrophilic and hydrophobic ends of the surfactant molecule [138, 139]. In other situations, the calculation of the HLB number is based on the structure of the surfactant

molecule and in others the HLB number is deduced from prior records obtained from emulsification experiments. It is good to bear in mind that HLB number of the surfactant does not give the efficiency or the effectiveness of the particular surfactant, it only gives information on the kind of emulsion, which can be formed from it. Some reports have also shown that a single surfactant could be used to produce an oil-in-water or water-in-oil emulsion. The phenomenon is dependent on the experimental conditions (temperature, the shear rate, oil or water concentration and ratio of the surfactant to oil ratio) at which the emulsion is prepared [7, 140]. But in most cases the choice of the surfactant for a specific type of emulsion is dependent on the HLB number. Oil-in-water emulsions could be made with surfactant with a wide range of HLB numbers (2 to 17). On the other hand to obtain the right HLB number for an emulsion system, two or more surfactants can be mixed according to the Bancroft rule to obtain the appropriate stabilisation effect. Typically a water-in-oil surfactant dissolves in the oil phase while an oil-in-water surfactant dissolves in the water.

2.4.3 Alginate as a non-surfactant emulsifier

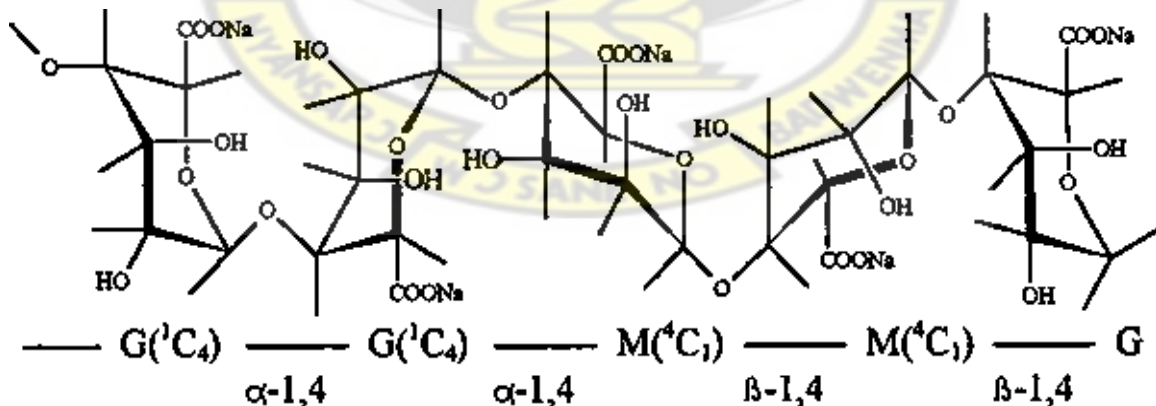


Figure 2-8: Chemical structure showing the G and M units of the Alginate molecule

Alginates are not toxic, they can be degradable biologically and occur in nature and are polysaccharide compounds found from seaweeds. Additionally they may be described as straight or linear copolymers consisting of (1-4)-linked β -D-mannuronic (M units) acid and α -L-guluronic (G units) acid [141, 142]. Their subunits are organized in blocks alongside the chain at the homopolymeric regions of M- and G-blocks. These blocks are arranged and interfered with sections of interchanging MG-blocks. The ratio and order of arrangements of the G and M units are very crucial for an alginate compound as it has effect for the physic-chemical characteristics of the molecule [143]. The alginate shows several different physico-chemical properties such as affinity for cations, gelling characteristics, chain rigidity etc. One of the most important characteristics of alginate compound is, its gelation properties in the company of cations carrying a +2 charge such as Ca^{2+} , which preferentially binds to the G-blocks within the alginate molecule in a more mutual way. This makes the G-blocks the focal structural feature in the creation of gels [144, 145]. The ability of the alginate compound to dissolve in aqueous solution is reliant on the cation linked to the alginate molecule and the pH. Sodium alginate dissolves in water and gels in the company of divalent cations such as Ca^{2+} and Mg^{2+} [146]. Alginate constituent is a crucial factor in alginate particle design, the percentage of sodium and calcium heavily impact the swelling and healing characteristics of the molecule. The viscosity of the alginate solution varies in quantity with the G unit. As the emulsification process go on, a high G block may lead to a premature gelation. This results in the formation of larger dispersions and highly porous gels. However, a high M unit produces high elastic weaker gels. The alginate compounds have been used in addition to other surfactant molecules to make better the stability of emulsions in delivery

systems. In addition, the strength of surfactant-alginate contacts at the oil droplet interface and the characteristics of the interfacial complex formed depends on the dispersion of ionized clusters on the surfactant molecules, stability of the surfactant molecule and the plasticity, charge dispersion and density of the alginate molecule [99, 147]. The interfacial membrane produced from the surfactant-alginate complex is normally denser and extra rigid as compared to that obtained from the surfactant molecules alone. It is therefore often preferred to use the interfacial complex formed from the surfactant-alginate interaction to make better the stability of emulsions especially as regards to ambient or environmental stress [9].

Utilizing alginate as a gelation agent in an emulsification process for the encapsulation of bioactive compounds for their application in drug delivery has been studied and reported extensively in literature. Xie et al (2010) [22] investigated the use of a one-step method to produce nanostructured composites.

Dang and Joo (2013) [23], studied the preparation of sodium alginate micro particles using a microfluidic flow-focusing device (MFFD) focusing on the production of gelation outside the device. With optimized flow conditions, microsized droplets of sodium alginate were prepared with the continuous phase being soybean oil and the alginate solution as the dispersed or discontinuous phase. After gelation, calcium alginate micro particles obtained were in the range of 100 to 250 μM . They concluded that the approach of manipulating the calcium alginate micro particles could be used in medical or biotechnological applications such as drug and cell delivery systems [23, 144].

2.4.4 Tween Surfactants –for the Stabilisation Oil-in-Water Emulsions

It is established that, oil-in-water emulsions are usually stabilised with high HLB number surfactants, which are referred to as the Tween surfactants. High HLB surfactants exhibit high hydrophilicity, which helps in the immediate O/W droplets formation or the quick dispersion of the preparation in the water phase [8, 133, 148]. The Tween surfactants are polyoxyethylene (POE) sorbitan compounds, nonionic and vegetable oil derivatives. They are routinely utilized in food, pharmacological and ornamental products [149, 150]. These surfactants are either classified according to their head group or the tail group found in the surfactant molecule. The total number of oxyethylene group (-C₂H₄O-) usually written in parenthesis after the polyoxyethylene in the systematic nomenclature represents the head group while the tail group is indicated and written as part of the common name usually identifying the type of Tween (such as 20,30,40,60,80) [130, 151]. The chemical nature of the tail group is linked to the kind of fatty acid from which a particular surfactant molecule is derived.

Palanuwech and Coupland (2003) [152], in their work on influence of surfactant kind on the ability of oil-in-water emulsions to stabilize to dispersed phase crystallisation, investigated the sweet (confection) coating of fat (CCF) emulsions (40 wt.%) which was made by putting together liquid fat with solutions (1-4 wt.%) of some carefully chosen polymeric and tiny molecule surfactants in a homogenization process for obtaining an average particle dimension of $0.71 \pm 0.05 \mu\text{m}$. It was observed that the crystallisation characteristics of the oil were dependent on the interfacial material and the thermal profile of the emulsion. The nature of the surfactant present showed little or no effect on the crystallisation temperature of the mass fat, but the crystallisation of the emulsified fat

was highly dependent on the kind of surfactant. The various kinds of surfactants chosen had varying tendencies in stabilizing the system against fractional coalescence in the course of thermal cycling. They observed that the viscosity of the interfacial stratum played an important role in identifying stable and unstable emulsions. Tween 20 was one of the tiny molecule uncharged surfactants, which gave dense layers with better stability than the less dense but charged strata of sodium dodecyl sulfate and docecyltrimethyl-ammonium chloride.

Hsu and Nacu (2003), [153] in their study of the performance of soybean emulsion stabilised by non-ionic surfactants, investigated the ability of Tween 20, (40,60,80 and 85) to stabilise an oil-in-water emulsion. They observed that even though all the emulsions produced under different surfactant selection were stable over a period, the concentration needed for each surfactant to successfully stabilise the emulsion system was dependent on the kind of Tween. In all it was observed that Tween 20 was capable of providing stability to the emulsion at a relatively low concentration, while the other Tween's (40,60,80 and 85) needed increased concentrations of their surfactant molecules in order to be able to provide stability to the emulsions. Tween 20 also produced droplets of very small size distribution as compared to the rest of the Tween surfactants and Tween 80 was the least efficient in decreasing droplet size. With regards to Tween 60, increasing concentration resulted in reducing droplet size until a threshold concentration above which no effect on the droplet size was observed. Droplet sizes in the emulsion from the Tween 85 kept decreasing with increase in their concentrations.

Rahate and Nagarkar (2007) [133] emulsified sunflower and sesame oils by utilizing a fusion of nonionic surfactants, such as Span-80, Tween-20, with natural polymer as additives. They found that stabilisation of emulsions made in the company of nonionic surfactants could be credited to the physical occurrence of the surfactants.

Polyethoxylated non-ionic surfactants are capable of dissolving in aqueous medium because the hydrogen bonds within the solvent molecules bonds with the oxygen atoms of polyoxyethylene chain. Combination of two or more different emulsifying agents is believed to show a “synergistic” interaction. In this kind of interaction the interfacial property of the mixture is more pronounced as compared with the interfacial properties exhibited by the individual components [7].

Considering the stabilisation advantage of such synergistic property, many industrial products and processes nowadays utilize of a combination of various types of emulsifiers to achieve an expected stabilisation effect. A perfect example of this application is found in the production of food grade emulsions where the selected surfactants have been used in combination with other emulsifiers such as proteins and surface modification agents like polysaccharides.

2.5 Encapsulation of Active Compounds in Oil-in-Water Emulsions

In the context of the current review, encapsulation is referred to as the process of trapping an active compound within the matrix of another substance. It is a technology that enables a range of materials of biological, chemical and physical interest to be safeguarded within the matrix and delivered. The technique works by creating an environment, which controls the interactions between the internal part and the outer part.

The overarching goal of the encapsulating technology in delivery systems is to provide protection for the entrapped active compound from unfavorable ambient environments, such as moisture light, and/or oxygen. Protection against these environmental conditions contributes to improving the storage period of the produce [155]. The substance entrapped in another substance may be described as core material, an active agent, the inner phase or even a fill, and the substance entrapping the inner substance could also be referred to as the 'coating', the membrane, a shell, the carrier material, the external phase, and a matrix. The presence of the external phase provides a barrier to overcome obstacles such as temperature and ultra-violet sensitivity, instability during pH fluctuation, low aqueous solubility and poor transportation rate. Encapsulation also offer various significant advantages such as providing efficient shield for the encapsulated active compound against environmental degradation, promotion of controlled release and planning a pre-programmed drug release profile to a specific therapeutic need and easy administration of many drug compounds. For this numerous advantages, encapsulation has become such a multipurpose technique which is applied widely in biomedicine, pharmaceuticals, food formulations and manufacturing, cosmetics and agriculture [156, 157].

In the food industry, encapsulation is found suitable especially in producing nutraceuticals and aliments of high value. Application of encapsulation technology is again seen in food production with fortified constituents, tailored flavour, colour, and texture or for preservation. It has been used for the addition of nutrients of probable healthiness benefits, including antioxidants and probiotics [158, 159]. When the production of functional foods is targeted, the preparation of foods product must take into

accounts the control and stability of the bioactive molecule present in the course of preparation and shelf life to circumvent the occurrence of unpleasant reactions in the food constituents and also to help monitor the food substance after its introduction into the human body.

Choi and co workers [160], investigated the physical characteristics of fish-oil encapsulated by two different methods. They first investigated the use of a water-soluble polymer, β -cyclodextrin (β -CD) as a matrix for encapsulating of the fish-oil through the aggregation method and also polycaprolactone (PCL) polymer that is not soluble in water, employing an emulsion – diffusion assay. Owing to diverse dietary benefits of fish oils, the study was targeted at improving the odour and the stability of the encapsulated fish oil against oxidation. They found that, fish-oil-laden in the β -CD at a blending ratio of 10:20 (β -CD:FO (w:w)) led to the most efficient encapsulation of 84.1%, and loading capacity of 62.7% with a leakage of 11.0% fish oil after freeze-drying. The rate of release of the fish oil from β -CD particles were also found to be slower in deionised water at 15 % and at 25% in NaCl. In terms of their storage stabilities, the β -CD–FO matrix of 10:20 w/w blending ratio kept 97% of fish oil in the particles in the course of 3 days after freeze-drying. Considering the emulsion–diffusion method, the PCL was found to effectively delay the release of the fishoil either within the fluid form or the solid form.

Pool and co-workers (2013), [161] investigated the impact of encapsulation on the physical form and release and/or bioaccessibility of hydrophobic bioactive portions (quercetin) in nano-emulsion-based delivery systems. Their work was aimed at determining whether the hydrophobic-crystalline-bioactive portion could be efficaciously

included in a nano-emulsion system and subsequently to assess at what level will this delivery system alter its bioaccessibility. Even though the physical form of the hydrophobic crystalline did not change in the emulsion system, their bioavailability was less and so they concluded that the lessons accrued from this investigation is crucial for the realistic design of delivery systems to integrate crystalline-hydrophobic-bioactive compounds into medicines and nutraceuticals, and to improve their bioaccessibility

Using the encapsulation technology in the manufacture of medicines may present some disadvantages including adding extra cost to the cost of production of a particular product. It may also increase the complexity in the method of production and the possibility of the final product having stability challenges. Nevertheless there has been an upsurge in utilizing this technique in diverse industries due to the following advantages:

- (a) Protection of the drug material from reacting with its environment thereby reducing the possibility of drug degradation;
- (b) Reduction of the possible occurrence of drug transfer or its evaporation;
- (c) Alteration of some of the physical properties of the original material;
- (d) Flexibility of targeted or controlled release of the drug material
- (e) Masking of taste of the internal drug material
- (f) Provision of separation for the various components of the drug mixture [162–164].

Many different drug compounds have been encapsulated using different technologies for their use in different therapeutic purposes. The encapsulation process has been used in

many applications in pharmaceutical formulations such as maintaining the potency of naturally occurring active compounds and in many synthetic formulations to improve their bioavailability [155, 165, 166].

2.5.1 Encapsulation Techniques

Most of the encapsulation techniques available are based on the production of droplets of the active compounds within a carrier material with different physicochemical properties. Currently diverse technology options exist for encapsulation in the confectionary and drug manufacture industries. These include spray drying, fluid-bed-coating, spray-chilling and spray-cooling as well as melt injection. Again there is also melt-extrusion, emulsification and Liposome entrapment [155, 167].

Dispersing an active component in a water-soluble solution of the carrier material represents the spray-drying technique. Atomization and the spraying of the blend into a hot compartment follow this. During the process of spray drying a thin layer (film) is produced at the droplet surface, thus delaying the bigger active molecules whereas the tinier water molecules are vaporized [168]. This is most widely used and the oldest encapsulation techniques and most commonly employed in the food and the pharmaceutical industry. The procedures involved in the spray drying technique are continuous, flexible and not so expensive to operate. It produces good quality particles of smaller sizes usually 10-400 μm . The size of the droplets is largely dependent on the surface tension force and the thickness of the liquid phase, the decrease in pressure throughout the nozzle, and the speed of the spray. In the course of drying, the size of the atomizing droplets is responsible for the duration of drying and particle size. The size of the particle obtained from this method affords their final products good sensorial and

texture characteristics. Even though the spray drying technique has been widely used in many food and pharmaceutical products, it is not without some undesirable factors such as the sophistication of the instruments used, the possibility of not having a uniform condition in the drying chamber and the difficulty associated with producing particles of a particular size [165, 169].

Fluid-bed-coating is that technology where a coating is applied on powder particles in a batch process; it is a well-known modified spray-dry approach. In the fluid bed coating method, the bioactive compound is suspended in air and the carrier molecules are sprayed onto it to develop a capsule [170]. In this technology, the elements to be coated by the fluid-bed should have a round shape and if possible must possess a small particle size distribution and should be able to flow freely. Particles with sharp edges are usually not used as the sharp edges may damage the coating during handling. The main distinction amongst the spray drying method and the fluid bed coating is that, in the fluid bed technology a broad number of carrier materials can be chosen; the carrier or matrix materials can be fats, proteins, carbohydrates etc. It is a useful method as it can be applied to encapsulate particles obtained from a spray dry method [169].

Spray-chilling also known as spray-cooling is the technique in which a droplet of melted lipids is atomized in a chilled compartment to result in a solidified lipid and ultimately their retrieval as fine particles. Also in this method, dispersions of the carrier material and the bioactive compound are prepared and cooled to form solid particles. It is worth noting that in this method fats with high melting point are usually used. The early set-up of a spray cooling experiment is like the spray-drying except that in the spray cooling the encapsulated compound is cooled to solidify rather than the evaporated water as seen in

spray drying. When the technique is termed as spray-chilling the particles are maintained at a lower temperatures [168].

Extrusion technologies consist of the dropping of droplets from an aqueous solution of a polymeric material such as carbohydrates. In principle the polymeric material (carbohydrates) to use for the encapsulation of the active component should be in the molten form. Two processes may be applied to encapsulate the active component in the polymer melt. There can be melt injection, in which the melted polymer and the encapsulated component is pressed through a filter and immediately followed by quenching by a cold, dehydrating solvent. This process is often referred to as a vertical screwless extrusion process and they usually produce encapsulates of particle sizes ranging from 200 to about 2,000 μm [169]. A smaller and more desired particle size can be achieved by reducing the extruded strands to the appropriate dimensions through vigorous stirring which leads to the breaking up of the extrudates into smaller pieces inside the cold dehydrating solvent. On the other hand the melt extrusion involves the use of screws placed in a horizontal position and there is no washing of extrudates surface. The extrusion technology is less hazardous but very laborious method of encapsulation. In extrusion, small droplets of the encapsulation material are forced through some kind of nozzles or through some smaller holes in a droplet-generating device. The droplet-producing device could be a simple micropipette, a syringe, a nozzle, a spraying nozzle, jet cutter or atomizing disk [168]. It is important to take into consideration the nozzle size of the droplet-generating instrument, as it is directly proportional to the droplets produced. Extrusion technologies are desirable for several reasons. Its application is gentle, does not involve the use of deleterious solvents, and the encapsulation process can

be done in the presence of oxygen or without it.

Emulsification is the application of emulsion technology for the encapsulation of bioactive compounds. It is usually applied in the encapsulation of bioactive agents in aqueous solutions. The encapsulated products can directly be used or after drying to get the powder form. The emulsion is made of two immiscible substances whereby one dispersed as droplets in the other [159, 171, 172]. The emulsions system so formed is thermodynamically unstable and separate out into the two different phases involved in the formulation. The stability of emulsion system can be achieved by proper formulation design for the phases and their interface formed. This is possible by a critical selection of some of the ingredients such as the choice of the emulsifier or texture modifiers used in the preparation [172–174]. Using high shear equipment with the ability to disrupt large molecules into smaller units commonly produces emulsions. Such techniques include stirring vessel with baffles, high shear mixing tools and ultrasonic homogenizer. These methods usually produce droplets of diameter ranging from 0.1 to 100 μm . to employ emulsion system to encapsulate an essential compound, the emulsion must prove to be stable especially during storage until its application and secondly, the emulsion's consistency upon application to enable the desired delivery.

Several methods have been established in order to increase emulsion stability hence increase the application of emulsion systems in encapsulation. Oil-in-water emulsion, may be spray dried or freeze dried to form a powdered end product. Such methods are used for the preparation of instant formulations used in beverages. The dispersed particles can also be modified by co-extrusion to produce encapsulates which are in turn used as templates for other processes [167]. Another important application that has evolved in

recent times is the emulsification of melted fat in an aqueous phase at a high temperatures. The disadvantage found with this method is that if the active component is not wholly soluble in the fat substance it may lead to an incomplete encapsulation [175].

Liposomes are kind of encapsulation technology whereby aqueous solutions of active compounds are enclosed in membrane of lipid molecules for an effective delivery. They are formed when the lipid compounds are dispersed in the aqueous medium using the colloid mill or microfluidization. The procedure in forming liposomes mainly is through interactions between the polar and non-polar lipid/water molecules. The liposomes can be used to entrap a hydrophilic drug in an aqueous matrix and entrap the hydrophobic drug within the bilayers of the lipid molecules. This encapsulation method is able to produce particles of sizes ranging from around 30 nm to some few micrometers. The application and the study of the liposomes in recent times is for its use as advanced pharmaceutical drug carriers. The use of liposomes is limited in food production since liposomes usually present chemical and physical stability problems during storage [157].

2.5.2 Encapsulation Efficiency of Emulsion-Based Delivery Systems

There are several challenges associated with developing a successful encapsulation in delivery systems based on emulsion products. Some challenges include instability of emulsion system, limited loading capacity, incomplete release pattern of encapsulated active component and the possible burst or diffusion within the emulsion system [176, 177]. These challenges contribute to the ineffective delivery of the encapsulated compounds and hence unsatisfactory release of the active component from the therapeutic and economic viewpoints. For this reason, it is important to investigate and monitor the efficiency of encapsulation in especially drug delivery systems. The

efficiency of encapsulation is usually characterized by the loading capacity, the particle size and surface morphology of the emulsion droplets. The factors affecting the efficiency of the encapsulation method in delivery systems may come from properties of the emulsion system and/or the encapsulated compound. From the encapsulated compound, the efficiency of encapsulation is dependent on the hydrophilic or hydrophobic nature of the active component and its interactions with the emulsion system. Concerning the emulsion properties, volumes of both the continuous and the disperse phase affect its efficiency, and the method of preparation also has great influence on the encapsulation efficiency. Methods for overcoming these challenges and, consequently, developing a more stable and effective delivery system have concentrated on using of stabilizing agents as well as other modification methods during production [176, 178–181]. Other research works have focused on the environmental conditions of the encapsulation process during production [182].

Several experimental methods have been used in the investigation of efficiency of encapsulation in delivery systems. The amount of active component entrapped (loading capacity) is usually measured by an HPLC method or a UV-spectrophotometer [178, 183, 184]. Determination of the size of the dispersed particles and their size distribution within the emulsion system shows the extent of stabilisation of the emulsion and the encapsulated compound in the emulsion system. It can also be used to confirm the presence of the active compound entrapped in the emulsion system. The particle size is measured using the dynamic light scattering system (DLS) instrument [160]. Many different microscopic methods have been used to characterize the morphology of the entrapped droplets [160, 182, 184].

CHAPTER 3

Materials and Experimental Methods

3.1 Materials

3.1.1 Vegetable Fat Samples

Fats used in this study are vegetable based fats. The fats were extracted from dried seeds from the ripe *Allanblackia* fruit and shea nuts, which were collected from the wild in the Western and Northern Regions of Ghana respectively and identified by Mr. P.Y. Adjei at the Department of Horticulture-KNUST, Kumasi Ghana. The seeds were cracked open to obtain the kernels after which the kernels were oven dried at 50 °C for 24 hours to ensure that samples dry completely. The dried seeds were then milled and the oil extracted by the press method. The oils were put into glass vials and kept at room temperature for future use.

3.1.2 Chemicals

HPLC grades hexanes, and methanol were obtained from Sigma Aldrich and were used without any further purification. Potassium hydroxide was obtained as a laboratory grade reagent from Sigma Aldrich Manchester UK. Chloroform-d (CDCl_3) and Tetramethylsilane (TMS) both analytical grade reagents were all obtained from Sigma Aldrich and used for the ^1H NMR analysis. The Sudan orange used in this study was of HPLC grade of $\geq 97\%$ with a molecular weight of 214.22, melting point of the range 143 – 146 °C and an absorption wavelength of 380 – 420 nm. This was obtained from Sigma-Aldrich, Manchester UK and used without any purification. Tween 20 with an HLB of

16.7 was purchased from Sigma Aldrich and used as the main surfactant in this study. Sodium alginate (sodium salt of alginic acid, a polysaccharide) was also obtained from Sigma Aldrich and used as a thickening agent in the study. The water (deionized water) used in all experiments was obtained from the Milli-Q water system (18.2 mΩ.cm at 25°C) from which distilled water through reverse osmosis unit was deionized. All other materials used in this study were without any extra purification or alteration of properties. All experiments were performed at the Organic Materials and Innovation Center (OMIC), at the School of Chemistry, The University of Manchester, United Kingdom

3.1.3 Concentration Units

Masses of all substances used in the experimental work were carefully chosen so as to obtain the needed absolute concentration of each of the component in the emulsion systems. Materials used in this work were estimated in percentage weight concentration of the component per the weight of the final product (wt/wt %). This is simply represented as % in the thesis for simplicity.

3.2 Experimental Methods

3.2.1 Fatty Acid Constituents Determination

3.2.1.1 Preparation and Determination of Fatty Acids Methyl Esters

The fatty acid constituents of the fats from *Allanblackia* (AB-GH) and shea butter (SB-GH) were determined as their methyl ester derivatives, which were prepared by dissolving 200 mg of the fat samples in 5 mL hexane and vortexed to ensure complete dissolution of the fat in hexane. A 200 µL of 2 N methanolic potassium hydroxide solution was added to the hexane fat mixture in a screw-top test tube and the cap

tightened. The solution was then strongly agitated continuously for 30 s. The mixture was left to stratify to obtain a clear to layer. The clear hexane layer was carefully transferred into a sample vial containing small amounts of sodium sulphate to remove the presence of any water molecules. The hexane phase containing the methyl ester and the sodium sulphate were allowed to stand for 15 min after which 1.0 μL of the hexane layer was injected via a split/splitless injector (split ratio 20:1) on GC/MS 7890/15975C Chemstation fitted with an autosampler (Agilent Technologies, USA). The oven temperature was programmed as follows; 125 $^{\circ}\text{C}$ for 3min, 125 $^{\circ}\text{C}$ to 206 $^{\circ}\text{C}$ at 3 $^{\circ}\text{C}/\text{min}$, holding at 206 $^{\circ}\text{C}$ for 7 min, 206 $^{\circ}\text{C}$ to 300 $^{\circ}\text{C}$ at 10 $^{\circ}\text{C}/\text{min}$. The total runtime was 30 min. The MS used electron impact ionization mode and full scan of m/z 40 – 560. The fatty acid components were identified by comparing their retention times with that of a fatty acid standard mix and confirmed by their mass spectra. Quantification was based on relative peak area. All analyses were performed in triplicates.

3.2.1.2 Determination of the Saturated and Unsaturated Fatty Acid Composition

^1H NMR was used to determine the saturated and unsaturated fatty acid compositions in the fat samples. In this method the fatty acids were determined as esterified fatty acid chains on a glycerol backbone, and quantified directly from the ^1H NMR spectra obtained by the correlation between the areas of a distinctive signal of each fatty acid and that of the glycerol moiety. The determinations of fatty acid composition by ^1H NMR spectroscopy were performed on a Bruker AVANCE 400 NMR spectrometer running at 9.4 T detecting the ^1H nuclei at 400.13 MHz. In this analysis, about 200 mg of the samples were directly transferred into 5-mm NMR tubes and dissolved to 500 μl with CDCl_3 with 0.05% TMS. The ^1H NMR spectra were obtained at room temperature (about

20 °C) by collecting eight averages, a relaxation delay of 1 s, a spectral width of about 7.0 ppm and 60 K data points, keeping a digital resolution of 0.05 Hz using a 5-mm multinuclear direct detection probe on the NMR instrument. Employing the exponential multiplication of the FIDs by a factor of 0.3 Hz prior to Fourier Transform with zero-filling to 60 K processed the ¹H NMR spectra. The relaxation delay to use for quantitative ¹H NMR spectra was measured by T1 measurements with the aid of the pulse sequence inversion recovery. All analyses were performed in triplicate.

3.2.2 Thermal Studies of Fat

Thermogravimetry and, differential scanning calorimetry are some of the techniques used in thermal analysis of materials. They have become extremely essential since give information about the mechanism of reactions, the kinetics, thermal stabilisation, phase transitions and heat of reaction of materials. In this study, thermogravimetry and the differential scanning calorimetry were used to investigate the change in sample behavior under controlled heating and cooling conditions. Both techniques provide fundamental information on the thermal characteristics and material properties of the samples. The thermal treatments employed were thermogravimetric analysis (TGA) and differential scanning calorimetric (DSC) methods. The TGA measures the decomposition pathway of materials with temperature change while the DSC measures the mechanism of the melting and cooling profiles of materials.

3.2.2.1 Thermal Decomposition of Fat

To determine the decomposition profile, about 10-14 mg of the fat samples were placed in a GPC platinum pan and loaded on the TGA balance. The system was purged with an inert gas (argon) and the sample analysed on a TA Instrument Q5000 IR Thermo

gravimetric Analyser (TGA) heating at a rate of 10 °C per minute from about 25 °C to a final temperature of 800 °C.

The thermogravimetric analysis is used to measure the change in weight of the material with change in temperature or time in a ordered atmosphere. The instrument principally measures the material's thermal stability, amount of filler in polymers materials; it can be used to measure the moisture and solvent content, and also the percent composition of constituents in a compound. A TGA analysis is performed by gradually raising the temperature of a sample. The weight of the material to be analyzed is determined by an analytical balance outside of the furnace. In the TGA, lost of weight is seen if the thermal event leads to the lost of volatile constituents, combustion processes may also involve mass loss, however physical transformations; including melting may not involve weight loss. A typical TGA thermograph shows a plot weight of sample with temperature or time. This gives information about the decomposition pattern of the material. Thermogravimetric method depends on an excessive level of accuracy in three measurements: mass change, temperature, and temperature change. The furnace may be set to a constant rate of heating, or to heat to obtain a constant weight loss with time. The TGA instrument can uninterruptedly weigh the sample during the heating to temperatures of up to 2000 °C. An increase in temperature leads to the decomposition the sample constituents and their various weight percentages measured.

3.2.2.2 Thermal Properties and Crystallisation Behaviour

The thermal properties of Shea butter and Allanblackia fats were investigated by a Perkin Elmer precise Diamond DSC with hyperDSCTM (Perkin Elmer, Inc. US) with a Refrigerated Cooling System (Perkin Elmer, Inc. US). Nitrogen flowing at a rate of 1

ml/min was used to purge the thermal analysis system. Indium (Perkin Elmer, Inc. US) was used to calibrate the instrument, azobenzene (Sigma Aldrich) and undecane (Sigma Aldrich) before data collection. The data obtained was processed by the instrument software (Pyris software, version 9.0.1.0174, Perkin Elmer, Inc. US.). The measuring principle of the DSC is to heat the sample with a linear temperature ramp and compare the rate of heat flow in the sample with that of unreactive material (reference sample). Any variations in the sample material linked with absorption or evolution of heat leads to the alteration in the differential heat flow this is then noted as a peak. The direction of the peak shows a heat loss (exothermic) or heat gain (endothermic) during the thermal event while the area under the peak is estimated to be directly proportional to the change in enthalpy. The DSC measurements give quantitative and qualitative information about physical and chemical changes involving processes leading to heat gain or heat loss or changes in heat capacity.

The DSC screens heat properties related to change in phase and chemical reactions as the temperature changes. Again, the difference in heat flow of the material and that of reference at the same temperature is recorded with change in temperature. The reference which is a unreactive material include alumina, or an empty aluminum pan. Since the DSC is at constant pressure, heat flow is equivalent to enthalpy changes:

$$\left(\frac{dq}{dT}\right)_p = \frac{dH}{dT} \quad \text{eqn 3.1}$$

where dH/dT is the heat flow measured in mcal sec^{-1} . The heat flow difference between the sample and the reference is:

$$\Delta \frac{dH}{dT} = \left(\frac{dH}{dT} \right)_{\text{sample}} - \left(\frac{dH}{dT} \right)_{\text{reference}} \quad \text{eqn 3.2}$$

During the endothermic process, heat is gained and that makes the heat flow to the material higher than the reference. Hence $\Delta dH/dT$ is positive. However, for the exothermic process, examples as crystallisation, oxidation reactions, and some decomposition reactions, heat is lost and that makes the heat flow to the material lower than the reference and so $\Delta dH/dT$ becomes negative.

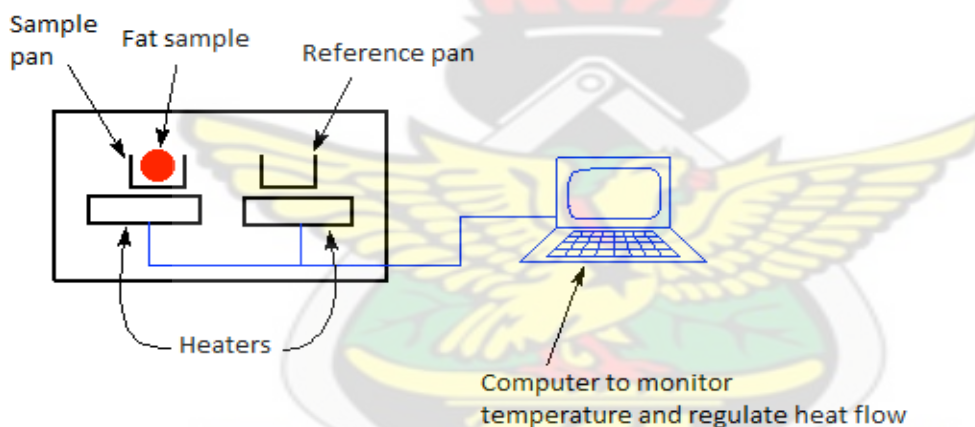


Figure 3-1: Schematic diagram of a Differential Scanning Colorimetric device, as the Diamond DSC from Perkin Elmer Instruments.

3.2.2.2.1 Melting and Cooling Profile the Fat Samples

The Allanblackia seed fat (AB-GH) and shea nut fat (SB-GH) sample was weighed (5-6 mg) into an aluminium pan and sealed. A hermetically sealed empty aluminium pan was used for the reference. Measuring the melting and cooling profiles, first of all the samples were heated rapidly from 30 °C to 70 °C at of 30 °C/min rate. The heated sample was held at the 70 °C for 10 mins to ensure completely melted fat and to destroy any nuclei

present. The samples were cooled to $-30\text{ }^{\circ}\text{C}$ at $10\text{ }^{\circ}\text{C}/\text{min}$ cooling rate and held for 10 min to ensure a fully crystallised sample. They were then heated again to $70\text{ }^{\circ}\text{C}$ at $10\text{ }^{\circ}\text{C}/\text{min}$ to investigate the melting profile of the fats.

3.2.2.2.2 Crystallisation at Different Cooling Rates

To determine the effect of cooling rate on crystallisation, the temperature was programmed by heating the sample rapidly from room temperature to $70\text{ }^{\circ}\text{C}$ at $30\text{ }^{\circ}\text{C}/\text{min}$ and held at the $70\text{ }^{\circ}\text{C}$ to erase any crystallisation memory. The samples were then subjected to cooling to $-30\text{ }^{\circ}\text{C}$ at $5\text{ }^{\circ}\text{C}/\text{min}$, $10\text{ }^{\circ}\text{C}/\text{min}$, $15\text{ }^{\circ}\text{C}/\text{min}$ and $20\text{ }^{\circ}\text{C}/\text{min}$ cooling rates. The DSC scans were collected on new samples to guarantee the same initial thermal pattern for all samples.

3.2.2.2.3 Isothermal Crystallisation by the DSC Method

The isothermal crystallisation patterns were obtained from a rapidly heated fat sample to $70\text{ }^{\circ}\text{C}$ and held for 10 mins to ensure a completely melted fat. The samples in melt were cooled to selected isothermal temperature of $-10\text{ }^{\circ}\text{C}$, $16\text{ }^{\circ}\text{C}$ and $20\text{ }^{\circ}\text{C}$ at a cooling rate of $10\text{ }^{\circ}\text{C}/\text{min}$ and held for 60 mins isothermal time. The various isothermal crystallisation profiles were obtained from the integration from the Pyris software, version 9.0

3.2.2.2.4 Isothermal Crystallisation Kinetics by the DSC Stop-and-Return Technique

The isothermal crystallisation was further investigated by the DSC stop-and-return technique [62]. From the same sample for the isothermal crystallisation analysis, the samples were reheated at different times from the various isothermal temperatures to $70\text{ }^{\circ}\text{C}$ at $10\text{ }^{\circ}\text{C}/\text{min}$, so as to record the melting profile of the components crystallised at the various isothermal periods. This procedure was repeated at varying time intervals to

investigate the crystallisation mechanism and their polymorphic transitions. Avrami theory was then applied to qualify the data obtained from the crystallisation process at 20 °C and 16 °C. Three kinetic parameters were derived from the fitting of the Avrami model. The kinetic parameters were the Avrami exponent (**n**), Avrami constant (**k**) and the half-time of crystallisation (**t**_{1/2}) obtained from the linearization of equation 3.3, where the logarithmic transformation of [-ln(1-X)] and t were plotted and the values of **k** and **n** calculated from the y-intercept and the slope respectively.

$$(1-X) = \exp^{(-ktn)} \quad \text{eqn 3.3}$$

where **X** is the fraction of crystal obtained at the time **t** during the crystallisation, **k** is the crystallisation rate constant and is dependent basically on crystallisation temperature, and **n** is the Avrami exponent, a constant associated the dimensionality of transformation. The value of **n** expresses the power dependence on the time of crystallisation and this is related to the processes governing the nucleation and the subsequent crystal growth mechanism during the crystallisation process [47]. The crystallisation rate constant **k**, represents a mixture of both nucleation and the growth rate constants, in relation to temperature change. The value obtained for **k** is relates directly to half-time of crystallisation (**t**_{1/2}) and the overall rate of crystallisation [185].

The relative amount of materials crystallised (**X**) with change in time were estimated from the integration of the isothermal DSC crystallisation curves. The areas under the crystallisation curves correspond to the total enthalpy of crystallisation, (**ΔH**_t). The relative amount of fat crystallised (crystal fraction) **X** at a given time was approximated

by the ratio of the partial enthalpy, (ΔH_x), at that time to the total crystallisation enthalpy. All measurements were taken in triplicates.

$$X = \Delta H_x / \Delta H_t \quad \text{eqn 3.4}$$

The half-time of crystallisation ($t_{1/2}$) gives the degree of the Avrami constant and this was estimated as follows

$$t_{1/2} = (0.693/k)^{1/n} \quad \text{eqn 3.5 [186]}$$

3.2.3 X-ray Diffraction (XRD) Analysis

X-ray diffraction pattern of crushed *Allanblackia* seed fat and shea nut fat were determined. The XRD data were collected using a Bruker D8 Discovery Powder X-ray Diffractometer, using a copper lamp ($\lambda = 1.52 \text{ \AA}$) to a voltage of 40 kV and 44 mA current. A 0.57 divergence slit, 0.57 scatter slit and 0.3 mm receiving slit were used. The wide-angle X-ray diffraction analysis (WAXD) was carried out by scanning the samples from 15° to 30° at $2^\circ/\text{min}$. The analysis was performed at 20°C and the XRD pattern obtained smoothed with a Fourier transformation by the X'pert high score plus software provided by the manufacturer. X-rays were passed through the samples and the scattered X-rays from the atoms gives the diffraction pattern, and subsequently provide information on the atomic arrangement inside the sample crystal network. The information about the arrangement of the atoms in the crystal network is interpreted according to the Bragg's Law.

$$n\lambda = 2d\sin\theta \quad \text{eqn 3.6}$$

The Bragg's Law describes the reasons for the cleavage faces of a crystal seem to reflect X-ray beams at a particular angle of incidence (theta θ), the wavelength λ of incident X-ray beam and n as an integer and d is the lattice spacing.

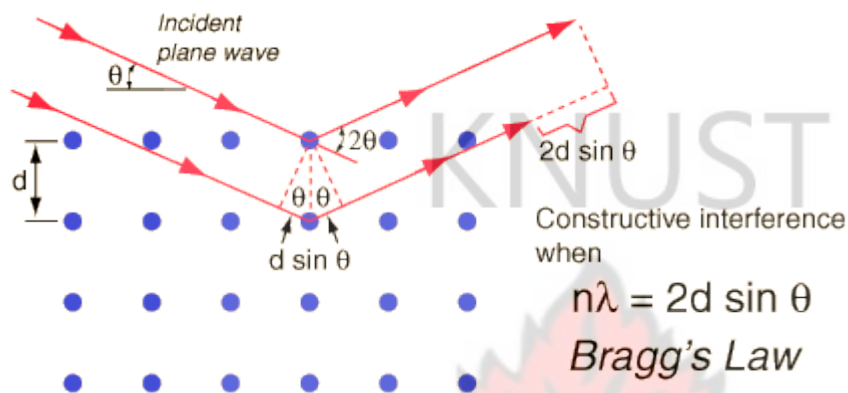


Figure 3-2: Schematic representation of the Bragg's Law in X-ray diffraction instruments.

3.2.4 Microscopic Analysis

The optical microscope uses the application of the visible light and lenses to enlarge images of smaller molecules. The light microscope generates an enlarged, comprehensive image of apparently undetectable objects or specimen. This established on the principles of transmission, absorption diffraction and refraction of light waves. The optical microscope may be used as the fundamental tool for phase identification.

The crystal morphology of Allanblackia seed fat and shea nut fat were studied at the selected fixed temperatures of 20 °C, 16 °C and -10 °C with an optical microscope, a Nikon OPTIPHOT-2 optical microscope fitted with a 5 megapixels DinoEye Eyepiece camera manufactured by Dino-Lite, Taiwan. From the melted (70 °C) samples, a

capillary tube was used to take a drop and transferred onto a microscope glass slide. The drop on the slide was covered with another slide to ensure uniform sample and desired thickness. After preparing the samples on the slides, the samples were brought to the required temperature in a controlled hood and three different visual field pictures were taken at a magnification of 4X

3.2.5 Preparations and Characterization of Colloidal Dispersions

3.2.5.1 Emulsion Preparation

By convention, oil-in-water (O/W) emulsions are produced through the homogenization an oil and an aqueous phase together by adding a surface active agent. Several different homogenizers such as high-shear mixers have used in the development of emulsions, high-pressure homogenizers and colloidal mills as well as ultrasonic homogenizers are available for the emulsification process. Choosing a specific type of homogenizer, the extent of homogenization and the conditions of its operations are dependent on the characteristics of the materials to be homogenized and the expected end product.

Dispersion of the fat particles in the aqueous phase in this study was done by two homogenizing methods to form an oil-in-water (O/W) emulsion with desired particle size viscosity. First the emulsions were prepared by continuous stirring of the melted fat/water/Tween 20/ sodium alginate mixture on a Heidolph MR Hei-Standard magnetic stirrer hot plate connected with the Heidolph temperature sensor Pt 1000 (Heidolph Instruments.co.uk) at 800 rpm and a 60 °C temperature. The second stage of the emulsion preparation was achieved by using a micro-tip of an ultrasonic cell disruptor

homogenizer (MisonixSonicator 3000, Misonix Inc. NY USA) for 6 minutes. No efforts were made to control the temperature during the homogenization process.

3.2.5.2 Allanblackia seed Fat/Water Emulsion

A known amount from 0.5 g to 2 g of Allanblackia seed fat, obtained as a solid fat, was placed in a screw top glass vial (50 mL) and heated to melting at 60 °C. Deionized water approximately 80 to 95 % of the final weight of dispersion was also carefully added to a separate glass vial. The pH was maintained at 7.0 with 5 mM sodium phosphate buffer. The fat-in-water emulsion systems were then developed by mixing the melted fat and the heated water at 60 °C with a magnetic stirrer hot plate at 1400 rpm for 10 mins after which an ultrasonic cell disruptor homogenizer (Misonix sonicator 3000) was used for 6 minutes intermittently at intervals of every 2 minutes to avoid over heating of samples.

3.2.5.3 Surfactant Stabilised Emulsion

In the preparation of surfactant stabilised emulsion, 0.1 g to 0.5 g (in the increment of 0.1) making up about 1 to 5 % of Tween 20 was added to the different concentration (5%, 10%, 15% and 20%) of melted Allanblackia seed fat and gently agitated at 60-65°C for 1 hr until completely mixed together. The oil/Tween 20 mixture was maintained at 60 °C temperature for 10 minutes after which it was then added to the heated (60 °C) deionized water and the mixture emulsified as described in section 3.2.5.2

3.2.5.4 Combined Surfactant/Biopolymer Emulsifier Mixture Stabilised Emulsion

In the preparation of the combined surfactant/biopolymer stabilised emulsions, different quantities of Tween 20 from 0.1 to 0.5 g (in the increment of 0.1) making up about 1 to 5 % of the total weight of final emulsion was added to the melted Allanblackia seed fat and

the mixture gently agitated at 60 - 65°C until completely mixed together and kept under continuous stirring at constant temperature of 60 °C and in a separate glass vial containing heated (60 – 65 °C) deionized water and a know quantity of sodium alginate 0.1 to 0.5 g (in the increment of 0.1) making up about 1 to 5 % of the total weight of final emulsion produced. The sodium alginate and water were agitated until there was complete dissolution of the sodium alginate salt in the water. The mixed system was continuously agitated at 60 °C for 10 minutes after which the oil/Tween 20 mixture was transferred to the water alginate mixture and the mixed solution emulsified as described in section 3.2.5.2

3.2.5.4 Emulsion Characterizations

The stability of the prepared (fat-in-water only, fat-in-water surfactant stabilised and fat-in-water combined surfactant/biopolymer stabilised) emulsions against aggregation such as creaming was assessed immediately after preparation and after 30 days of preparation. The occurrence of creaming was investigated by visual observation and measuring the volume fraction of creaming layer, the emulsion morphology and microstructure determined by microscopy and the dynamic light scattering instrument.

3.2.5.4.1 Determination of Volume Fraction of Creaming Layer

To measure the volume fraction of creaming layer, immediately after the preparation of the emulsions, 10 mL quantities were sampled into a 25 mL graduated glass vial and allowed to stay for 30 hours after which the extent of creaming assessed. The extent of separation (formation of a creaming layer) was determined by measuring the volume change in creaming layer formed expressed as the volume fraction of creaming ($V_{f_{Cr}}$) if

any, after the 3 hours period and also 30 days after the emulsion preparation. This was achieved by relating the observed volume of creamy layer (V_{Cr}) formed to the total volume of emulsion in vial V_{em} as adopted from Pichot, (2010) [187] with slight modifications.

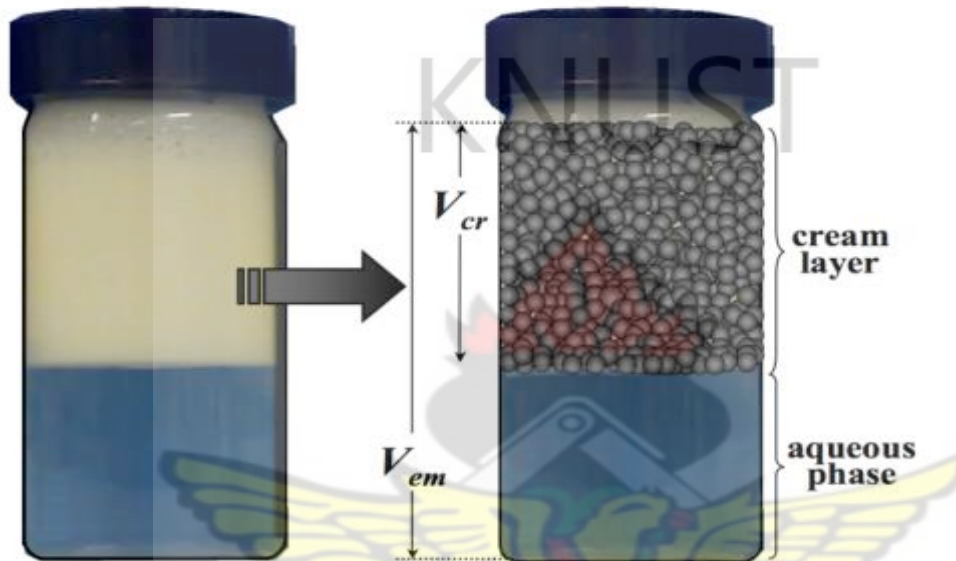


Figure 3-3: Sketch representing an emulsion structure: showing creaming and the particle distribution in the cream layer as adopted from Pichot (2010) [187].

The occurrence of creaming in the emulsion systems were quantified by the expression:

$$Vf_{Cr} = (V_{Cr} / V_{em}) \quad \text{eqn 3.7}$$

where V_{Cr} represents the volume of the top creaming phase and V_{em} the total volume of the emulsion.

3.2.5.4.2 Crystal Morphology and Microstructure of the Dispersed Fat Particles

The morphology and microstructure of the dispersed fat particles were studied by the Scanning Electron Microscope (SEM) and optical microscope. The SEM is used to

investigate the morphology and microstructure of materials. It works by scanning a focused electron beam over the surface of an object to create an image. As the electrons are focused on the object, the electrons interact with the object leading to the production of signals that are used to produce information about the composition, microstructure and morphology of the object.

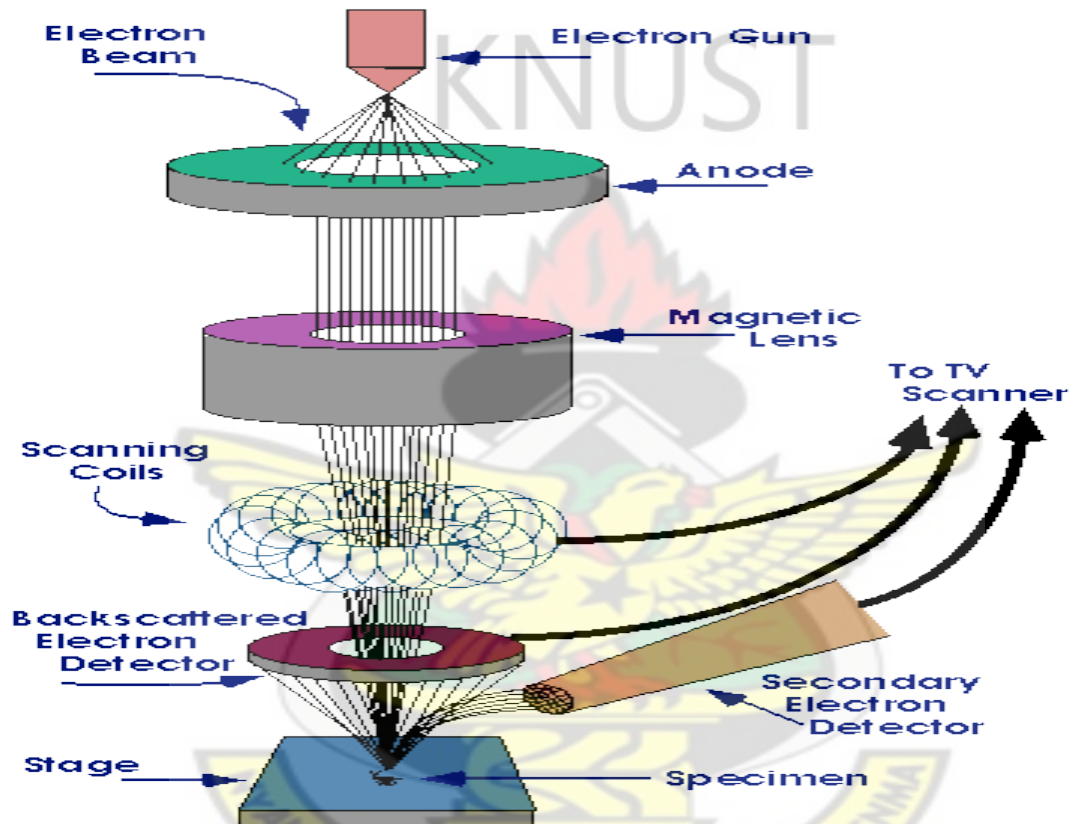


Figure 3-4: A Scheme representing operations scanning electron microscope [188]

In this study, emulsions prepared from the different fat/water combinations at varying Tween 20/sodium alginate ratios were diluted (1%) with deionized water and a drop placed on an SEM pin stub specimen mount. The images were captured by a field emission high resolution Scanning Electron Microscope Philips XL 30 FEG that operates both at low accelerating voltage (200 V) and high accelerating voltage (30 kV).

Again, two drops of 1% diluted emulsion solution were put on (75 mm by 25 mm) microscopy slides using a capillary tube and spreading it carefully on the microscope slide to avoid the development of any possible bubbles. The microstructure and droplet distributions observed with an optical microscope, a Nikon OPTIPHOT-2 optical microscope fitted with a 5 megapixels DinoEye Eyepiece camera manufactured by Dino-Lite, Taiwan. Three different visual field pictures were taken for each spotted sample at a magnification of 4X. In all about 100 different emulsions were analyzed.

3.2.5.4.3 Particle Size Measurements

The size of the fat particles size was measured using the Zetasizer Nano series from Malvern Instrument. The Zetasizer instrument measures the size of the particles by employing the Dynamic Light Scattering (DLS) technique, the mechanism of the instrument allows the measurement of particle sizes in the sub micron region [189]. The DLS detects the Brownian motion of the particles and link it with the size of the particles. As particles move randomly in dispersion, they interact with solvent molecules within which they move and this type of movement is termed the Brownian motion. As the particles move randomly the particle size is related to the speed of motion by the Stokes-Einstein equation.

The DLS instrument consists of six different components. The first is a laser which provides light to illuminate the particles inside the sample cell. As the laser beam passes through the sample, the beam of rays are scattered by the particles. It also has a detector which measures the intensity of the scattered light.

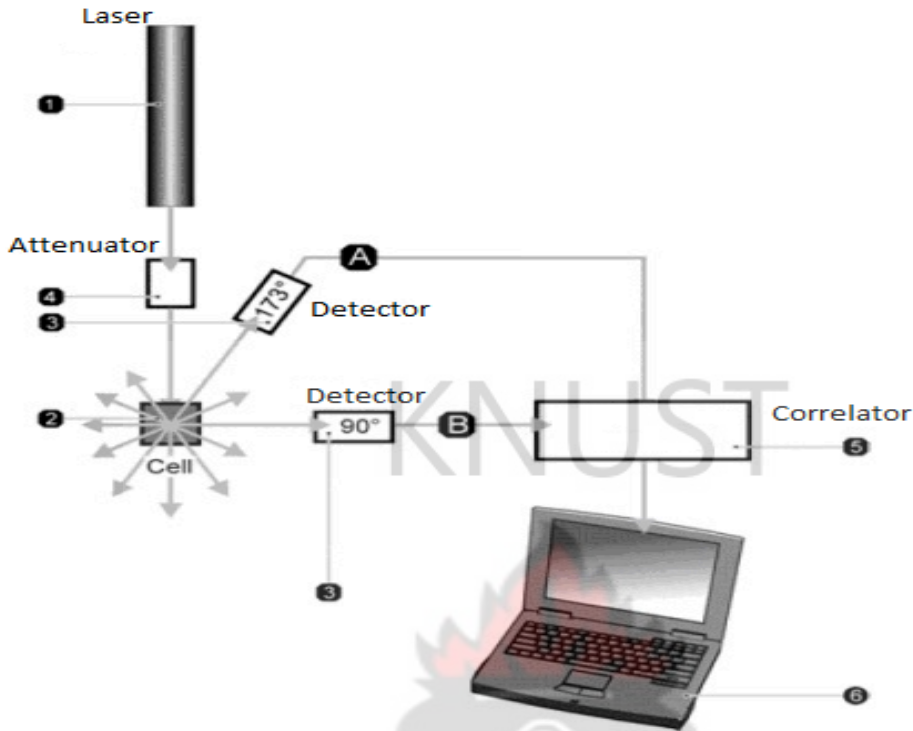


Figure 3-5: Schematic representation of the Zetasizer Dynamic Light Scattering (DLS) device, from Malvern Instruments.

The Zetasizer-Nano ZS instrument He-Ne laser with wavelength 632.8 nm gave the measured diameter of the particles. The instrument measures and display the mean diameter established on the intensity of scattered light. The emulsions prepared from the different fat/water ratios (5/95, 10/90, 15/85 and 20/80), in varying amounts of Tween 20 surfactant and also from different ratios of Tween 20/sodium alginate mixtures were diluted to concentration of 1% and their pH maintained at 7.0. Small volumes of the diluted dispersions were placed in a standard optical glass cuvette 10 x 10 x 45 (mm) and the cuvette and its content placed in the Zetasizer-Nano ZS instruments for analysis.

The software of the Zetasizer-Nano ZS instrument uses the refractive index of the

dispersant and its viscosity, and the refractive index of the dispersed phase and finally its absorption. The Malvern Instrument provides a list of properties of the most common materials used as dispersant and dispersed samples. The refractive index of water was selected as 1.32 and that of fat particles as 1.46. At the 25 °C measurement temperature, the viscosity of water was given as 0.8870 mPa-s with the absorption of the fat particles given to be 0.001.

3.2.5.5 Determination of the Rheological Parameters of the Emulsions

Two different rheological analysis, namely; steady state shear stress-shear rate analysis and dynamic (oscillatory) analysis were studied by using a strain controlled advanced rheometric expansion system (ARES). ARES works as a mechanical spectrometer that subjects a sample to either a sinusoidal or steady shear strain deformation. It measures the force spent by the sample in response to this shear strain.

In measuring the rheological parameters, the force of deformation is expressed as the stress or force per unit area. The level of deformation subjected to a material is known as the strain, which may also be expressed as sample displacement relative to pre-deformation sample dimensions. The sample deformation can be either simple shear or linear deformations. The ARES instrument measures the deformational energy and the viscosity of the material and relate it to Hooke's and Newton's laws respectively. The steady shear testing employs constant rotation to operate strain. When a steady shear rate is reached, the shear stress is measured as a function of the shear rate. The stress-to-shear-rate ratio yields the steady shear viscosity. Measurements are typically made around a varied series of shear rates to study the shear rate dependence of the sample.

For viscoelastic materials, the phase angle shift (δ) between stress and strain occurs among the elastic and viscous boundaries. The viscoelastic material generates a stress signal which can be divided into two components namely: an elastic stress (σ') that is in phase with strain, and a viscous stress (σ'') that is in phase with the strain rate ($d\delta/dt$) but 90° out of phase with strain. Occasionally, the elastic stress may be termed as in-phase while that of the viscous stress may be termed as out-of-phase. The elastic stress determines the level at which the substance shows characteristic property of an elastic solid. In much the same way, the viscous stress determines the level at which the substance acts as an ideal fluid. The viscous and elastic stresses can be linked to material characteristics over the ratio of stress to strain, or modulus. Thus, the ratio of the elastic stress to strain is referred to as the elastic (or storage) modulus (G'), which represents the ability of a material to store energy elastically. The ratio of viscous stress to strain is termed the viscous (or loss) modulus (G''), and this measures the material's capacity to give off energy. Additionally, the complex modulus (G^*) also measures the total endurance of the substance to deformation. If these measurements are made using a linear geometry instead of shear geometry then the letter E is used to represent the modulus, instead of G. In some cases it is suitable to define the ratio of the material strain to material stress. This is known as compliance, and is represented by a J in shear testing, and a D in linear testing. As in case of modulus values it is possible to define both elastic (J' or D') and viscous (J'' or D'') components to the complex compliance (J^* or D^*). The tangent of the phase angle shift of stress and strain also known as $\tan \delta$ measures the damping character of the material.

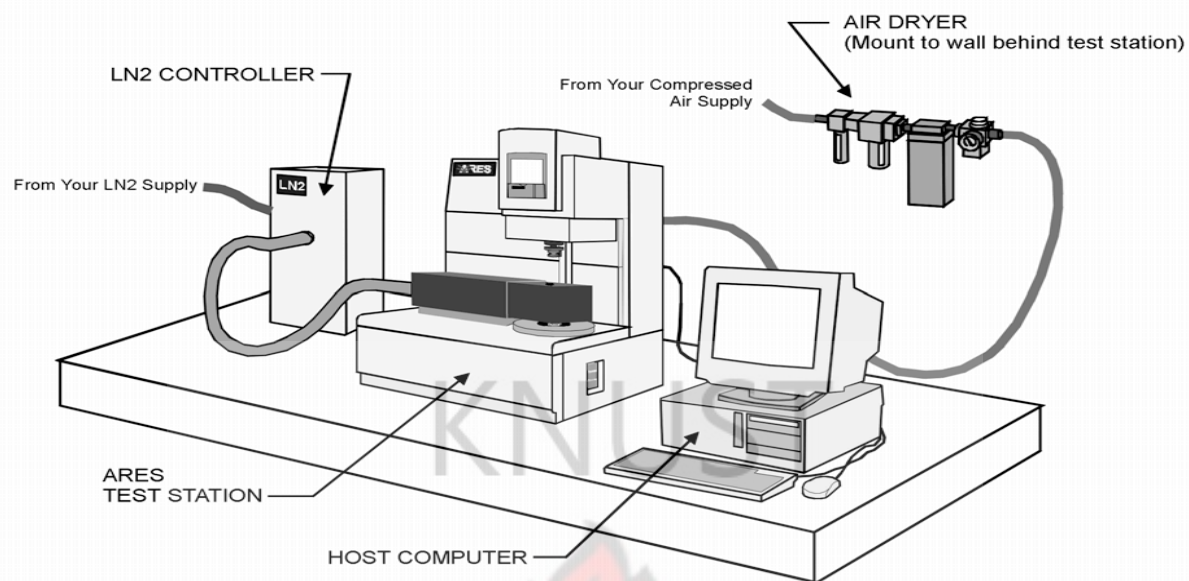


Figure 3-6: A Sketch of the ARES Viscometer [190]

To study the long-term physical stabilisation of the emulsions, three different batches of the emulsion systems stored for 30 days containing different amounts of fat/water ratios (5/95, 10/90, 15/85 and 20/80) in the presence of increasing Tween 20 and sodium alginate contents were analyzed with respect to their rheological properties

1. The long-term stability of emulsions with respect to changing concentration of sodium alginate whiles Tween 20 and fat content are held constant,
2. The long-term stability of emulsions with respect to changing concentration of Tween 20 with sodium alginate and fat content held constant.
3. The long-term stability of emulsions with respect to changing fat content with Tween 20 and sodium alginate concentration held constant on the rheological properties of the emulsions.

3.2.6 Preparation and Efficiency of Encapsulated Particles

3.2.6.1 Preparation of the Encapsulated Particles

The solid fat encapsulated Sudan orange dye particles (ESODP) were prepared by adding about 0.2 g of the Sudan orange dye to an already melted 1.5 g (constituting 15/85) solid fat at 65 °C and the emulsion prepared by the simple homogenization method as described in the previous section 3.2.5.2.

3.2.6.2 Encapsulation Efficiency

The efficiency of encapsulation of the solid fat-in-water emulsion was estimated by evaluating the loading capacity of the emulsion system, the extent of leaching of the encapsulated dye and the swelling properties of the encapsulated emulsion.

3.2.6.2.1 Determination of Amount of Dye Encapsulated

To determine the amount of dye entrapped in the solid fat-encapsulated sudan orange dye particles, the ESODP were air dried to remove any traces of water molecules remaining on the surface of the molecules. After obtaining completely dried particles, the particles were transferred into an air dried beaker and ethanol added to dissolve the entrapped dye and subsequently measured using a Varian's Cary 5000 UV-Vis NIR spectrophotometer, equipped with a Cary series WinUV software 2002. The instrument has a wavelength range of 175-3300 nm and the wavelength accuracy of 190-900 nm. The average dye incorporated was estimated according to the Lambert-Beer law. Expressed as a logarithmic transformation between the transmission **T** of light throughout the material, the product of the absorption coefficient of the substance **a** and the distance the light travels through the materials **l**. This is expressed as

$$T = I/I_0 = e^{-al} = e^{-\epsilon lc} \quad \text{eqn 3.8}$$

where I_0 and I are the intensities of the incident light and the transmitted light respectively, a is the absorption coefficient of the substance, ϵ is the molar absorptivity and c the molar concentration.

The transmission expressed as the absorbance becomes

$$A = -\log(I/I_0) \quad \text{eqn 3.9}$$

Therefore when the absorbance becomes linear with the concentration, the equation is expressed as follows

$$A = \log I_0/I = \epsilon lc \quad \text{eqn 3.10}$$

$$\text{Therefore } A = \epsilon lc \quad \text{eqn 3.11}$$

A wavelength of 450 nm was employed in the detection of the Sudan Orange dye absorbance. About 0.20 g of the Sudan orange dye was added to an already melted 1.5 g of the vegetable fat and the mixture homogenized as explained earlier to complete the encapsulation process. The loading capacity was estimated as follows;

$$\text{Percent encapsulation (\%E)} = \frac{\text{Actual amount of dye loaded (g)}}{\text{Original amount of dye used in the experiment (g)}} \times 100 \% \quad \text{eqn 3.12}$$

3.2.6.2.2 Leaching Studies

The extent of leaching of the encapsulated dye was determined by placing 0.36 g of the dried ESODP samples on a filter paper and stored at 21°C for 24 hours to monitor any leakage of the internal phase onto the filter paper used for the analysis. Again in another study, a 0.38 g portion of the same dried sample kept on the filter paper then incubated at

37 °C for 1 hour after which its weight measured every 30 minutes for 6 hours. Percent leaching (%L) was expressed as;

$$\%L = \frac{W_i - W_f}{W_i} \times 100 \% \quad \text{eqn 3.13}$$

where W_i is weight of initial sample before incubation and W_f represent weight of samples after incubation. All weights were measured in grams.

3.2.6.2.3 Swelling Studies

The effect of swelling of the encapsulated solid fat emulsions by absorbing water or other ingredients in the presence of an aqueous solution was investigated as a function of time. About 0.23 g of the dried ESODP samples were soaked in deionized water on a watch glass for one hour after which the samples were filtered, air dried and weighed every 5 minutes. Care was taken in handling the swollen particles to avoid the possible occurrence of breakage and erosion. The percent swelling was calculated as

$$\% \text{ Swelling} = \frac{(\text{wet weight} - \text{dry weight})}{\text{dry weight}} \times 100 \% \quad \text{eqn 3.14}$$

3.2.6.3. Characterization of the Solid Fat Encapsulated Sudan Orange Particles

3.2.6.3.1 Particle Size and Size Distribution

The average size of dye-loaded ESODP was measured by the Malvern DLS technique. Dilutions of the ESODP suspension were prepared with deionized water and subsequently sonicated for 60s to ensure well-dispersed particles before the

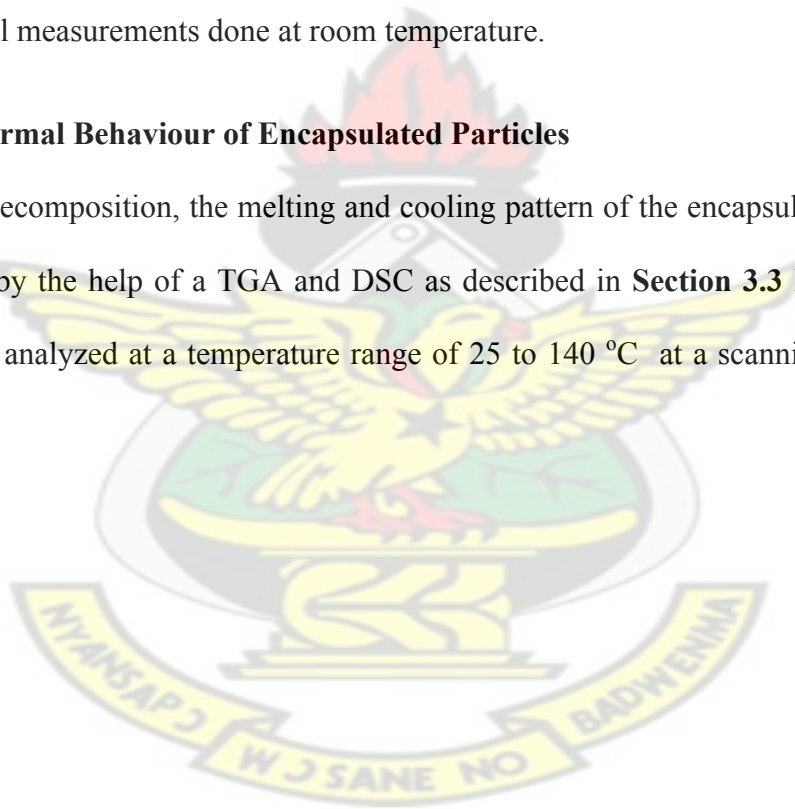
measurement. Optical microscopy was used to investigate the particle size distribution and to understand the microstructure of the encapsulated particles formed.

3.2.6.3.2 XRD Analysis

The ESODP samples were carefully pressed into the sample holder to ensure there were no pockets of lumps present. The samples were pressed to achieve a smooth flat surface. The ESODP were exposed to an X-ray diffraction (Bruker D8, Discover) using a monochromatic Cu K α radiation ($\lambda=0.154\text{nm}$) in the range of 5° to 50° at a scanning rate of $2\theta/\text{min}$. All measurements done at room temperature.

3.2.6.3.3. Thermal Behaviour of Encapsulated Particles

The thermal decomposition, the melting and cooling pattern of the encapsulated particles were studied by the help of a TGA and DSC as described in **Section 3.3** For DSC, the samples were analyzed at a temperature range of 25 to 140°C at a scanning rate of $10^\circ\text{C}/\text{min}$.



CHAPTER 4

Chemical Constituents and Thermal Behaviour of Allanblackia Seed Fat and Shea Butter

The use of vegetable fats as raw materials in many food products and other industrial applications has gained interest due to the excellent properties they exhibit, such as high production, cheap, stability to thermal oxidation and their plastic behavior at room temperature. Knowledge of the fatty acids composition and the consequence of these fatty acids on thermal behaviour of vegetable fats is important. Since it gives information on the functionality of the fat substance. However, it is also imperative to note that the physico-chemical properties of any vegetable oil or fat depend on the climatic conditions and the vegetation of the place where it is produced.

In this chapter, the aim of the study was to determine and compare the fatty acid composition of two vegetable fats of tropical origin namely: Allanblackia seed fat (AB-GH) and Shea nut fat (SB-GH), and to determine the effect of the fatty acid composition on their physical behaviour. The fatty acid constituents were determined by analytical methods and the physical properties were investigated with change in temperature. The melting and crystallisation profile as well as the occurrence and/or existence of polymorphism (different crystal phases) and polymorphic transitions and the crystal morphology of the fat substances are discussed.

4.1 Determination of the Fatty Acid Constituents of Allanblackia Seed Fat (AB-GH) and Shea Butter (SB-GH)

4.1.1 GC/MS Analysis of AB-GH and SB-GH

Table 4-1 shows the fatty acid composition of AB-GH and SB-GH. From the data obtained, it is clear that both AB-GH and SB-GH contains stearic and oleic acid as their major fatty acid components. AB-GH contains about 58 % saturated fatty acids of which about 57 % is stearic acid, with palmitic acid and arachidic acid constituting 1 % of the total fatty acid composition. AB-GH also contains about 42 % unsaturated fatty acids which is basically made of oleic acid (42 %). SB-GH was shown to consist of about 51 % saturated fatty acids, which is made up of about 47 % stearic acid and 4 % palmitic and arachidic acids. SB-GH also contains about 49 % unsaturated fatty acids consisting of about 45 % oleic acid and 4 % linoleic acid. The high-saturated fatty acid content in both AB-GH and SB-GH accounts for their characteristic solid state at room temperature and their melting at elevated temperatures.

Table 4-1: Levels of fatty acid composition in shea butter and Allanblackia fat determined by the GC/MS

ID	C _{16:0}	C _{18:0}	C _{18:1}	C _{18:2}	C _{20:0}	T.Sat,	T.Unsat.
AB	0.81±0.23	56.93±0.61	42.16±0.16	N/D	0.11±0.30	57.78±0.14	42.16±0.15
SB	2.83±0.45	47.14±0.74	44.58±0.13	4.20±0.12	1.09±0.21	51.06±0.40	48.78±0.24

Allanblackia seed fats contains about 45 – 58 % stearic acid, 40 – 51 % oleic acid and an iodine value of about 40 which shows the amount of unsaturation present in the fat or oil

[80, 81, 191]. Shea butter is also reported to contain 36 % stearic acid, 50 % oleic acid and about 59 % iodine value [192].

Fatty acids in fats and oils are found as esters on a glycerol backbone forming the triacylglycerol (TAG) content of the particular fat or oil and this TAG accounts for about 95-97 % of the fat or oil composition [34, 193]. The physical and chemical properties of the fats are mainly influence by the fatty acids and their TAG compositions and this is used to characterize and identify fats and oils [45]. Therefore from fatty acid data (Table 4-1) it can be deduced that the randomisation of the fatty acids over the glycerol backbone may lead to the formation of saturated-saturated-saturated (SSS) triacylglycerols, saturated-saturated-unsaturated (SSU) triacylglycerols, saturated-unsaturated-unsaturated (SUU) triacylglycerols, and unsaturated-unsaturated-unsaturated (UUU) triacylglycerols. The presence of the different composition of the fatty acids in the TAG structure accounts for the characteristic chemical and physical behaviour of the fats. The European Food Safety Authority has reported that *Allanblackia* seed fat contains 69 % stearic-oleic-stearic (SOS) and 23 % stearic-oleic-oleic (SOO) triacylglycerides (TAGs) [194]. Shea butter has also been reported to contain about 10 % trioleic (OOO), 35 % stearic-oleic-oleic (SOO), 40 % stearic-oleic-stearic (SOS) and 8 % palmitic-oleic-stearic (POS). It also contains other TAGs made up of linoleic acid, arachidic acid in minor quantities [195]. The difference in the quantity and fatty acid profile of the shea butter affords it a wide variety of TAG composition in the fat sample. The structure of the fatty acids in the TAG content of the various fats gives it a complex chemical structure, which may have a direct relation with the thermal behaviour of the *Allanblackia* seed fat

and shea butter fat samples. From the above results and discussions, the thermal properties of both samples were studied using the differential scanning calorimetric techniques in order to establish the characteristic profile of Allanblackia seed fat and shea butter fat with heat flow and the results recorded and discussed in section 4.3. This knowledge can be used to prove the importance of shea butter and Allanblackia seed fat in industrial applications.

4.1.2 ¹HNMR Analysis of AB-GH and SB-GH

The ¹HNMR spectra obtained for AB-GH and SB-GH gave chemical shifts (ppm) representing saturated and unsaturated fatty acids. The spectra also showed the presence of the glycerol protons confirming the existence of the fatty acids as esters of glycerol. Details of the results are shown in Figure 4.1 and Table 4.2. For this study fats from the Allanblackia seeds and shea nuts were dissolved in chloroform-D and the ¹HNMR spectra obtained. The percentage fatty acids were calculated using standards and computing (integration) the area under the curves. From the observed chemical shifts, AB-GH is shown to contain about 60 % saturated fatty acids and 40 % unsaturated fatty acids while SB-GH contains 50 % saturated acids and 50 % unsaturated acids. Earlier studies have examined the degree of unsaturation of different vegetable oils and fats using ¹H NMR spectroscopy [196–198] and the results obtained compares favourably with results obtained for both shea nut fat and the Allanblackia seed fat.

Table 4-2: Chemical shifts obtained from the AB-GH and SB-GH fats corresponding functional groups of saturated and unsaturated fatty acids

AB-GH fat samples		
Signal	Chemical Shift (ppm)	Functional group
a	0.85-0.90	-(CH ₂) _n -CH ₃ (terminal methyl group)
b	1.21-1.37	-(CH ₂) _n (methylene group)
c	1.55-1.65	-OCO-CH ₂ -CH ₂ - (acyl chains)
d	1.97-2.05	-CH ₂ -CH=CH- (allylic group)
e	2.27-2.33	-OCO-CH ₂ - (acyl chains)
f	4.10-4.32	-CH ₂ OCOR (glyceryl group)
g	5.23-5.28	>CHOCOR (glyceryl group)
h	5.31-5.35	-CH=CH- (olefinic protons)
SB-GH fat samples		
a	0.79-0.92	-(CH ₂) _y -CH ₃ (terminal methyl group)
b	1.19-1.39	-(CH ₂) _n (methylene group)
c	1.57-1.70	-OCO-CH ₂ -CH ₂ - (acyl chains)
d	1.97-2.06	-CH ₂ -CH=CH- (allylic group)
e	2.17	=CH-CH ₂ -CH= (bis-allylic group)
f	2.26-2.35	-OCO-CH ₂ - (acyl chains)
g	4.08-4.35	-CH ₂ OCOR (glyceryl group)
h	5.22-5.28	>CHOCOR (glyceryl group)
i	5.31-5.40	-CH=CH- (olefinic group)

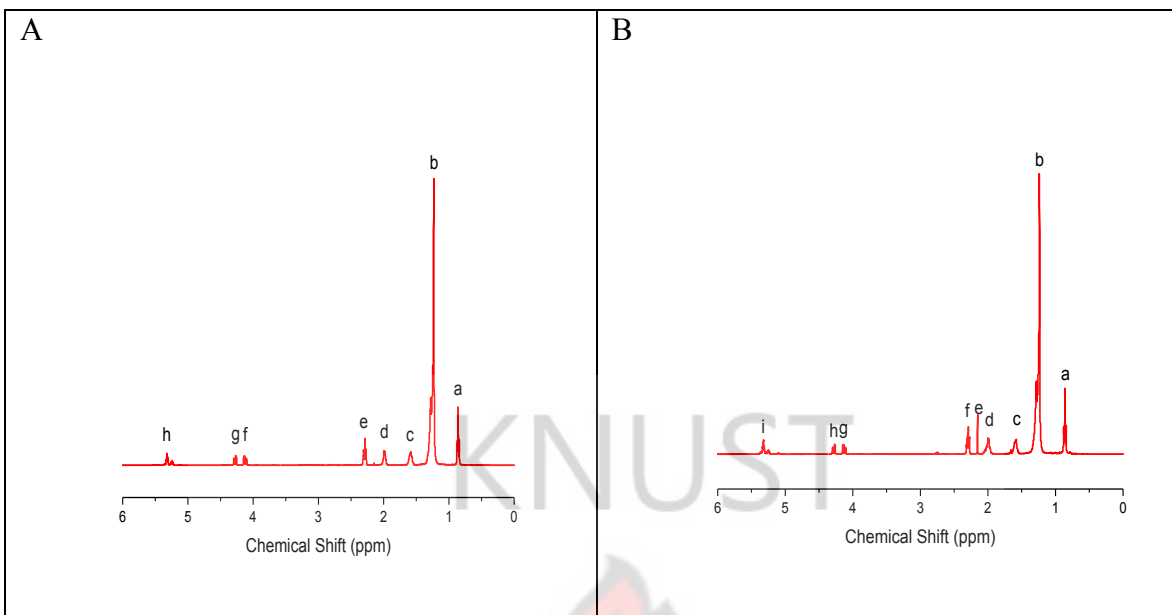
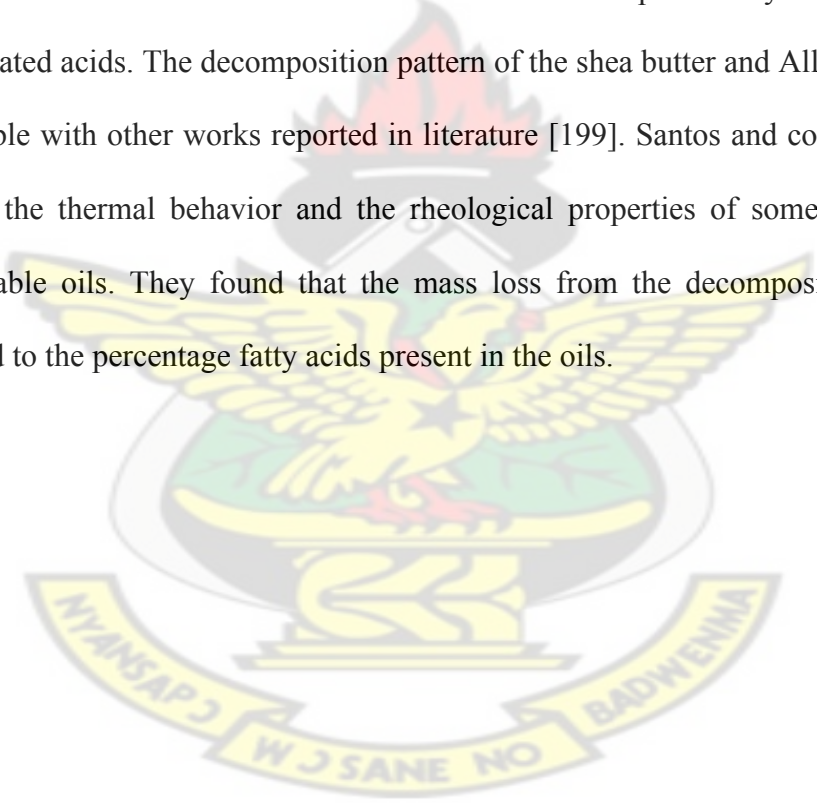


Figure 4-1: ^1H NMR spectra showing the saturated and unsaturated fatty acids of: (A) AB-GH and (B) SB-GH

4.2 Thermal Decomposition of AB-GH and SB-GH by Thermogravimetric Analysis (TGA)

The decomposition profile obtained from the TGA shows a two-step decomposition pattern for SB-GH and a single step decomposition profile for AB-GH (Figure 4.2). It was observed that both samples were thermally stable up to 200 °C after which SB-GH began to decompose from the initial weight of 12.84 mg to about 11.30 mg (change in weight 1.54 mg), which represents the composition of about 12% of the total fat sample at temperatures from 200 to 350 °C. The initial 12 % weight loss in the SB-GH maybe attributed to the loss of highly unsaturated fatty acid component. The unsaturated fatty acid compounds have low melting point and hence during the heating process they easily vapourise and hence decompose. After this initial decomposition step, SB-GH gave second step of decomposition, which was rapid and ended at about 450 °C at which there

was a complete decomposition of all the fat samples. The first step is attributed to the decomposition and evaporation of molecules of TAGs obtained from low melting fatty acids such as the polyunsaturated and monounsaturated acids (OOL and OOO) which may be present in the SB-GH while the second and major step is attributed to the TAGs consisting of saturated and monounsaturated (SOO, SOS and POS) fatty acids which, from the GC/MS analysis constitute the major chemical composition. The decomposition profile of AB-GH samples gave primarily a single step and this attributed to the simple fatty acid constituents of the AB-GH which is made up of only saturated and monounsaturated acids. The decomposition pattern of the shea butter and Allanblackia fat are comparable with other works reported in literature [199]. Santos and coworkers [52] also studied the thermal behavior and the rheological properties of some commercial edible vegetable oils. They found that the mass loss from the decomposition process corresponded to the percentage fatty acids present in the oils.



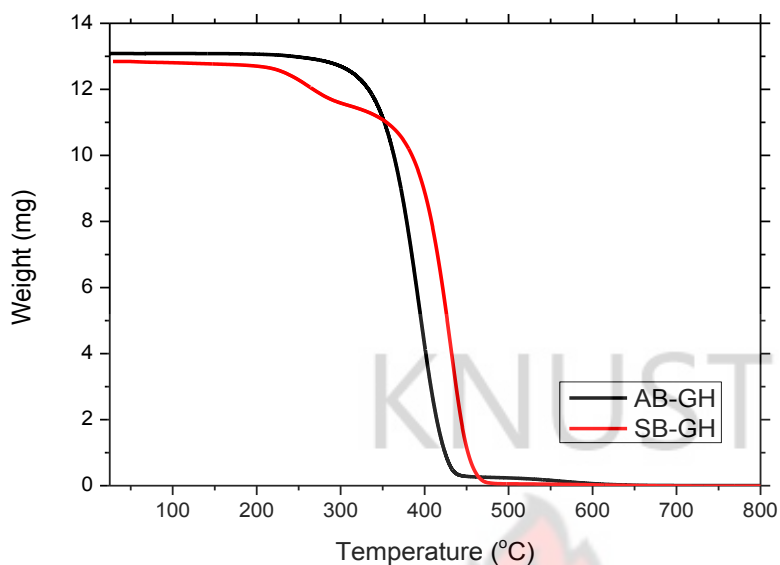
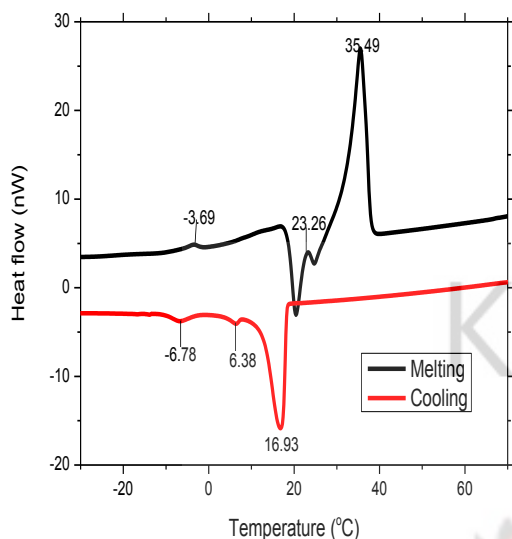


Figure 4-2: Thermal decomposition profile of AB-GH and SB-GH obtained from the TGA starting at 25 °C to 800 °C at 10 °C/min

4.3 Crystallisation and Melting Behaviour by the DSC Method

Change in heat flow is an important phenomenon in the use of fat in industrial processes. A change in temperature directly affects the handling of fat and in their subsequent applications and hence affects their product performance [45]. In this study, the melting and cooling profiles of AB-GH and SB-GH were investigated as the samples were heated to 70 °C and cooled to -30 °C at 2 °C/min cooling rate. The effect of the heat change on their physical properties were recorded as the melting and cooling curves and shown in Figure 4.3.

A



B

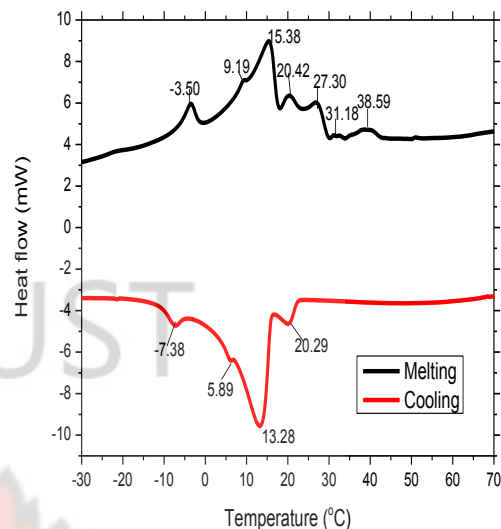


Figure 4-3: Melting and cooling profile of fat samples obtained at temperatures between -30 °C to 70 °C at 2 °C per minute from DSC: (A) melting and cooling curves of AB-GH and (B) melting and cooling curves of SB-GH

During the heating process, AB-GH and SB-GH showed different melting profiles. The peaks observed under the AB-GH curve, were a peak at a temperature and enthalpy variation of -3.69 °C and 0.94 J/g respectively. This peak may represent the melting temperature of TAGs (such as UUU) consisting of low melting fatty acid components and may be present in small quantities in the *Allanblackia* seed fat hence their smaller magnitude. After the first melting endotherm, an exothermic peak appeared at about 21 °C temperature. This observation may result from recrystallisation of some of the high melting components, which began melting at low temperatures. After the recrystallisation process, the fats began to melt again showing a major peak at 35.49 °C temperature and 83.35 J/g enthalpy change and may account for the existence of TAGs made up of high melting fatty acids as their major components. The melting profile of *Allanblackia* can be

explained as follows: during the heat flow, low melting TAGs which could consist of triunsaturated (UUU) fatty acids such as trioleic acid (OOO) or possibly TAGs made up of diunsaturated monosaturated (UUS) fatty acids, such as dioleic monostearic acid (OOS) is melted out first. This is followed by the recrystallisation of some of the high melting TAGs, which had initially co-melted with the low melting components at the lower temperatures. As the temperature increases, a larger proportion of the high melting TAGs which could consist of disaturated monounsaturated (SSU) fatty acids such as palmitic oleic stearic acid (POS), distearic oleic acid (SOS) crystallizes out and since the *Allanblackia* seed fat contains basically SOO and SOS TAGs [194], the melting endotherms observed may be attributed to these TAGs. The melting profile of SB-GH showed multiple endotherms, a total of about seven different endothermic peaks were observed (figure 4-3B). These peaks were of different shapes and sizes and correspond to different individual fat components of different chemical structure and/or the occurrence of polymorphic transformations. The shea butter fat from the GC/MS analysis was observed to contain three different saturated fatty acids namely palmitic acid, stearic acid and arachidic acid as their major fatty acid component which are of different carbon chain lengths. The existence of trioleic (OOO), stearic-oleic-oleic (SOO), stearic-oleic-stearic (SOS), palmitic-oleic-stearic (POS) and other TAGs made up of linoleic acid and arachidic acid in minor quantities accounts for the different melting peaks profiles.

The cooling profiles observed under both AB-GH and SB-GH, however, were not complex as compared to their melting profiles. *Allanblackia* seed fat gave three exothermic peaks. A sharp and narrow peak occurred as the first and main exotherm, at

temperature of 16.93 °C and with an enthalpy change of -45.42 J/g. This peak may correspond to the observed major melting component and may be attributed to TAGs made up of large amounts of the high melting saturated fatty acids such as the SOS TAG. The shape of the first crystallization peak occurring at the 16.93 °C (narrow and sharp) gives an indication of pure composition of the TAG present. The presence of two other crystallisation peaks at temperature and enthalpy of 6.33 °C and -1.08 J/g, -6.78 °C and -2.97 J/g respectively can be attributed to sequential crystallisation of TAG compounds of different low melting fatty acids compositions. The SB-GH cooling curve showed four crystallisation peaks at temperatures 20.29 °C, 13.28 °C, 5.89 °C and -7.38 °C with enthalpies -1.76 J/g, -37.83 J/g, -0.29 J/g and -1.45 J/g respectively. In general, peaks observed under the SB-GH cooling curve were broad and shaped similar to the peaks observed in their melting profiles. This is because as the fat sample is being cooled from the melt, the high melting components, which showed a high melting temperature crystallizes first, followed by the low melting and subsequently the lowest melting components as observed by Che Man and Tan (2002) [45] and Vereecken et al (2010) [200]. The broad peak also indicates the presence of different varieties of TAG compounds. Comparing *Allanblackia* and shea butter, it can be seen that both their melting and cooling profiles are different, shea butter has more fatty acid constituents compared to the *Allanblankia* seed fat hence their behaviour under the different thermal treatments. The observed difference in the melting and cooling curves within the same fat sample has also been discussed by other researches in this area [60, 200]. The appearance of broad peaks as seen in Figure 4-3B, is a characteristic of the presence wide range TAGs compounds. This observation was reported by Liu et al (2013) [47] in their

preparation of specialty fats from beef tallow and canola oil by chemical interesterification. There is also the possibility of dilution of the crystallisation temperatures as a result of the association with TAGs of high melting point with TAG of low melting point. The triacylglycerol structure has a direct effect on the shape and appearance and temperature of the crystallisation peak [201]. To further understand the cooling process of shea butter and Allanblackia seed fat, the crystallisation processes at different cooling rates were also studied and the results presented in section 4.4 below.

4.4 Thermal Behaviour with Increasing Cooling Rates

In this section, the DSC was used to follow the thermal events that occur during the crystallisation process of the fat samples at different cooling rates. The mechanism in this process is that, as the melted fat is cooled from a temperature above its the crystallisation temperature of a particular high melting component, the high melting fat, which is kinetically favoured at that temperature quickly forms crystals. When the favoured component is completely crystallized the next available component that is kinetically favoured also crystallizes. This process continues until the final crystallisation temperature is reached. This leads to the growth of diverse crystalline phases containing the maximum concentration of the kinetically favoured component at the particular crystallisation temperature [45]. The strategy employed in this study was to investigate the behaviour of the subdivided exothermic regions of SB-GH and AB-GH at increasing cooling rates. Knowledge of their behaviour under different cooling rates will help in processing Allanblackia and shea butter into different industrial products.

In the DSC analysis, the melted samples were cooled from 70 °C to -30 °C at different scanning rates of temperature program (i.e. 5, 10, 15 and 20 °C/min) and the results obtained are shown in Figure 4-4. The cooling curves are presented according to their cooling rates with their exothermic peaks identified as a, b, c, and d. The thermal data obtained from the crystallisation curves are detailed in Table 4-3. All crystallisation temperatures are quoted and refer to the maximum peak temperatures.

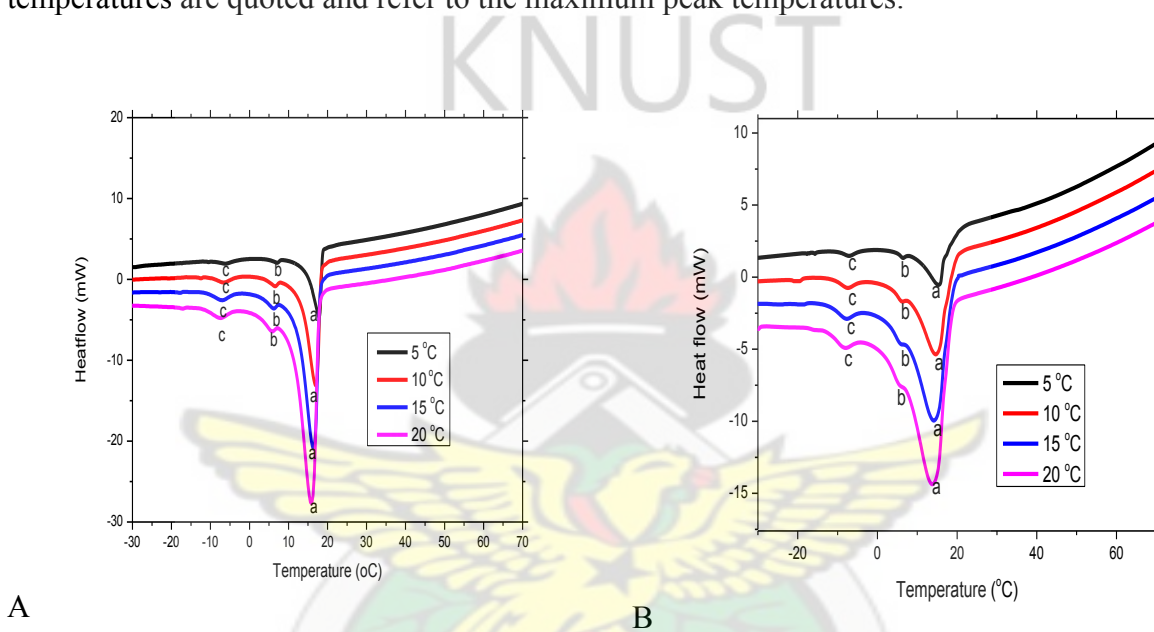


Figure 4-4: DSC crystallisation profile of AB-GH and SB-GH from -30 °C to 70 °C at different cooling rates: (A) crystallisation profiles of AB-GH with change in cooling rates from 5 °C/min to 20 °C/min and (B) crystallisation profile of SB-GH with change in cooling rates from 5 °C/min to 20 °C/min

From the DSC investigations, increasing cooling rates leads to the crystal peaks of the observed cooling curves increased in size and their crystallisation temperatures also show a marginal decrease. As shown in Figures 4-4A and 4-4B, SB-GH and AB-GH gave three main crystallisation peaks under all the different cooling programs. For the AB-GH

curve, the three main peaks primarily consisted of a major peak occurring at a temperature between 15 to 20 °C and 14 to 16 °C for the SB-GH. The two other peaks even though smaller in magnitude, occurred in the melting profile for all the cooling regimes. They occurred at temperatures between 5 to 10 °C and -10 to -5 °C respectively for both AB-GH and SB-GH. Detailed results of the crystallisation temperatures and their respective enthalpy change are presented in Table 4-3.

Table 4-3: Temperature (Tp) and the enthalpy change (ΔHc) recorded for AB-GH and SB-GH at increasing cooling rates

Peaks		a		b		c	
	Cooling rates (°C/min)	Tp (°C)	ΔHc (J/g)	Tp (°C)	ΔHc (J/g)	Tp (°C)	ΔHc (J/g)
AB	5	17.82±0.02	58.93±0.29	7.13±0.02	0.88±0.02	-6.07±0.03	1.46±0.13
	10	16.98±0.02	59.68±0.36	6.49±0.01	1.17±0.01	-6.57±0.01	1.86±0.04
	15	16.38±0.01	59.89±0.22	6.03±0.12	1.21±0.08	-6.97±0.01	2.06±0.13
	20	15.80±0.16	60.27±0.36	5.67±0.05	1.31±0.06	-7.52±0.00	2.23±0.01
SB	5	15.57±0.03	49.69±0.48	6.43±0.03	0.30±0.89	-6.93±0.14	2.26±0.03
	10	14.96±0.01	66.34±0.15	6.08±0.10	0.47±0.06	-7.49±0.10	2.45±0.02
	15	14.61±0.01	66.59±0.03	5.65±0.01	0.55±0.08	-7.84±0.13	2.60±0.03
	20	14.28±0.16	67.21±0.16	5.34±0.05	0.76±0.09	-8.19±0.01	2.79±0.17

The occurrences of these peaks may be as a result of the fractional crystallisation of different melting TAG components. The major exothermic peak is as a result of the

presence of TAGs consisting of trisaturated (SSS) or disaturated mono-unsaturated (SSU) fatty acid, which is then followed by the low melting components as, discussed under the melting and cooling profiles.

As the sample is cooled at the slow rate (5 °C/min), the kinetics of the crystallisation process also proceeds at a slower manner. TAGs of comparable chain lengths have time to interact with each other, co-crystallise and subsequently fractionate. At the 5 °C/min cooling rate, there is the formation of more discrete peaks and a reduction in overlapping of peaks. Again, at the slower rates the TAG molecules have enough time and hence the occurrence of molecular rearrangement and organisation. This leads to the formation of pure and few crystals. However, the fast cooling forces the molecule to organise into crystals under conditions with limited time to ensure the association of only pure compounds. Quicker cooling usually results in high amount of compounds crystallising with lower purity. At the high cooling rates such as moving through 10 °C/min to 20 °C/min, the rapid formation of high solid fat content at the particular crystallisation temperature leads to the cooling of higher melting TAGs more rapidly and therefore forming an under cooled initially crystallised solid which is produced within the liquid phase of the melted fat. This phenomenon leads to a rapid rise in viscosity of the melted fat, thus limiting mass transfer, this forces the fat molecules to crystallise rapidly into mixed crystals. The mixed crystals merges leading to the broadening cooling peaks as seen in Figures 4-4A and 4-4B. This observation is in agreement with other studies in the literature that as the melted fats and oils systems are crystallised under rapid cooling conditions, higher melting TAGs will be rapidly undercooled and initially crystallised, developing a solid within the liquid phase and the triacylglyceride chains which come

into crystalline lattice require a certain relaxation time, resulting in lag-period compared to the cooling process and it increases with increasing cooling rate [202]. The locations of the exotherms were influenced by the rate of the crystallisation process as the peaks shift to lower temperatures with the increasing cooling rates. The shift of crystallisation peaks to the lower temperatures is caused by the reduction in crystallisation temperatures due to the dilution of high melting TAGs by low melting TAGs. The dilution occurs when the high melting TAGs co-crystallise with the low melting components due to the fast cooling program [45]. The decrease in crystallisation temperature with increasing cooling rates has also been discussed as related to the formation of stable polymorphic forms. The presence of polymorphic forms was discussed by Campos and coworkers [203], in their work on the effects of cooling rate on the structure and mechanical properties of milk fat and lard. They observed that with slow cooling rate, the β polymorph which is present crystallises at higher temperatures while at a rapid cooling rate the metastable β' polymorph which is present crystallises at lower temperatures. Again, at a slow cooling rate, there is enough time to permit the occurrence of molecular organisation; this results in the availability of fewer crystals of higher purity being obtained and thereby presenting a smaller peak size [47, 204]

As observed from the above discussions, it can be stated that change in the rate of cooling of the fat is an efficient way to effect the crystallisation process and effectively change the crystal network structure and their subsequent physical functionality. But, the degree of change in the physical structure cannot be significantly attributed to the change in the cooling. Therefore further work to understand the effect of marginal changes of the physical functionality due to change in rate of cooling is important.

4.5 Isothermal Crystallisation Studies

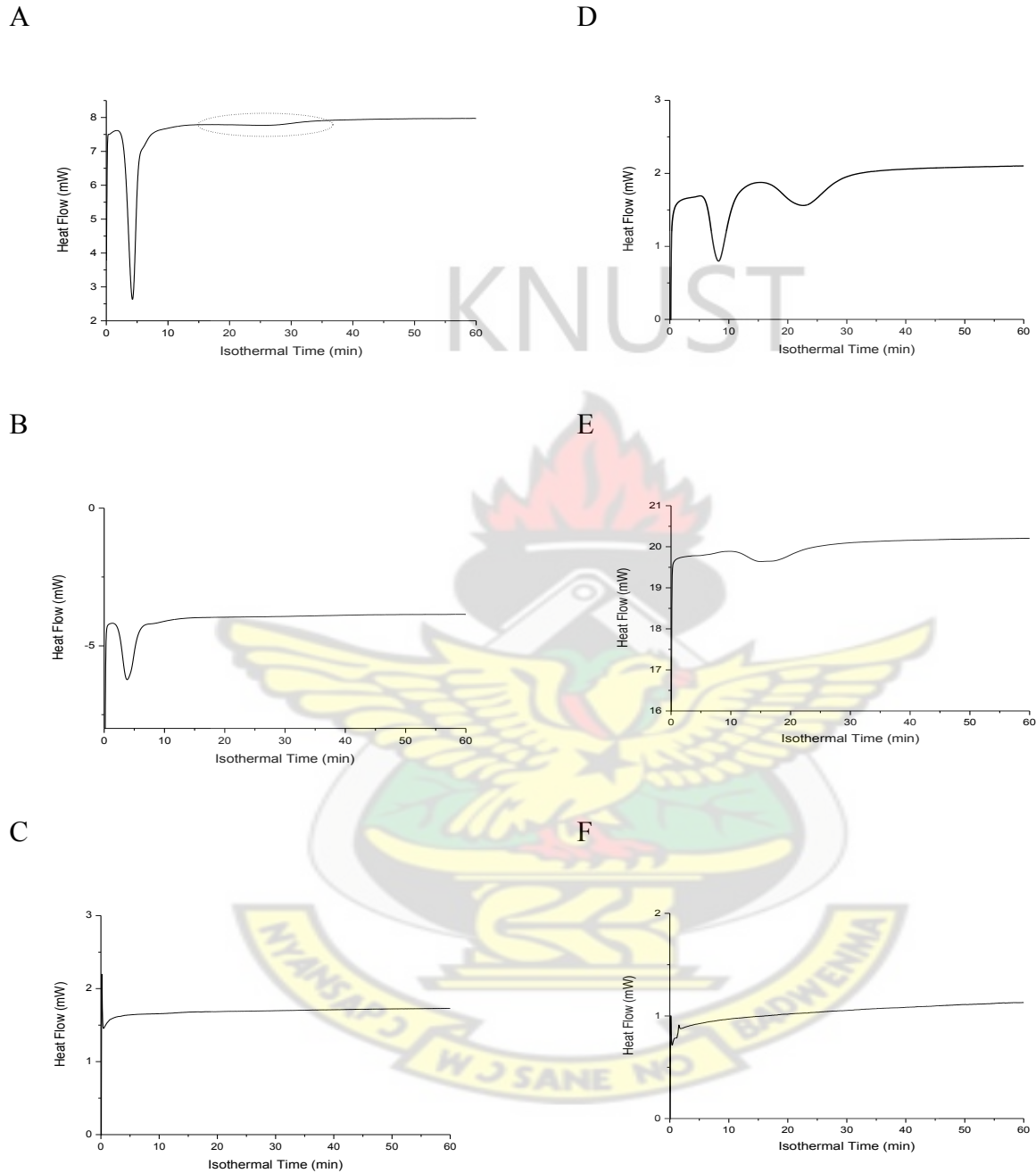


Figure 4-5: Crystallisation profiles of AB-GH and SB-GH at isothermal time of 60 minutes for the DSC experiments: (A) crystallisation profile of AB-GH at 20 °C, (B) crystallisation profile of AB-GH at 16 °C, (C) crystallisation profile of AB-GH at -10 °C, (D) crystallisation profile of SB-GH at 20 °C, (E) crystallisation profile of SB-GH at 16 °C and (F) crystallisation profile of SB-GH at -10 °C

The isothermal properties of the crystallisation process of the fat samples were further studied. The isothermal crystallisation curves of SB-GH and AB-GH as obtained from the DSC analysis at three crystallisation temperatures (-10 °C, 16 °C and 20 °C) are shown in Figure 4-5.

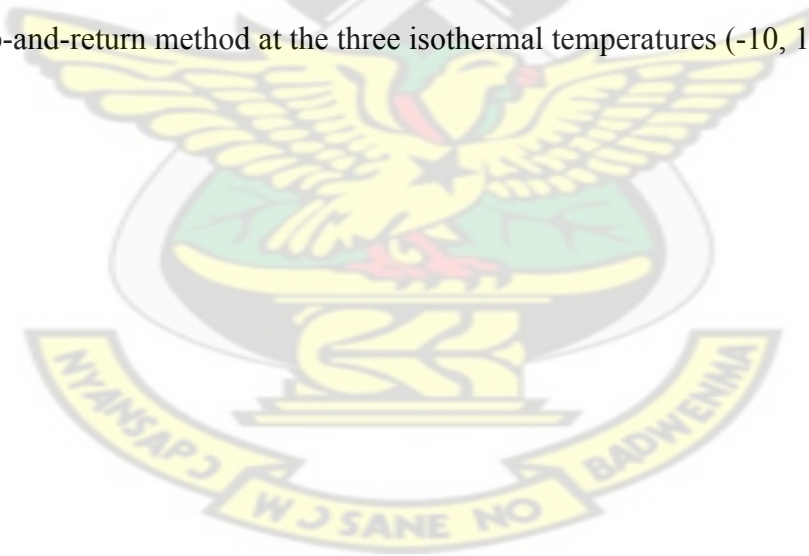
AB-GH at 20 °C, (Figure 4-5A) gave two crystallisation peaks at the end of the isothermal period (60 mins). The first peak, which is narrow and sharp, occurred within 10 mins into the isothermal time, after which a second very broad and slightly visible peak occurred from between 20 to 40 mins isothermal time. At 16 °C, AB-GH gave a single peak between 1 to about 7 mins isothermal time. The peak at -10 °C isothermal temperature was observed to have started the crystallisation during the cooling process. Considering shea butter in the isothermal process, two peaks were also observed at between 5 to 15 mins and between 15 to 25 mins isothermal time for the 20 °C temperatures. Single peaks were observed at isothermal temperature of 16 and -10 °C., with the peak for the -10 °C occurring during the cooling period. The two peaks at the 20 °C for both AB-GH and SB-GH may be as a result of sequential crystallisation of fractions of the fat with different melting properties. During the study of cooling patterns of SB-GH and AB-GH in this study, it was observed that both samples gave exothermic peaks around the 20 °C temperature, which was concluded to be as a result of the presence of high melting TAGs which could result from mixtures of high melting saturated fatty acids and monounsaturated fatty acids such as trisaturated (SSS) and disaturated monounsaturated (USS). The presence of such mixtures during the isothermal period receives enough time by which the components are able to separate into pure components hence exhibiting different crystallisation peaks during the isothermal period.

The occurrence of the peaks can also be potentially due to a rapid formation of a metastable polymorph (an α fat crystal) at the start of the isothermal process which was then followed by a transition into more stable β or β' crystals [60]. The narrow and broadened nature of the peaks corresponds to the different TAG mixtures found under the 20 °C temperature. A broad peak corresponds to wide range of different TAG compounds while a narrow peak shows a more pure and low range TAG compounds. At -10 °C, the peaks for both SB-GH and AB-GH were all observed to have occurred during the cooling process. Even though this peak may be attributed to the low melting fat components, their quantification is difficult as during the isothermal period the appearance of the peak does not begin from the baseline after the cooling process and therefore cannot be integrated. Also from the curves obtained for both SB-GH and AB-GH, it can be seen that the crystallisation to some extent started during the time of cooling and this indicated by the measured heat flow after the cooling step and before the presence of the crystallisation peaks. In light of the above discussion the stop-and-return technique was used to investigate the isothermal crystallisation kinetics of the fat samples and the results presented and discussed in section 4.6.

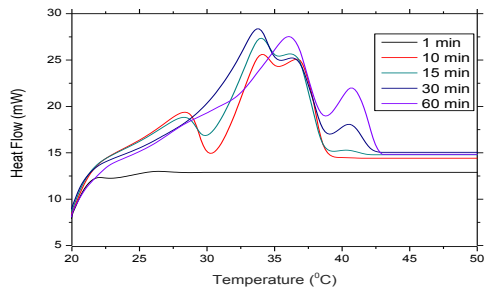
4.6 Studies of Crystallisation Kinetics by DSC Stop-and-Return Method

In order to understand the phase transition behaviour that occurs during the crystallisation process of Allantoin and shea butter, the stop-and-return technique of DSC was employed to study their crystallisation kinetics. The DSC that has been reported to be sensitive, high-resolution and extensive method by several authors in the study of crystallisation kinetics of fats and oils [62] was used in this study. The method is established from measuring the heat flow obtained as the crystallisation progresses and

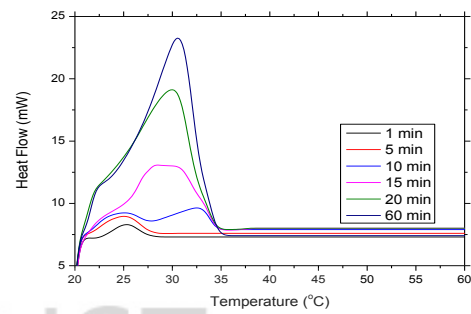
results in phase or polymorphic transitions. During the isothermal period, sometimes the crystallisation takes place immediately the cooling process begins or the occurrence of a polymorphic transformation simultaneously with the crystallisation process. This occurrence makes it difficult to integrate the cooling curves obtained. In this regard, the DSC stop-and-return method is used in this work to study the crystallisation kinetics. From the isothermal crystallisation curves, the stop-and-return method was used to further investigate the crystallisation process. In this study, the crystallisation process were interrupted at different times and re-melted, to find the melting profile, the crystallised fat at a particular time of the isothermal crystallisation period. The obtained melting peaks were integrated, to give an idea of the amount of the crystallised fat. Figures 4-6 from A to F shows the melting endotherms of SB-GH and AB-GH obtained from the stop-and-return method at the three isothermal temperatures (-10, 16, 20 °C).



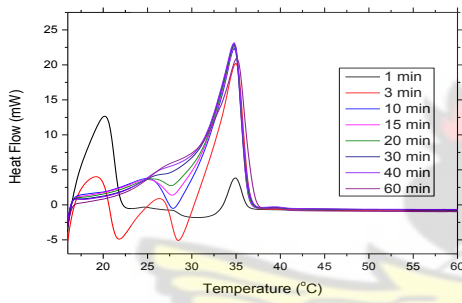
A



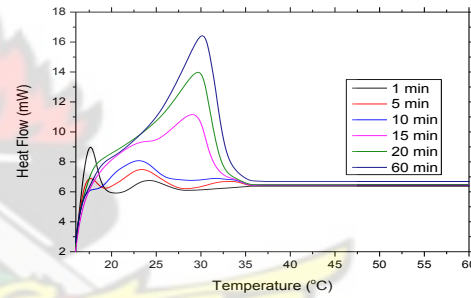
D



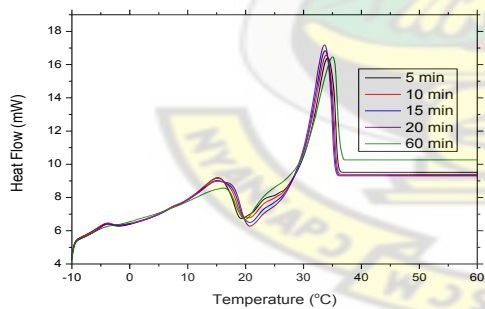
B



E



C



F

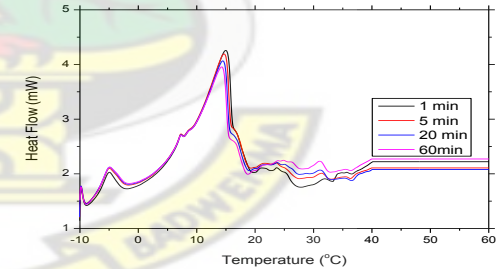


Figure 4-6: Melting profile at every minute during the isothermal period where crystal fractions are melted under the DSC stop-and-return method (A) melting curves of AB-GH at 20 °C (B) melting curves of AB-GH at 16 °C (C) melting curves of AB-GH at -10 °C (D) melting curves of SB-GH at 20 °C (E) melting curves of SB-GH at 16 °C (F) melting curves of SB-GH at -10 °C isothermal crystallisation temperatures

The melting curves at the isothermal temperature of 20°C for AB-GH (Figure 4-6 A) gave a profile which consist of the appearance of two peaks within the first and third minutes during the isothermal process, as the crystallisation process progresses (10 to 40 mins); there is the appearance of a third peak after which a two peak profile is seen at the 50 to 60 mins of the isothermal time. The peaks were observed to be closely associated with each other and also some of the peaks did not return to the baseline. The shapes and sizes of the peaks were not regular and appeared to change as the isothermal time increases. This profile gives an indication that at the 20 °C, temperature, several events occur in the crystallisation of the *Allanblackia* seed fat, firstly there is possibility of co-crystallisation of low melting TAGs with the high melting TAGs at that temperature which may result in the appearance of the two melting peaks immediately the crystallisation started. Since vegetable fats are multifaceted mixtures of TAGs, their crystallisation processes may lead to the growth of many kinds of crystal as a result of polymorphism or association growth of several crystal types [205]. The occurrence of polymorphic transformations is observed with melting peaks appearing at lower temperatures, some of the peaks disappeared after some time or shifted to higher temperatures as the crystallisation process progresses. The above observations were compared with data for the evolution of peak maxima of the melting profiles (Figure 4-7A).

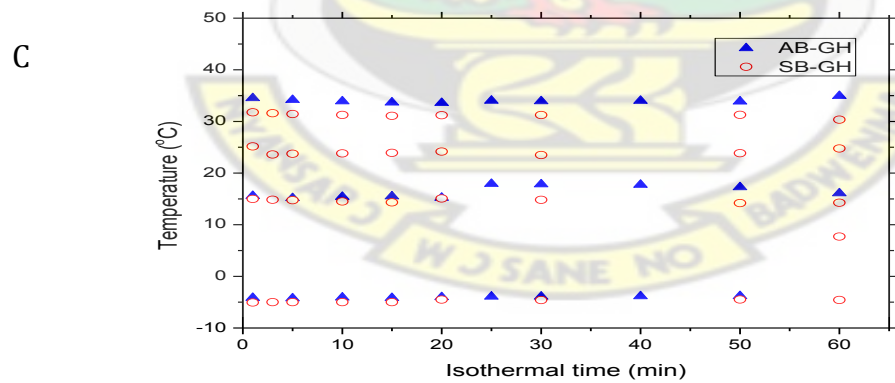
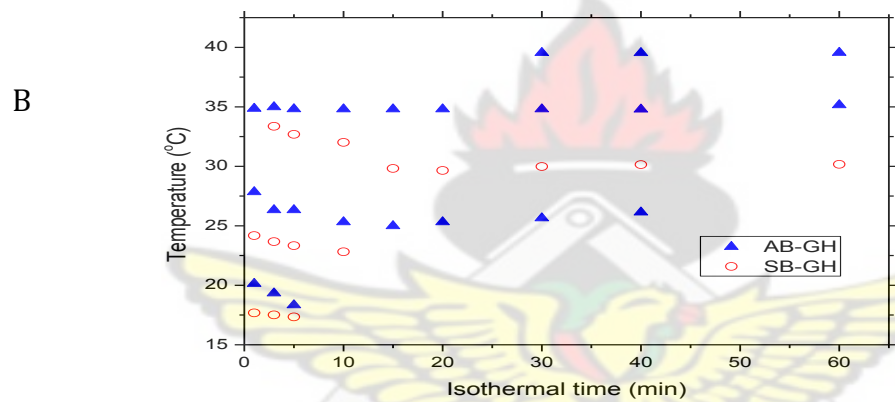
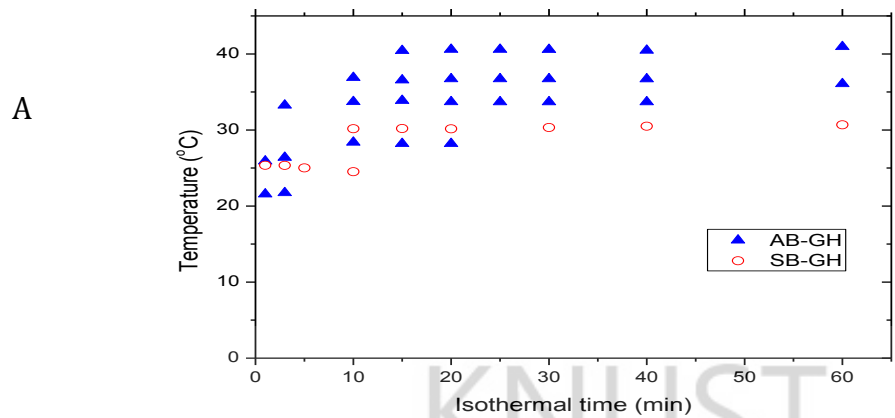


Figure 4-7: Comparison of the appearance of the melting peaks at different time recorded from the stop-and-return DSC experiments: (A) peaks maxima profile of AB-GH and SB-GH at 20 °C (B) peaks maxima profile of AB-GH and SB-GH at 16 °C and (C) peaks maxima profile of AB-GH and SB-GH at -10 °C crystallisation temperatures

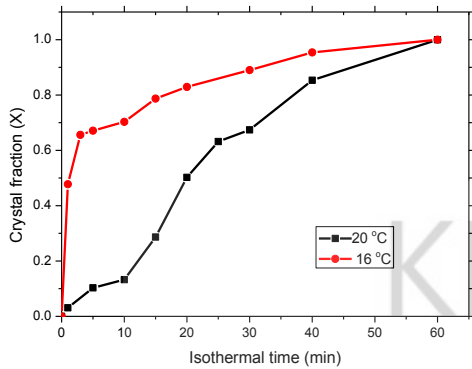
The peak maxima profile confirms the observation of two peaks initially (1 min) after which three peak profiles were observed from the 5th to the 40th minute and finally a two peak profile (50th to 60th min). Peaks occurring at low melting temperatures disappeared while the high melting ones remain as the process progresses. The disappearance of these low melting peaks may confirm the formation of less stable polymorphs of fat components which is later transformed into a more stable polymorph, since different polymorphic forms show different melting points and enthalpies at a given time [206]. Additionally, from the data obtained, the high melting peaks which appear later during the isothermal process and remain unchanged may also be attributed to the sequential crystallisation of different fat components. At the isothermal temperature of 16 °C, AB-GH gave rather complex melting endotherms from the stop-and-return method. At the start of the isothermal period (from 1 min), multiple endothermic peaks were observed and the peaks seem to present a more regular shape while the magnitude of their sizes change as the period of the isothermal process changes. There is also the presence of exothermic peaks in the melting profiles, this also changes as the isothermal time increases and finally disappears at high isothermal periods. The observed exothermic peaks in the melting profile during the isothermal crystallisation process is as a result of recrystallisation which represents a transition of a less stable polymorph to more stable form. This is because the more stable polymorph has a higher melting temperature [207]. During the crystallisation process, these components begin to melt when the temperature is applied but this changes as they quickly recrystallize to form a stable polymorph. This exothermic peak disappears as the isothermal period increases. The size of the third major peak increases. This observation is confirmed by the peak maxima graph, which displays

the appearance of three peaks within the first 10 mins of the isothermal process at a melting temperature of about 15 – 35 °C. The low melting peaks disappear as the isothermal process progresses and this is an indication of the existence of polymorphic transformations. The existence of the high melting peaks, which do not change with change in isothermal time, shows the existence of fractional crystallisation of different fat components at the 16 °C isothermal temperature. At -10°C, Allantblackia seed fat gave a three melting endotherm, which remained constant as the crystallisation process progressed to the end. This phenomenon may be attributed to the sequential crystallisation of different fractions as a result of the existence of distinct TAG components within the crystal fats formed at that temperature. This behaviour was also confirmed by the appearance of peak maxima.

At 20 °C, the SB-GH curves from the stop-and-return method gave essentially one melting endotherm. This peak showed a smaller magnitude in initial stages of the crystallisation process. As the time increased the magnitude of the peaks also increased. This behaviour was also seen in the appearance of peak maxima profile. This phenomenon can be described as systematic crystallisation processes where the fats during the crystallisation process initially forms crystal nuclei which gradually result in an increase in the crystal size as the isothermal process progresses. In general, the change in shape and increase size of the endotherms as the isothermal time increases, can be explained by the fact that at the initial stages, there is the formation of a nucleus of fats which can be formed from TAGs with low melting profile in a process termed as nucleation, which crystallises and serve as a seed for crystallisation and subsequently the formation of molecular aggregates and its subsequent crystal growth [61, 200]. The

melting temperature of the nuclei changes as the crystal nucleus begins to experience the formation of molecular growth after which there is no significant change in temperature of the melting endotherms. At 16°C, SB-GH gave 3 melting peaks within the first 5 mins of the isothermal crystallisation process. As the process progresses the low melting peaks disappears resulting in only one peak left at the end of the isothermal period of 60 mins this observation also compares with the peak maxima profile. This behaviour is best described as the occurrence of a less stable polymorph which gradually disappears into a more stable polymorph as the crystallisation progresses. At -10 °C, shea butter showed a multiple melting profile. The size and shape of the peaks were consistent from the initial stage of the crystallisation processes to the end of the isothermal period of 60 mins. This is due to the occurrence of sequential crystallisation of low melting TAGs. The observed multiple melting peaks which was confirmed by the maximum peak appearance profile may be attributed to the fact that shea butter contains large amount of oleic acid and some linoleic acid, both of which are low melting fatty acids. According to Stapley et al (2006) [64], in their study of the thermodynamic and kinetic aspects of fat crystallisation, they found that the melting and crystallisation properties of TAGs are very sensitive and so even small difference in fatty acids composition may result in significant change in the crystallisation profile. Therefore at the -10 °C, the TAGs present may consist of different combinations of these low melting fatty acids hence the observed profile. There can also be the possibility of the existence of co-crystallisation of some of the high melting TAGs which might have crystallised out during the cooling process and this explains the nature of the isothermal crystallisation peaks observed at the -10 °C temperature for both SB-GH and AB-GH (Figures 4-6C and F).

A



B

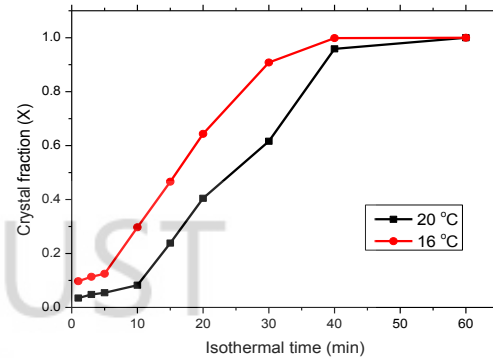


Figure 4-8: Formation of crystal fractions as a function with time: (A) Fractions of crystals formed for AB-GH at 20 and 16 °C crystallisation temperatures and (B) Fractions of crystals formed for SB-GH at 20 and 16 °C crystallisation temperatures

Plotting the amount of crystal fractions formed with time during the isothermal period as shown in Figure 4-8, it was observed that the crystallisation process in SB-GH at both 20 °C and 16 °C (Figure 4-8 B) were much slower at the initial crystallisation stage (first 10 mins) as compared with *Allanblackia* at the same time for the 20 °C and 16 °C (Figure 4-8 A). The nature of the crystallisation process can be characterised by two main processes, namely, the nucleation process and crystal growth. During the cooling process, the components that experience a kinetically favoured temperature initially crystallise out therefore forming a solid crystal within the melted fat. This initial solid fat formed becomes the seed (nucleus) on which further crystallisation occurs. This initial crystallisation is termed the nucleation stage and the building up of any further crystallisation is termed the crystal growth [208]. The shape of the crystal fraction verses time curves can give important information of the crystallisation mechanism of the fat

samples [208]. From the curves, it can be seen that the samples showed an s-shaped curve at both temperatures, suggesting a two-step crystallisation process. The two-step crystallisation process may be due to the formation of fat crystals as a result of polymorphism or concomitant growth due to the presence of different mixtures of TAGs. This observation has been discussed by Foubert and his co-worker (2003) [205]. During the isothermal period, there is the formation of a crystal nucleus at the beginning of the crystallisation process after which there is the accumulation of fat until the end of the isothermal process (60 min). However, at 16 °C the s-shape of the AB-GH curve, was not very distinct as a large amount of the fat is formed at the initial nucleation stage. This observation can be as a result of super-cooling of high melting TAG components in the Allanblackia sample leading to a large amount of fat forming at the nucleation stage.

Applying the Avrami crystallisation theory, the percentage of crystallinity of fat with time was fitted with the Avrami model. From the Avrami equation, the exponent (n), the constant (K) and the half-time of crystallisation ($t_{1/2}$) were calculated (Table 4.3.) and used to characterise the crystallisation kinetics [185]. According to the theory, the n value is estimated to be a reflection of the nucleation and the mechanism of crystal growth. A high n value signifies a complex mechanism for the crystal growth and the smaller the n value indicates a faster nucleation and a more rapid crystal growth [47]. From the data obtained it was found that Allanblackia fat at 16 °C has the smallest n value, hence a faster nucleation stage thereby confirming the large amount of crystals formed (about 70 %) within the first 10 minutes of the isothermal period (Figure 4-6B). This can be due to the presence of high melting fat fractions which co-crystallise with the low melting fats.

Additionally the K value tells the rate of crystallisation and corresponds to the driving forces of the crystallisation process. The Allanblackia fat at the 16 °C gave a high K value meaning an increase in the driving forces of the crystallisation process. The driving force of crystallisation depends on the nature of the cooling process (super-cooling or super-saturation conditions). During the crystallisation of the Allanblackia fat it is observed that some amount of the high melting components co-crystallise with the low melting TAGs. These high melting components are said to be super-cooled at the 16 °C temperature and therefore this may result in the rapid crystallisation rate. From the half-time of crystallisation ($t_{1/2}$) which is the time at which the crystallisation process is about 50% complete it is suggested that the crystallisation is about 50% complete within the first 3 minutes ($t_{1/2} = 1.613$ min). Values obtained for n , K and $t_{1/2}$ suggest that the crystallisation of AB-GH at the 20 °C temperature is much slower as compared with the crystallisation of AB-GH at 16 °C. Considering SB-GH, it is observed that at both the 16 and 20 °C the crystallisation was relatively slow (n) = 1.415 and 1.163 respectively. However, after the nucleation stage the crystal growth was much faster at the 16 °C isothermal temperature ($t_{1/2} = 13.740$ mins).

Table 4-4: Isothermal crystallisation kinetics parameters; Avrami exponent (n), the crystallisation rate constant (K) and the half-time of crystallisation ($t_{1/2}$) obtained from fitting the isothermal crystallisation curve at 16 and 20 °C temperature for AB-GH and SB-GH

Samples	T (°C)	n	K (min)	$t_{1/2}$ (min)
AB-GH	20	1.204±0.041	0.016±0.001	22.872±0.032
	16	0.333±0.017	0.591±0.008	1.613±0.015
SB-GH	20	1.163±0.059	0.016±0.003	25.541±0.041
	16	1.415±0.032	0.017±0.076	13.740±0.062

4.7 X-ray Diffraction (XRD) Studies of Fat crystals at Room Temperature

The XRD studies were used to investigate the polymorphic behaviour of fat crystals from AB-GH and SB-GH stored at room temperature over a period of time. From the literature, the short spacing at 4.15 Å represents the existence of an α polymorph while the occurrence of the two intense signals at 4.2 and 3.8 Å corresponds to β' polymorph. The presence of a β polymorph is characterized by a very strong intense signal at 4.6 Å [209]. Figure 4-9 shows the X-ray diffraction patterns of AB-GH and SB-GH. It is observed that the polymorphic behavior of both samples showed very strong intense short spacing signal around 4.6 Å and medium signals in the region of 5.4 Å, 3.9 Å and 3.6 Å which indicates the presence of β polymorphs in the fat crystals of AB-GH and SB-GH at room temperature. However, AB-GH exhibited in addition, signals at around 4.2 Å and 3.8 Å which indicates the presence of a β' polymorph. The existence of both β and β' polymorphs in the AB-GH fat stored at room temperature can be explained as follows:

during the formation of the fat crystals, the initial formation of crystals of the high melting fatty acid TAGs leads to the increase in viscosity as it begins to crystallize and this causes a reduction in molecular mobility of crystals formed which consequently leads to the formation of mixed crystals. This phenomenon has also been described by Acevedo et al (2012) [210].

The presence of the unstable β' polymorph gives the AB-GH fat crystals a functionality and desirability advantage over the SB-GH. This property is attributed to the crystal size (1 mm) and the needle-shaped morphology of the β' polymorph as described in the literature [44, 211]

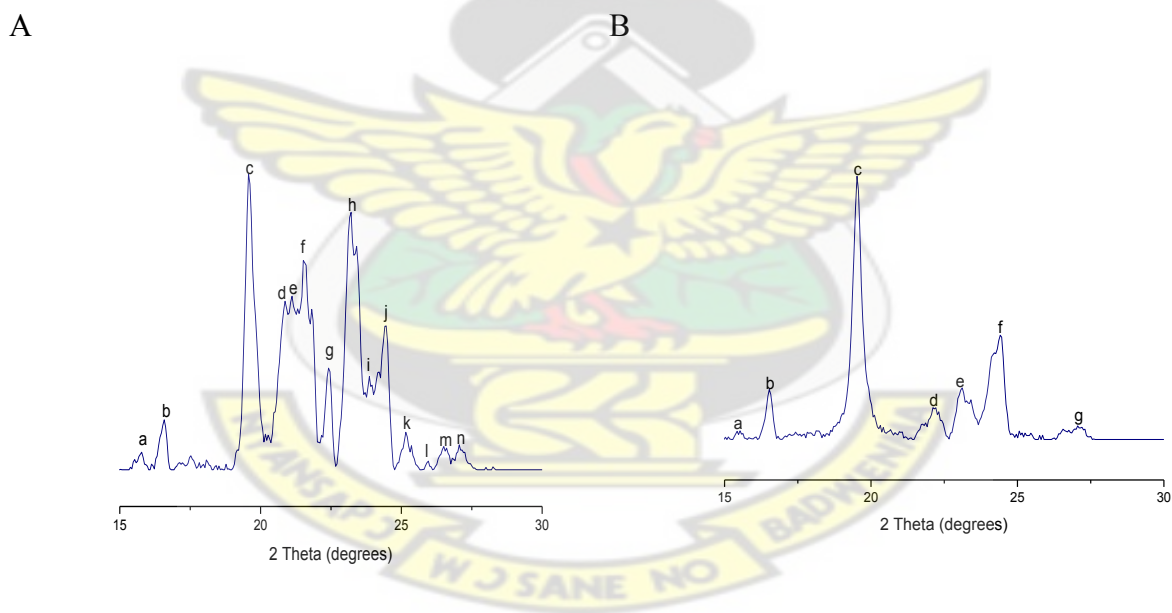


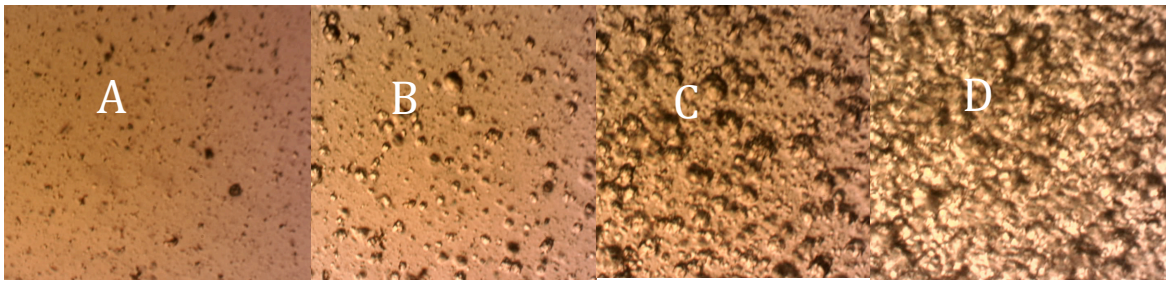
Figure 4-9: Diffractions obtained from the powder XRD analysis for fat kept at room temperature for six months: (A) XRD profile for AB-GH and (B) XRD profile for SB-GH

Table 4-5: Signals and their corresponding d-spacing (Å) obtained from the X-ray diffraction patterns for AB-GH and SB-GH fat samples.

AB-GH		SB-GH	
Signal	d-spacing (Å)	Signal	d-spacing (Å)
a	5.62	a	5.70
b	5.36	b	5.36
c	4.58	c	4.56
d	4.25	d	4.01
e	4.20	e	3.85
f	4.12	f	3.64
g	3.96	g	3.29
h	3.83		
i	3.73		
j	3.364		
k	3.54		
l	3.43		
m	3.36		
n	3.29		

4.8 Crystal Morphology

Optical microscopy was used to investigate and understand the microscopic physical properties, visual images of the microstructure of the fats at various stages of the crystallisation processes. The microstructure of the fat crystal network at 70°C, 20 °C, 16 °C and -10 °C was visualised to predict their structure as the fat crystallises from the melt (at 70 °C) until a completely solidified fat crystal network is formed at -10 °C. The photomicrographs are shown in Figure 4-10.



AB-GH



SB-GH

Figure 4-10: Visual images of AB-GH and SB-GH as obtained from the optical microscope at (A) 70 °C, (B) 20 °C, (C) 16 °C and (D) -10 °C

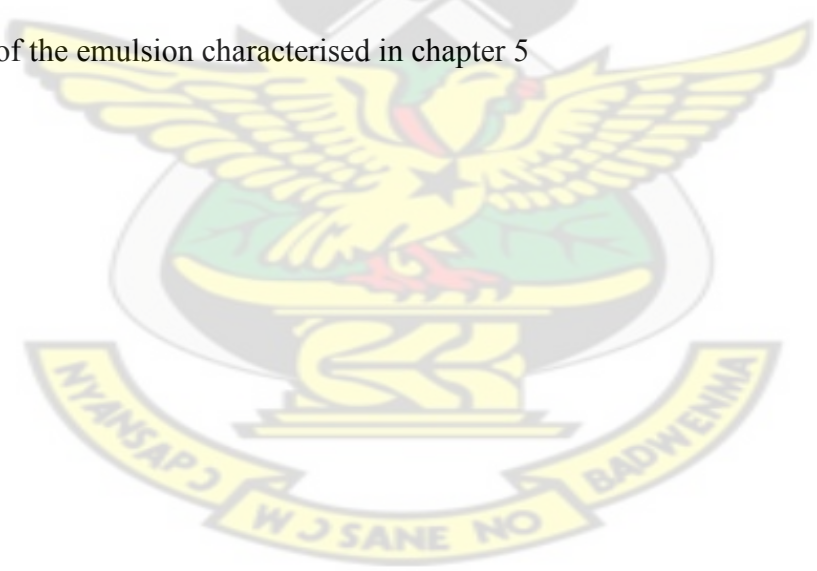
From the optical images, it can be seen that as the fat begins to crystallise from the melt (from 70 °C to -10 °C), Allanblackia seed fat and the shea nut fat presented different crystals morphologies. As the crystallisation process begins at 20 °C, it is observed that the crystals formed within the Allanblackia melt give distinct rounded solid fat particles and the number of these solid crystalline fat increases as the temperature decreases from the 20 °C to the 16 °C and finally to -10 °C. The profile of the shea butter shows that the crystals formed are associated with each other and therefore does not form distinct crystal fractions. Going through the crystallisation process of both samples, it can be seen that as the crystallisation process starts at the 20 °C, the crystals formed at that temperature represents the seed crystals upon which there is crystal growth until a completely solid fat is achieved. At the 70 °C, both fat samples are in their melted form and they appear as a

clear yellowish liquid. The photomicrograph as observed can also be used to confirm the crystallisation mechanism observed under the isothermal crystallisation kinetics as studied by the DSC method. The formation of a larger and denser crystal networks by shea butter as compared to the individual fat crystals of Allanblackia may be used as an indication of the presence of strong association and interactions within the crystal structure of shea butter. The different fatty acids constituents lead a greater attractive force between the molecules and therefore easily associate to form the solid. Again, shea butter at $-10\text{ }^{\circ}\text{C}$ presented a somewhat needle-like crystal morphology while Allanblackia presented more spherical crystal morphology. In addition it was also observed that the microstructure of the shea butter at $-10\text{ }^{\circ}\text{C}$ became less homogeneous as compared to the crystals formed at the $20\text{ }^{\circ}\text{C}$ and $16\text{ }^{\circ}\text{C}$ and this may be as a result of the presence of different TAGs (e.g OOO, SOL, POL and OOL) composition which can lead to the growth of diverse mixed crystals.

4.9 Conclusion

The results obtained from GC and ^1H NMR indicate a high saturated fatty acid, mostly stearic acid, in the Allanblackia seed fat and the shea nut fat. The high saturated fatty acid content accounts for the high melting point of the fats. The research has shown that numerous significant variations were found in the thermal properties of the Allanblackia seed fat and shea butter with temperature change. The cooling profiles indicated three main events in their crystallisation mechanism. The initial peak was detected at a high temperature which is possibly associated to the high stearic acid fraction, the two crystallisation peaks detected at low temperatures, may be associated with the olein fractions in the vegetable fats. The phase transformations of both the Allanblackia seed

fat and the shea nut fat are found to be dependent on the thermal processes occurring at each temperature change and this is evident by the change in the cooling profile with change in the cooling rate. Additionally, the crystallisation peaks were been found to shift gradually as the rate of cooling increased. For the isothermal crystallisation, with respect to the Avrami model, it was observed that when the crystallisation temperature increased, the n value increased for the Allanblackia seed fat whiles the n value reduced with increasing temperature for the shea nut fat. The mechanism of crystallisation was observed to involve a two-step process involving nucleation and the crystal growth. Having determined the crystallisation patterns and a detail thermal profile of the Allanblackia seed fat and the shea nut fat, the Allanblackia fat was selected and used as the dispersed solid fat for the formulation of an oil-in-water emulsion system and the stabilisation of the emulsion characterised in chapter 5



CHAPTER 5

Formulation, Stabilisation and Characterisation of Fat Particles-in-Water Emulsions – Effect of Tween 20 and Sodium Alginate Mixtures

Many products from the food and pharmaceutical industry are based on oil droplets dispersed in water. Effects of the formation of the fat crystals affecting the stability of emulsion system are reviewed thoroughly in the literature. However, few works have reported on the influence of solid fat on the mechanism of the emulsion stability. Work done so far has been on the utilisation of fat crystal network for protection of oil droplets as they occur in the emulsion but little or no work is done on the formulation, characterisation and the stabilisation mechanisms of a complete solid fat particle dispersed in aqueous medium. Having studied the fatty acids constituents and the thermal behaviour of shea butter and Allanblackia seed fat, the Allanblackia seed fat was selected as the vegetable fat of choice and used as the dispersed phase in the formulation of oil particles dispersed in water. This chapter looks at the influence of Tween 20 and sodium alginate mixtures on the stabilisation of fat particles-in-water emulsions against coalescence and particle aggregation is discussed. The stabilisation process of the emulsions has been described in terms of change in concentration of the Tween 20, sodium alginate and the amount of fat used in the emulsions formulation. Also, the work looked at how the fat content affects the size of the particles formed. Finally rheological measurements were used to determine the stabilisation of the emulsion in the long terms

5.1 Formulation of Fat Particles-in-Water Emulsions

Stability of the fat particles-in-water emulsions at pH 7 was first investigated against aggregation and coalescence without the use of any emulsifier at various fat/water ratios of 5/95, 10/90, 15/85 and 20/80. A creamy emulsion was produced immediately after homogenisation, which indicates an evenly spread of solid particles the continuous aqueous phase. Images were taken soon after the homogenisation process by the light microscope and this confirmed the formation of discrete and evenly distributed fat particles. The observed creamy emulsions were found to separate out into two complete layers as shown in Figure 5-1A; a solid fat upper layer and a clear aqueous layer within the first 30 minutes after the homogenisation. The extent of separation of the two phases was found to be dependent on the amount of fat present. After the homogenisation, the particles formed were in constant motion and the particle tends to move close to each other resulting in collision; as the particles collide, the thin film of continuous aqueous phase separating the fat particles may break down hence particles aggregate. Also, close contact of the fat particles increases the van der Waals internal attractive forces more than the electrostatic repulsive force and this may lead to the formation of aggregates of fat particles [135]. There was no coalescence as the dispersed fat phase immediately formed rigid solid particles when the temperature began to reduce as soon as the homogenisation was completed. The observation of an upper fat layer and lower aqueous layer was not surprising since solid fat particles are less dense than the aqueous phase and will move towards each other to form a network structure in the upper layer. However, having shown the prominence of instability of the fat particles dispersed in water emulsion in

this section, the use of a surfactant to improve the interfacial properties of fat particles was investigated and discussed in the next section.

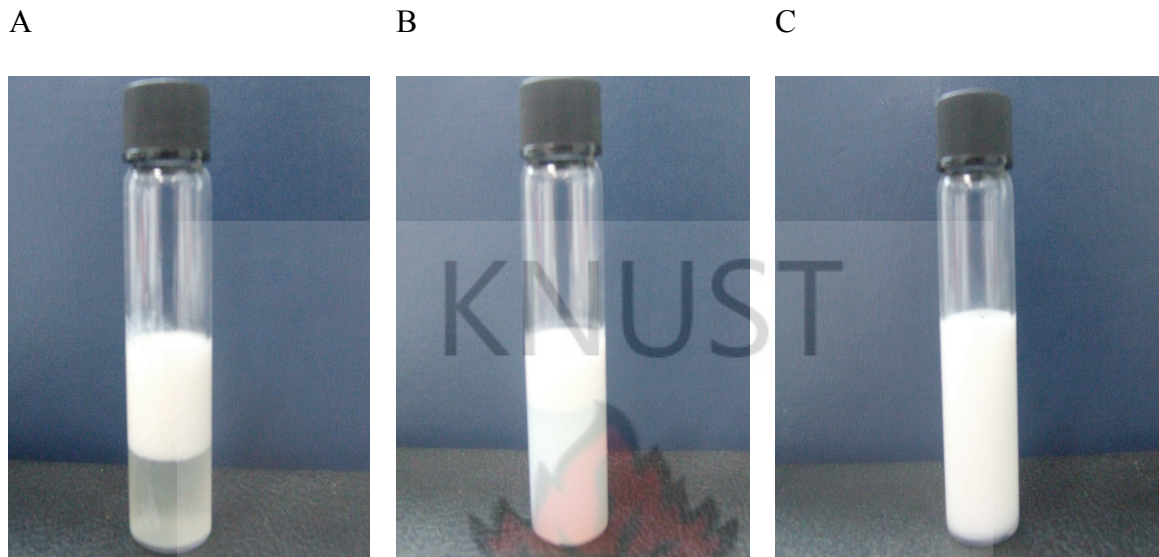


Figure 5-1: Visual observation of emulsions after 1 hour of homogenisation (A) dispersed fat particles in water without any emulsifier (B) dispersed fat particles in water with Tween 20 surfactant (C) dispersed fat particles in water with Tween 20 and sodium alginate mixture

5.2 Surfactant Stabilised Fat Particles-in-Water Emulsions

Having shown the inability of fat particles to form a stabilised oil-in-water emulsion, modification of the emulsion was considered by the addition of a surface-active compound to help improve the interfacial properties of the dispersed fat particles. Tween 20 with an HLB of 16.7 was selected and assessed for improved stabilisation of the dispersed fat particles. Contribution of Tween 20 on the emulsion stabilisation process was investigated by following the change in emulsion characteristics at 1 to 5% Tween 20 compositions. The presence of the Tween 20 produced emulsions with evenly distributed dispersed fat particles in the continuous aqueous phase. The stabilised

emulsions lasted for 3 hours after which the emulsions began to break down into two layers. There was the observation of a creamier upper layer and an opaque aqueous lower layer (Figure 5-1 B) and the level of separation (as measured by the volume ratio of creaming) was affected by both the amount of fat present and the concentration of Tween 20 used. Due to the amphiphilic character of the Tween 20, reduced the interfacial tension generated at the water/particle interface. This process leads to improved stability of dispersed fat particles. In 3 hours after emulsion preparation, some of the fat particles began to experience de-adsorption of the surfactant molecules hence the ability of the particles to aggregate upon collision. The cloudy lower layer may be due to excess surfactant molecules dispersed in the water or as a result of the ability of some of the fat particles to maintain the adsorbed surfactant molecules, which helped to improve the surface tension, generated during the emulsification process. At the 5/95-fat/water ratios, some of the destabilised fat particles were observed to move to the upper most layers to form solid mass, which can be an indication of the occurrence of coalescence immediately after the emulsification process before the complete solidification of the liquid fat droplets. From the results obtained, it can be explained that the addition of Tween 20 enables both the dispersed particles and the continuous phase to experience an improved interfacial properties hence a stabilised physicochemical behavior of the emulsions with time. However, emulsion breakdown as a function of time suggests the inability of the Tween 20 to completely stabilise the fat particles in water emulsion in the long term.

5.3 Mixed Surfactant/Biopolymer Emulsifier System in Stabilised Fat-in-Water Emulsions

The presence of the Tween 20 in the emulsion system was observed to introduce a level of stability to the dispersed fat particles. However, as discussed above, this observed stability was only prominent for a while after which some of the dispersed particles lost their stability and began to aggregate. In order to obtain a more stabilised system, there was the need to increase the viscosity of water by adding the sodium alginate thickener. The sodium alginate (sodium salt of alginic acid) is a polysaccharide which works together with Tween 20 to improve the interfacial properties in the emulsion system. The effects of the mixed sodium alginate and Tween 20 as a combined-emulsifier system on the stabilisation of the fat-in-water emulsion was investigated by using varying concentrations of the sodium alginate (1 – 5% in the increment of 1%) and Tween 20 (1 – 6% in the increment of 1%). A well-developed emulsion was observed (Figure 5-1C). The emulsions produced were investigated in details by the characterization of their particle distribution, particle microstructure and the occurrence of creaming as discussed in the following sections.

5.4 Characterisation of the Dispersed Fat Particles-in-Water Emulsions

The effect of the various ingredients namely; the fat content, sodium alginate and the Tween 20 on the stabilisation mechanism of the emulsion system was investigated. Different batches of emulsions were prepared by a systematic variation of the concentrations of the fat, sodium alginate and Tween 20. The stability of the prepared fat particles-in-water emulsions were determined from the measured particle size of the fat particles distributed in the creaming layer with time. Again the emulsion stability was

determined from the measurement of volume fraction of creaming layer and also by examining the fat particle microstructure.

5.4.1 Effects of Fat Content on emulsion Stabilisation

Emulsions containing small amounts of fat concentrations (5%) irrespective of the amount of sodium alginate and Tween 20 present with the exception of those containing 1% sodium alginate, gave a well developed emulsion with uniformly distributed dispersed particles without any separation within the first 24 hr after preparation. However, the emulsions appeared to separate out after the 24-hr period, which was evident in the results obtained from the volume fraction of the creamy layer. A significant increase in the size of the fat particles with time over 30 days period. As the fat content in the emulsion system increased (5% to 20%), the level of stability observed also increased. In order to achieve stability for the fat particles in the emulsion systems it was necessary to consider increasing the fat content above the 5% threshold. Solid fat crystals in the emulsion with high fat concentration regimes were indeed able to stabilise fat particles in water emulsions with little or no phase separation occurring immediately or 30 days after the emulsification process. It was observed that the efficiency of stabilisation increased with increasing fat content (Tables 5-1 to 5-4).

Table 5-1: Average size of particles (PSD) with their standard of deviations of emulsion (5/95) mixed-emulsifier stabilized emulsions and the volume fractions of creaming layer ($V_{f_{cr}}$) with change in sodium alginate and Tween 20 concentrations.

		Tween 20					
Sodium Alginate		1.0	2.0	3.0	4.0	5.0	6.0
1.0	PSD	168.5±2.22	145.5±1.81	136.7±1.48	132.4±1.57	131.4±0.61	131.4±0.61
		213.4±1.42	207.0±1.40	201.6±4.17	200.1±4.56	200.3±2.57	200.1±2.05
	$V_{f_{cr}}$	0.68 0.29	0.80 0.29	0.84 0.29	0.86 0.29	0.90 0.29	0.90 0.29
2.0	PSD	145.0±1.89	140.9±1.30	134.8±1.64	130.9±0.90	130.2±0.80	130.1±0.33
		193.5±2.83	187.8±1.13	185.5±1.01	185.0±1.60	185.4±1.89	185.2±3.19
	$V_{f_{cr}}$	1.00 0.30	1.00 0.33	1.00 0.35	1.00 0.35	1.00 0.33	1.00 0.34
3.0	PSD	140.7±1.59	138.1±1.46	131.8±1.91	130.5±0.46	129.6±0.47	129.1±0.48
		187.4±4.65	186.6±1.30	184.1±1.52	184.3±0.98	184.9±1.44	184.3±1.03
	$V_{f_{cr}}$	1.00 0.48	1.00 0.51	1.00 0.58	1.00 0.56	1.00 0.58	1.00 0.58
4.0	PSD	162.1±0.78	160.9±0.45	161.9±2.01	160.4±0.93	160.3±0.88	160.0.70
		181.5±1.96	181.4±1.30	181.2±2.22	182.4±1.62	182.4±0.91	181.2±0.45
	$V_{f_{cr}}$	1.00 0.65	1.00 0.67	1.00 0.66	1.00 0.68	1.00 0.68	1.00 0.68
5.0	PSD	163.0±1.16	163.9±1.62	162.3±1.81	162.4±1.07	162.7±0.37	162.5±1.26
		182.9±0.51	182.0±1.94	181.5±0.98	182.3±0.79	182.3±1.34	181.0±1.68
	$V_{f_{cr}}$	1.00 0.65	1.00 0.68	1.00 0.70	1.00 0.68	1.00 0.72	1.00 0.70

PSD and $V_{f_{cr}}$ data was collected soon after the homogenization process and after 30 days (in red ink)

Table 5-2: Average size of particles (PSD) with their standard of deviations of emulsion (10/90) mixed-emulsifier stabilized emulsions and the volume fractions of creaming layer ($V_{f_{cr}}$) with change in sodium alginate and Tween 20 concentrations.

		Tween 20					
Sodium Alginate		1.0	2.0	3.0	4.0	5.0	6.0
1.0	PSD	163.5±2.28	144.1±1.00	141.4±1.02	140.9±1.38	140.7±0.61	140.1±1.07
	$V_{f_{cr}}$	215.6±1.27 0.82 0.48	184.1±1.72 0.96 0.61	178.6±1.74 1.00 0.68	177.1±1.00 1.00 0.68	177.8±1.09 1.00 0.66	177.4±1.05 1.00 0.68
2.0	PSD	143.1±1.21	140.3±0.59	139.8±0.45	139.8±0.65	139.1±0.69	139.4±0.34
	$V_{f_{cr}}$	185.1±3.48 1.00 0.60	182.6±1.65 1.00 0.68	176.6±1.63 1.00 0.72	175.9±0.87 1.00 0.74	175.5±1.78 1.00 0.72	174.6±0.73 1.00 0.73
3.0	PSD	142.5±1.71	139.9±1.18	140.1±0.45	139.8±2.00	139.8±0.24	139.4±0.62
	$V_{f_{cr}}$	183.4±1.72 1.00 0.68	180.6±1.11 1.00 0.82	174.4±1.68 1.00 0.86	174.3±1.11 1.00 0.86	174.5±1.10 1.00 0.88	174.7±1.43 1.00 0.88
4.0	PSD	160.9±2.77	160.4±0.50	161.3±0.94	161.7±2.00	160.9±0.71	161.2±1.03
	$V_{f_{cr}}$	162.2±1.86 1.00 0.94	160.2±1.09 1.00 0.95	161.2±1.20 1.00 0.94	161.7±1.30 1.00 0.98	161.4±0.41 1.00 0.92	161.3±0.61 1.00 0.92
5.0	PSD	163.5±1.05	162.4±1.79	162.5±1.81	162.2±1.07	162.2±1.24	162.8±0.77
	$V_{f_{cr}}$	163.7±0.51 1.00 0.95	162.5±0.99 1.00 0.95	162.6±1.65 1.00 0.96	162.6±0.79 1.00 0.98	162.5±0.92 1.00 0.95	162.2±1.71 1.00 0.95

PSD and $V_{f_{cr}}$ data was collected soon after the homogenization process and after 30 days (in red ink)

Table 5-3: Average size of particles (PSD) with their standard of deviations of emulsion (15/85) mixed-emulsifier stabilized emulsions and the volume fractions of creaming layer ($V_{f_{cr}}$) with change in sodium alginate and Tween 20 concentrations.

		Tween 20					
NaAlg		1.0	2.0	3.0	4.0	5.0	6.0
1.0	PSD	164.0±0.87	144.5±0.58	141.9±1.35	139.7±1.27	139.3±1.37	139.7±0.88
	$V_{f_{cr}}$	178.3±3.32 1.00 0.44	145.2±3.40 1.00 0.44	141.5±0.43 1.00 0.46	139.9±0.61 1.00 0.45	139.2±1.31 1.00 0.48	139.4±0.34 1.00 0.48
2.0	PSD	142.9±0.90	140.5±0.86	138.8±1.13	139.6±1.20	139.4±0.34	139.0±1.05
	$V_{f_{cr}}$	146.8±0.76 1.00 0.90	142.2±2.50 1.00 0.98	139.3±0.37 1.00 1.00	139.5±0.57 1.00 1.00	139.7±0.85 1.00 1.00	139.8±1.64 1.00 1.00
3.0	PSD	139.7±1.46	138.5±0.70	137.9±1.90	136.8±0.94	136.7±0.71	136.5±0.91
	$V_{f_{cr}}$	143.8±2.12 1.00 0.91	139.3±1.71 1.00 1.00	139.4±1.56 1.00 1.00	138.2±1.96 1.00 1.00	139.0±0.57 1.00 1.00	137.7±1.02 1.00 1.00
4.0	PSD	161.2±1.13	160.5±0.86	160.5±0.40	160.5±1.20	160.8±0.78	161.2±0.39
	$V_{f_{cr}}$	162.5±1.07 1.00 0.95	161.7±1.28 1.00 0.97	161.2±1.07 1.00 0.96	161.2±1.35 1.00 0.98	161.1±0.95 1.00 0.98	161.6±1.27 1.00 0.98
5.0	PSD	163.2±0.54	161.2±1.52	161.3±2.09	161.6±0.42	161.8±1.54	161.9±0.31
	$V_{f_{cr}}$	164.1±1.23 1.00 0.90	162.1±2.11 1.00 0.91	161.6±1.68 1.00 0.90	161.8±0.49 1.00 0.90	161.8±0.74 1.00 0.90	161.8±0.34 1.00 0.90

PSD and $V_{f_{cr}}$ data was collected soon after the homogenization process and after 30 days (in red ink)

Table 5-4: Average size of particles (PSD) with their standard of deviations of emulsion (20/80) mixed-emulsifier stabilized emulsions and the volume fractions of creaming layer ($V_{f_{cr}}$) with change in sodium alginate and Tween 20 concentrations.

		Tween 20					
NaAlg		1.0	2.0	3.0	4.0	5.0	6.0
1.0	PSD	153.0±1.88	144.0±0.66	143.0±2.15	141.1±1.31	139.3±1.37	141.8±0.70
	$V_{f_{cr}}$	153.3±2.04 1.00 0.94	143.8±0.87 1.00 0.98	143.0±1.23 1.00 1.00	143.2±1.84 1.00 1.00	139.2±1.31 1.00 1.00	143.4±1.65 1.00 1.00
2.0	PSD	142.4±0.24	141.4±2.22	140.1±1.56	139.9±1.22	139.4±0.34	139.1±0.49
	$V_{f_{cr}}$	143.0±1.03 1.00 1.00	143.2±0.37 1.00 1.00	143.1±1.28 1.00 1.00	141.7±1.84 1.00 1.00	139.7±0.85 1.00 1.00	142.1±1.53 1.00 1.00
3.0	PSD	141.3±1.61	139.4±1.07	139.5±0.86	140.1±0.43	136.7±0.71	139.9±0.59
	$V_{f_{cr}}$	142.5±0.49 1.00 1.00	140.3±1.72 1.00 1.00	140.3±1.72 1.00 1.00	139.9±0.61 1.00 1.00	139.0±0.57 1.00 1.00	140.8±0.97 1.00 1.00
4.0	PSD	162.1±1.45	161.4±0.79	161.4±0.79	161.1±0.57	160.8±0.78	161.0±0.94
	$V_{f_{cr}}$	163.1±1.02 1.00 1.00	162.0±1.35 1.00 1.00	162.0±1.35 1.00 1.00	161.4±0.90 1.00 1.00	161.1±0.95 1.00 1.00	161.8±0.90 1.00 1.00
5.0	PSD	163.7±0.66	163.2±0.73	163.2±0.73	163.2±0.57	162.8±1.00	162.8±0.37
	$V_{f_{cr}}$	163.9±0.53 1.00 1.00	163.5±1.08 1.00 1.00	163.5±1.08 1.00 1.00	163.1±0.43 1.00 1.00	163.1±0.95 1.00 1.00	163.6±1.57 1.00 1.00

PSD and $V_{f_{cr}}$ data was collected soon after the homogenization process and after 30 days (in red ink)

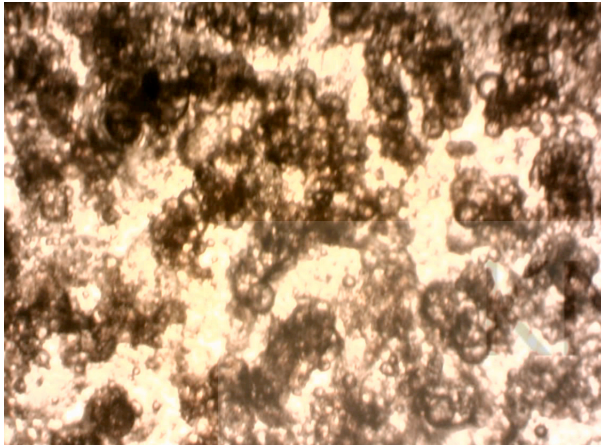
A visual observation showed that there was an improved stability against creaming within the first 24 hours due to the presence of the combined emulsifier system. At low fat content (5 %), there was a steady increase in the separation after the first 24 hours. This can be explained based on the fat/water ratio. At low levels fat content, a small amount of fat particles are generated within the emulsion system as compared with the volume of the continuous water phase (95%). These particles as generated are widely spread and

spaced to fill up the total volume of the emulsion system. The particles are in constant motion and since they are less dense compared with the aqueous phase, they travel up faster with no or little obstruction in the aqueous phase. They settle on top of the aqueous phase and form aggregates leading to the creamy upper layer. The formation of the aggregates is observed from the microstructure image (Figure 5-2A). The extent of separation was significantly more affected with increasing concentration of the sodium alginate content and this is because the sodium alginate content makes the viscosity of the aqueous increase hence reducing the speed of the particles movement. A slow rate in the particle movement results in the reduction of the association of the fat particles and hence improved aggregation, leading to the formation of creamy layer. Increase in the fat content from the 10 – 20%, showed a significant improvement on the stabilisation of emulsions. It was observed that emulsions produced remained uniformly creamy for all concentrations of both sodium alginate (1-5%) and tween 20 (1-6%). The presence of fat increases the thickness of the emulsion system after the homogenisation process. In the presence of high level of fat, there is a reduction in the amount of water used and a huge number of fat units are dispersed. Increased fat particles will cause a reduction in the speed and distance at which the particles travel and collide. The large distribution of particles also provides proximity, which supports particle-particle interaction within the continuous aqueous phase. A three-dimensional structure is formed, which can encase the aqueous phase thereby improving the stabilisation of the emulsion system. At 15 and 20% fat content emulsions were to large extent stabilised over a period of 30 days. At 15% fat concentration, a completely stable emulsion was formed and observed for the 30 days with a minimal volume separation occurring at low sodium alginate concentration.

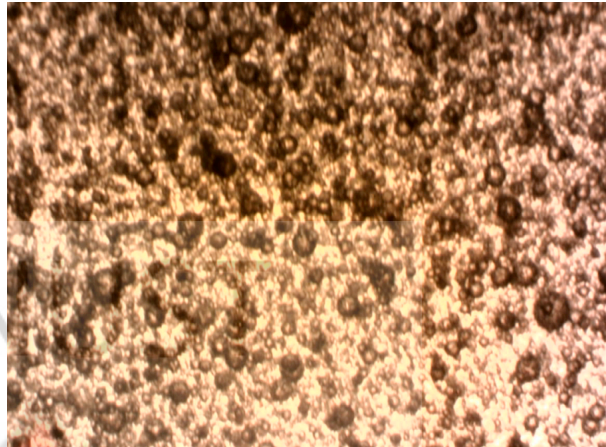
Also increase in the fat content caused an increase in emulsion thickness and the resultant stable emulsion was formed as shown in Table 5-3. With 20% fat, a uniformly dispersed creamy emulsion was formed for the first 24 hours after which there was some level of separation and a subsequent formation of a semi-solid (paste) creamy layer (Table 5-4).

The stability of the emulsions were established as they maintained their physical appearance and also confirmed by the fact that there was little or no change in their particle sizes (Table 5-1 to 5-4). Stabilisation of the emulsion systems seems to be effective at high levels of the crystallized fat in the emulsifier system. Stabilisation of the fat particles was also affected by the presence of both the Tween 20 and the sodium alginate molecules in the emulsification process. At low concentrations (1%) of Tween 20 and sodium alginate in a low solid fat content (5%) emulsion, the emulsifier system was unable to keep the emulsion stable. By increasing the solid fat content ($> 5\%$), the stabilisation effect of both the Tween 20 and the sodium alginate was very much seen, especially within the first 24 hours after the emulsion preparation. Another observation worth noting is the fact that low amount of sodium alginate in the combined emulsion system was able to introduce a level of stability into the emulsion system after preparation even for low solid fat content (5%) emulsions. The continuous motion of the particles was affected by the presence of both Tween 20 and the sodium alginate. The Tween 20 and sodium alginate worked synergistically to provide an effective distance between the dispersed fat particles such that they prevent particle-particle interaction or provide only a partial contact, hence their ability to prevent a total breakdown of the emulsion system.

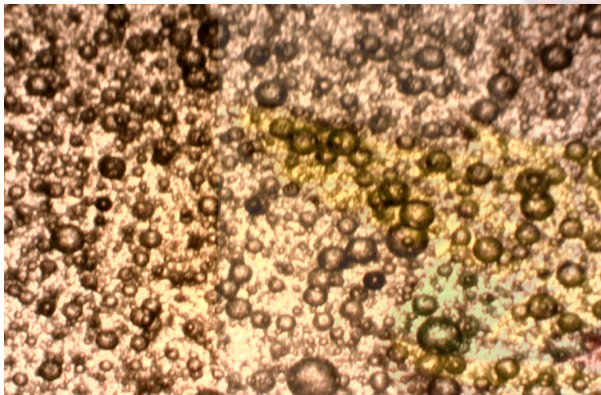
A



B



C



D

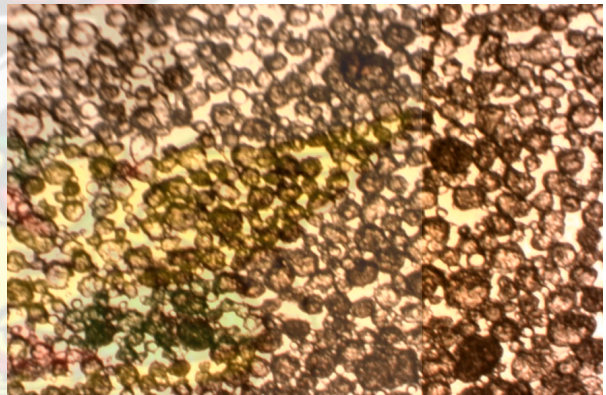


Figure 5-2: Light microscopic images of fat particles in water in the presence of both Tween 20 and sodium alginate at (A) 5/95 % fat/water (B) 10/90 % fat/water (C) 15/85 % fat/water (D) 20/80 % fat/water ratios

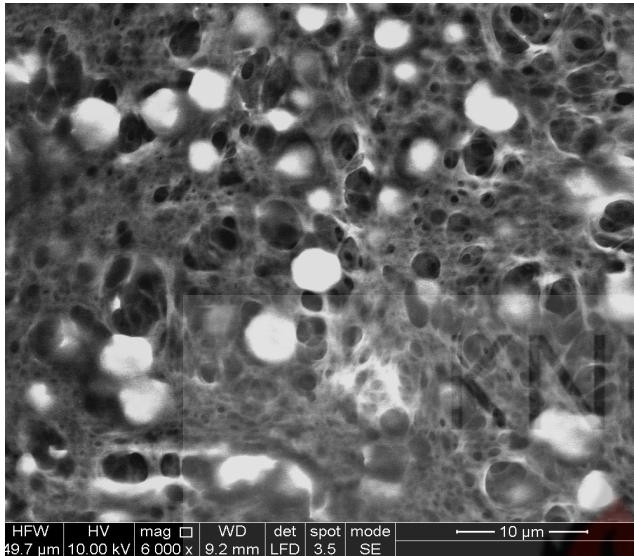
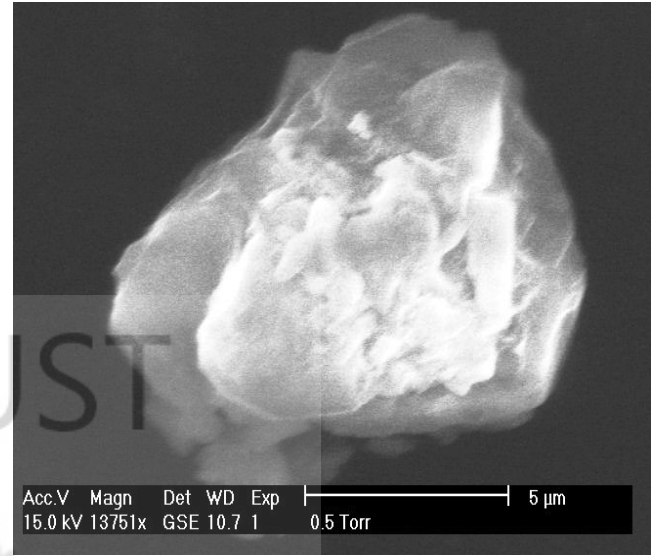
A**B**

Figure 5-3: SEM images of the dispersed fat particles in the emulsion system of 18/85 fat/water composition at 3 % sodium alginate and Tween 20 content

The SEM photographs showed the crystallized fat (figure 5-3). The micrographs show a confirmation of solidified crystal fat particles, which has been entrapped by the alginate gel within the emulsion system.

5.4.2 Effects of Tween 20 and Sodium Alginate Concentrations on the Emulsion Particle Size

The presence of Tween 20 and sodium alginate significantly improved the stabilisation of the emulsions for all fat/water ratios used. The effect of each of the components (i.e Tween 20 and sodium alginate) in the combined emulsifier stabilisation process was investigated and discussed by considering their effect at different concentrations in a systematic manner. The effect of increasing the concentration of Tween 20 (1 to 6% in the increment of 1%) while the concentration of the sodium alginate is held constant as

well as the effect of increasing concentration of the sodium alginate (1% to 5% in the increment of 1%) with the Tween 20 held constant were investigated. Increasing the concentration of Tween 20 from 1 to 3% gave a reduction in the size of fat particles formed. After the threshold concentration of 3% any further increase in the Tween 20 showed very little or no change on the particle sizes. The change in particle size with increasing concentration of Tween 20 was found to be independent of the amount of sodium alginate present. The size of the particles reduced in the emulsions as the concentration increases from 1 to 3% after which the particles increase in size irrespective of the amount of Tween 20 content.

A

B

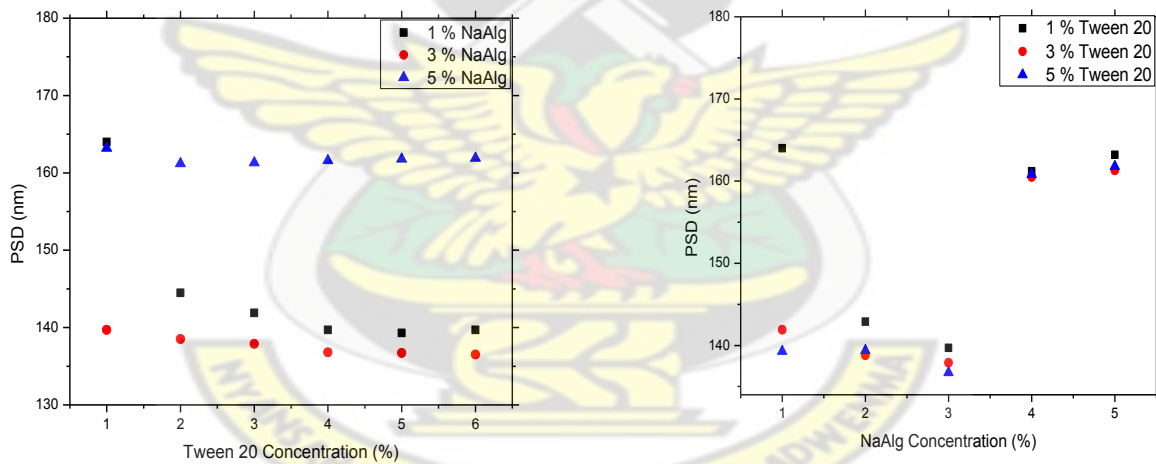
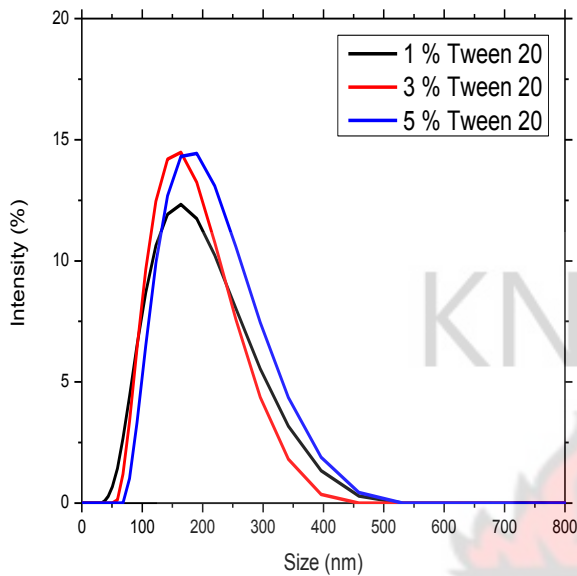


Figure 5-4: Average particle size (PSD) of the 15/85 fat/water particles in the emulsions (after homogenization) with respect to increasing (A) Tween 20 content at different amounts of sodium alginate (B) Sodium alginate at different amounts of Tween 20

A



B

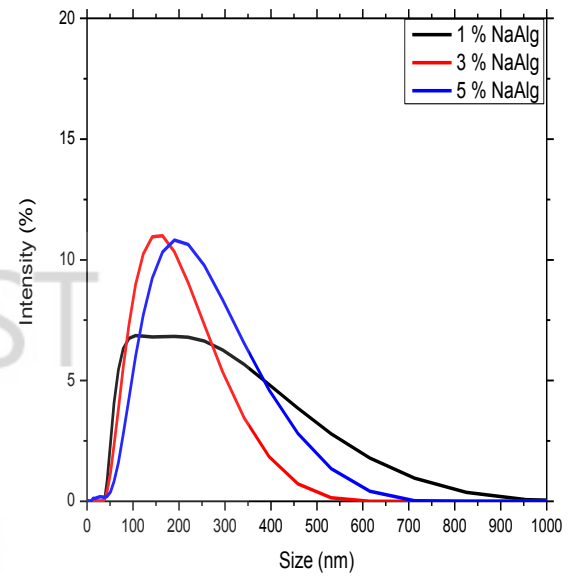


Figure 5-5: Particle size distributions of emulsions prepared at different contents of (A) Tween 20 at 3% sodium alginate (B) Sodium alginate at 3% Tween 20

Tween 20 is adsorbed at the water and fat droplet interface during the emulsification process and forms an interfacial layer around the fat droplet; this causes a lowering of the surface tension between the dispersed fat droplet and the continuous water phase. Therefore increasing Tween 20 content causes an increase in the number of molecules forming the interfacial layer hence a more lowered interfacial tension and a reduction in the droplet-droplet contact results.

Another important fact is that an increase in the Tween 20 concentration, also gives the ability to increase the flow rate in the emulsion system. This facilitates or promotes droplet break-ups during the emulsification process. The high flow rate prevents the

possibility of coalescence immediately after the emulsification process. As the flow rate is directly related to the rapid reduction of the interfacial tension, a high Tween 20 concentration increases the repulsion between the fat droplet causing a reduction in particle aggregation hence a stable size distribution within the emulsion system. The increase in sodium alginate concentration leads to high viscosity of the aqueous phase, and helps to reduce the rapid movement of the dispersed particles hence a reduction in the collision of the particles. The particle size significantly influence stabilisation of the final emulsion system in both in the short and long terms. The presence of the Tween 20 and the sodium alginate in the emulsification system both have a threshold concentration beyond which their presence has no significant effect on keeping the emulsion stable. As concentration of the Tween 20 increases it reaches its threshold concentration beyond which any further increase does not affect the particle size. This is because at the threshold concentration, the droplets have the maximum molecular coverage at the interfacial layer; hence increasing of the surfactant molecule further significantly does not affect the surface tension in the system. At this point the emulsion particle size becomes only limited by the emulsification process and therefore remains unchanged. However, with respect to the sodium alginate content, the rapid increase in viscosity introduced to the continuous water phase as the sodium alginate increases beyond its threshold concentration affects the speed of the emulsification process and hence the production of larger droplets.

A



B



Figure 5-6: Visual photographs of emulsions prepared at fat/water ratio 15/85 after 30 days (A) at 3% sodium alginate with increasing concentration of Tween 20 (B) at 3% Tween 20 with increasing concentration of sodium alginate

From a visual observation, a whitish creamy emulsion with little or no phase separation was formed and lasted for a period of 30 days as the concentration of the Tween 20 increases (Figure 5-6 A). This observation also confirms the little or no change in the size of the particle in the emulsion systems even after 30 days period. This phenomenon is due to the fact that at the 3% sodium alginate concentration, when there was high content of Tween 20. This leads to the formation of smaller particles, which exhibit stronger and effective packing. Considering the effect of sodium alginate on the emulsion stabilisation mechanism (Figure 5-6 B), the visual images gave a completely creamy emulsion with no phase separation even after 30 days for emulsions formed at 3% and 4% sodium alginate content. However, at 5% sodium alginate, there was some level of separation. This

observation confirms the result obtained from the particle size measurement (Table 5-1 to 5-4).

5.5 Rheological Characterization for the Long-term Physical Stability of the Emulsions

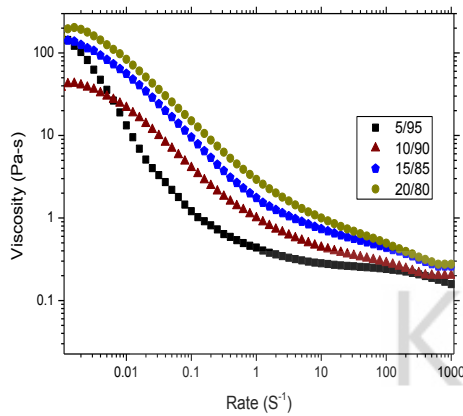
Long-term stabilisation mechanism of the well-developed emulsion produced in Sections 5.4 (after 30 days) was investigated using rheological measurements. The use of rheology, which is an accelerated tool to predict the physicochemical properties of emulsion, gives a good understanding of the physical stability of the emulsion system. Different rheological parameters from the steady state shear stress-shear rate measurements; constant stress measurements and the dynamic (oscillatory) measurements were used to assess the breakdown processes that occur in the emulsion leading to an unstable emulsion in the long term. Long-term physical stability of the emulsions at temperature variations, induced stress caused by transportation and the consistency of the emulsion are indicators for a good industrial application. In this study the effects of the amount of fat, the Tween 20 content and the sodium alginate content in the emulsion systems against the viscous and elastic responses were assessed.

5.5.1 Effect of Stress on the Stability of Emulsion Against Creaming

Reduction of creaming in an emulsion is usually achieved by using polymers of high molecular weight or thickeners in the continuous aqueous phase. Sodium alginate, a polysaccharide copolymer was used as a thickener for the continuous aqueous phase. The long-term stability of the emulsion produced in this study against creaming was investigated by measuring the change in viscosity with shear. These investigations were conducted at varying concentrations of fat and increasing sodium alginate and Tween 20

content. In general the viscosity decreased with shear rate increase (Figure 5.7), until the rate reached 1000 s^{-1} where the viscosity of the emulsions was almost constant. Therefore all emulsions types were described as exhibiting pseudoplastic behaviour. Hence the emulsions showed a reasonable to prominent shear-thinning character [95, 212], with high viscosities at low shear rates. The shear-thinning phenomenon is a typical characteristic of weak associative connections of fat droplets as due to weak droplet network structure. From Figure 5-7 A it was observed that there was a sharp reduction in viscosity as the shear rate increases for emulsion produced from 5/95 fat/water ratio. This sharp reduction reduces as the fat content increases. This may be due to the fact that the existence of the fat increases the thickness of the emulsion, hence their resistance to shear. The change in viscosity can also be used to confirm the fact that the solid fat particles form a network structure in the emulsion system, which begins to breakdown as the shear increases. Figure 5-7 B also gives a slow rate of decrease in the viscosity with the increase in shear rate. The presence of the sodium alginate leads to the development of a gel-like continuous phase hence an increase in the viscosity. Such behaviour was somehow expected as the viscosity of the emulsion is highly affected by the presence of thickeners [94, 108].

A



B

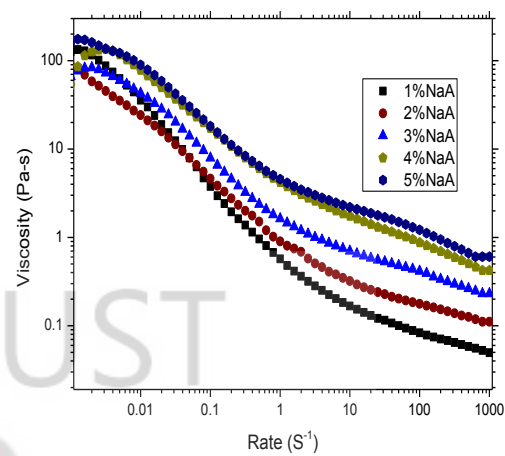


Figure 5-7: Shear-rate dependence of viscosity for A) stabilised fat particles in water emulsions with different fat concentrations at 3% Tween 20 and 3% sodium alginate and B) stabilised 15/85 fat/water particles in water emulsions with different sodium alginate concentrations

From the plot of viscosity versus the shear rate, the emulsion can be considered a non-Newtonian system, which demonstrate viscous behaviour with change in shear rate. The Power Law theory was further used to describe the linearity of the linear portion of the viscosity shear rate curve from the equations below.

$$\sigma = k\dot{\gamma}^n$$

eqn 5.1

where η is the viscosity (Pas), $\dot{\gamma}$ the shear rate (s^{-1}), k the consistency index and n is the Power Law index. The n gives information on the effects of shear on the emulsion system. The smaller the n value the more shear-thinning the system is ($n < 1$), if the value of n is equal to 1 ($n = 1$), the emulsion exhibits a Newtonian behavior and finally when n is large ($n > 1$) shear-thickening is observed [212].

Table 5-5: Data obtained after fitting the Power Law model on the viscosity/shear rate plot

Sodium alginate concentrations (%)	<i>k</i>	<i>n</i>
1	3.16	0.86
2	7.94	0.69
3	12.59	0.81
4	19.95	0.49
5	34.67	0.62
Fat concentrations (%)	<i>k</i>	<i>n</i>
5	1.41	0.43
10	5.62	0.60
15	15.85	0.74
20	22.39	0.79

The linear portions of the plots are readily fitted to the Power Law model with their derived Power Law parameters as shown in Table 5-5. From the viscosity/shear rate plots, it can be seen that as the shear rate increases, the viscosity reduces and indicates constant viscosity at high shear rates. This phenomenon explains the pseudo-plastic behavior of shear-thinning systems as observed by Tzoumaki et al (2011) [101] and Koocheki et al (2009) [107]. Comparing the plots with the data obtained from the Power law model, there is indication that the consistency index, k increases as the sodium alginate concentration increases. An n values less than 1, confirms shear-thinning of the emulsion systems. Shear-thinning behaviour in emulsions can be interpreted as demonstrating the presence of weak attractive forces between the emulsion droplets,

which give rise to the formation of a weak elastic gel-like network [213]. The application of a shear stress causes the droplets to move away from each other. A low shear stress in the presence of high attractive forces acting on the emulsion droplets leads to an elastic physical response of the emulsions. Hence the shear energy is elastically stored as an extension of the bonds between the dispersed droplets. The resistance to flow provided by the network that arises from these weak interaction forces is, however, readily overcome by the application of a shear force to the system. This phenomenon can be attributed to the presence of the sodium alginate and a rheological modifier in the emulsion system. Figure 5-7 A gives a graphical description of how changing fat–water composition affects the functional relationship between viscosity and shear rate. The data demonstrates that as the level of fat in the emulsion increases, there is a corresponding increase in the both consistency index, k and the n values pointing to shear-thinning behavior.

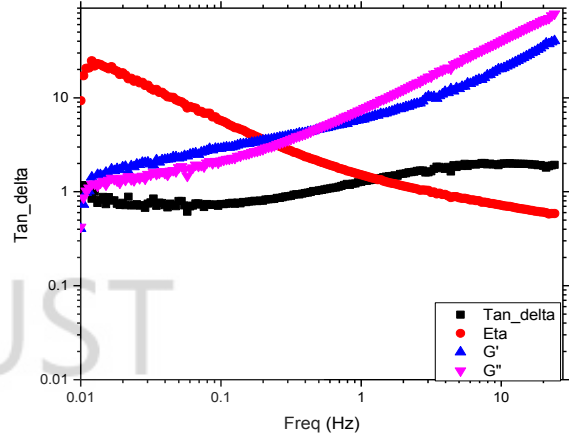
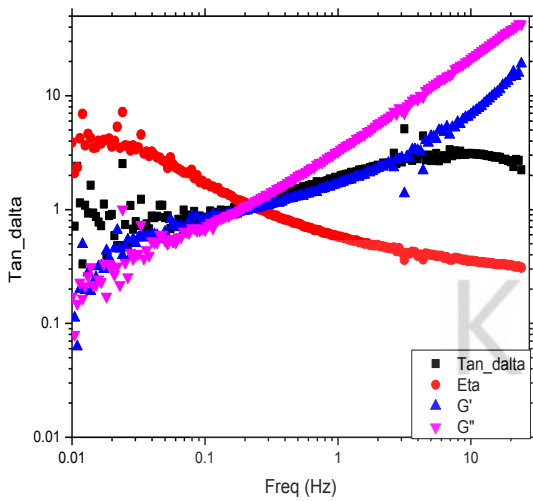
5.5.2 The Viscous and Elastic Responses of the Emulsion-Oscillatory Measurements

This section describes the viscous and elastic responses (viscoelastic behaviour) of the emulsion system by applying dynamic oscillatory measurements. A strain of amplitude γ_0 and frequency ν (Hz) was applied in a sinusoidal manner using a strain controlled ARES rheometer to measure the corresponding stress. The degree of network growth can be deduced from measurements of the viscoelastic properties; since a highly developed network demonstrates a high level elastic response to shear. Additionally, the storage modulus and loss modulus gives information of whether the emulsion is strongly or weakly associated. When weakly associated the system is described as liquid like.

Figure 5-8 shows a graph of the effect of increase in fat content on the viscoelastic properties of the emulsion. The data obtained show how the storage modulus, G' , the loss modulus G'' , the complex viscosity η^* and tan delta (δ) change as a function of frequency. For the emulsion with fat/water ratio of 5/95, low G' and G'' were recorded initially. These were similar at frequencies of 0.01 to 0.4 Hz after which both G' and G'' increased steadily with increasing frequency with the G'' showing higher magnitude than G' . A lower G' and the dependence of both parameters on the frequency indicate a minimal or no network structure within the emulsion system and therefore the emulsion exhibiting a liquid-like behavior. The low fat content leads to a limited number of fat particles hence a weaker network connection. The weaker network results in their failure to accommodate strain therefore a viscous system is observed. However, this viscous behavior changes as the fat concentration increases (Figure 5-8B – 5-8D). Changing from 10/90 to 20/80 fat/water ratio emulsions, showed strong dependency of G' and G'' as frequency changes. The magnitude of G' is observed to be higher than G'' at low frequencies until a critical frequency is reached where there is a crossover from huge G' to small G' and small G'' to a huge G'' .

5/95

10/90



15/85

20/80

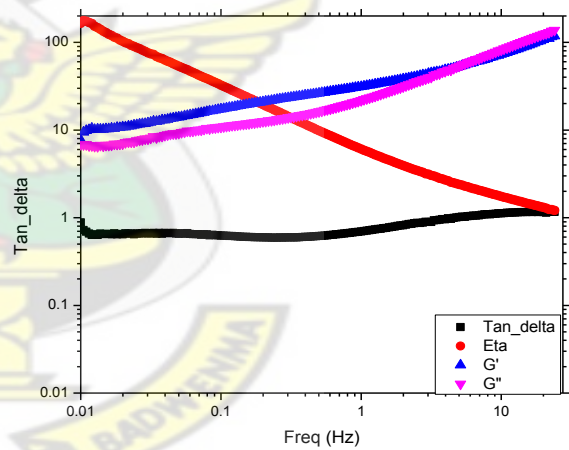
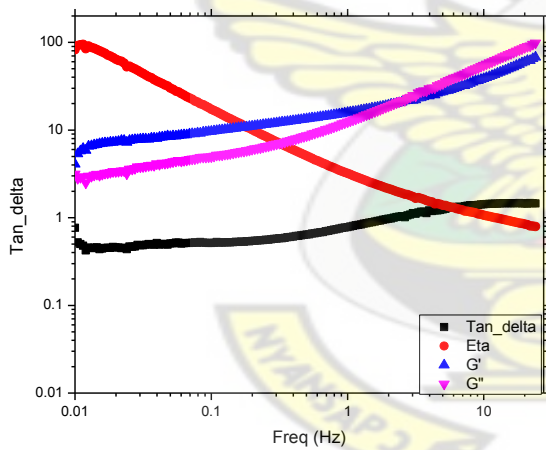


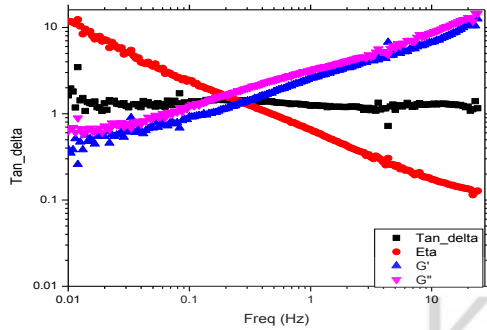
Figure 5-8: A graph of frequency sweep test of emulsions, which shows viscoelastic responses to shear of emulsions prepared from 5/95, 10/90, 15/85 and 20/80 fat/water content in 3% Tween 20 and sodium alginate. The diagram gives the storage (G') and loss (G'') moduli, complex viscosity (Eta^*) and $\tan \delta$ for emulsion with increasing fat content.

The frequency (0.4, 0.8, 4.0, 8.0 for 5/95, 10/90, 15/85, 20/80 respectively) at which the crossover occurred was also found as functionally determined on the fat/water ratio. As the fat content increases, the emulsion exhibits a solid-like behaviour, which is characterized by high G' . It is explained as follows: the presence of the solid fat droplets results in the development of a complex connection within the emulsion system. This leads to the exhibition of a characteristic solid behavior. This solid character is more prominent at low frequencies because at such frequencies the force acting on the emulsion is low and therefore the emulsion is able to keep the network connection. However, as the frequency increases, the network connection is only able to accommodate the force within the oscillation period to the 'critical frequency' after which the network system is completely destroyed leading to the change over from the more elastic system to a viscous system. Furthermore at high frequencies there can be a possible alteration of the total interaction potential due to the adsorbed non-ionic surfactant (Tween 20) or a combination effect of the surfactant and the modifier (sodium alginate) may cause steric repulsion. This may result in a weak gathering of particle-particle network structure, and can rearrange to contain the strain hence the droplet network breakup. The network gets stronger as the fat content increases up to 20 % and a large number of fat particles are present in the emulsion system leading to a highly connected system. This subsequently leads to the increase in the frequency at which the crossover occurs. The frequency at which the crossover occurs was found to be dependent on the fat/water content. This can also be attributed to the fact that the fat presents a crystal network, which contributes to developing of the droplet/droplet connections. The observed reduction in the complex viscosity with increase in frequency

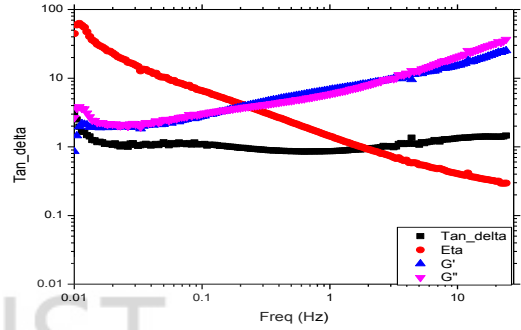
also implies the presence of a network structure, which breakdown as the frequency increases. The dependence of the complex viscosity Eta^* on the frequency indicates that even though there is the existence of the particle-particle inter-connection, the interaction forces between them is weak and hence a breakdown occurring with increase in frequency. This phenomenon is analogous to the apparent viscosity decrease observed with the increase in shear-rate, and is a characteristic of non-Newtonian systems.

The presence of sodium alginate showed a significant effect on the viscous and elastic responses. High values for both G' and G'' were obtained as seen in figure 5-9. Both storage modulus (G') and the loss modulus (G'') increased frequency increases. There was also a marginal decrease in the storage modulus as the frequency increased but this was minimal and so the values obtained for both the G' and the G'' were closely related. The percentage of the sodium alginate leads to the formation of a highly solvated layer near the oil-water interface by forming a conjugated Tween 20-sodium alginate moiety thereby enhancing the steric effect. From this, elevated energies are needed to disintegrate the conductivity of the fat particles. Again the sodium alginate dissolves in the water and forms an overlap concentration network in solution through simple entanglement of their hydrated chains [9]. The sodium alginate forms a 3-dimensional network leading to their elastic rheological behavior. The strength of the network formed is dependent on the number of points (i.e. entanglements), which build up the network, nature and amount of the modifier in the water.

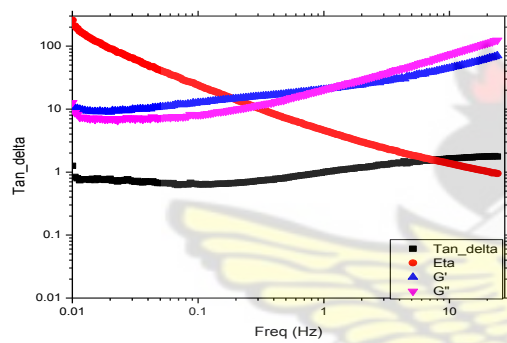
1%NaAl



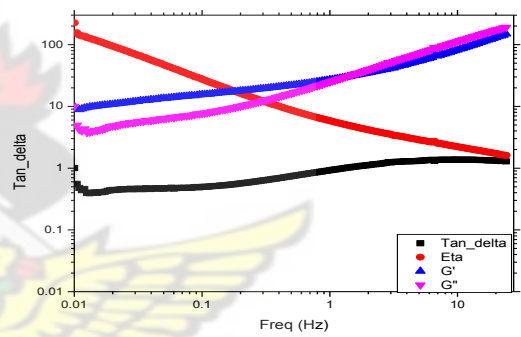
2 % NaAl



3 % NaAl



4 % NaAl



5 % NaAl

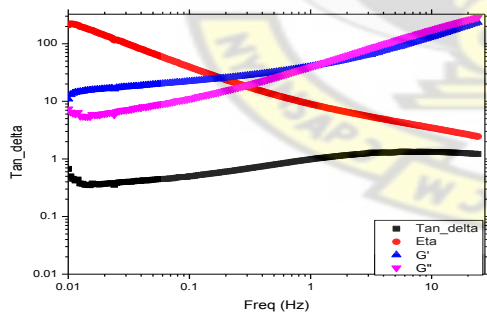


Figure 5-9: A graph of frequency sweep test of emulsions, which shows viscoelastic responses to shear shear of emulsions prepared from 15/85 fat/water content in 3% Tween 20 with increasing sodium alginate. The diagram gives the storage (G') and loss (G'') moduli, complex viscosity (Eta^*) and $\tan \delta$ for emulsion with increasing sodium alginate content.

Considering the data obtained for $\tan \delta$ measurements, it was observed that $\tan \delta$ was less than 1 at low frequencies but as the frequency increases the $\tan \delta$ values increase to become greater than 1. The presence of sodium alginate and the fat particles increases the thickness of the emulsions by forming a network connection hence their solid-like nature. However, at high frequencies this connectivity is destroyed resulting in the development of a liquid-like system. $\tan \delta$ measures the relative magnitude of G' and G'' . When the emulsion has $\tan \delta$ higher than 1, the system is characterised as liquid-like. Values of $\tan \delta$ give information on the viscoelastic nature of the emulsions.

The phase angles as shown in Figure 5-10, values obtained provide information, which confirms the viscous and elastic reaction in the emulsions. For a purely elastic system the phase angle is 0° , and it is 90° for viscous systems. From the study the phase angles measured range from 15° to 80° (Figure 5-10) the emulsion behaviour can be expressed as viscoelastic. For a viscoelastic system, the phase angle takes values in the range of 0 to 90° . As the frequency increases the phase angle also increases till it gets to a steady state after which no change occurs with increasing frequency. At this point the emulsion system is said to show a more viscous behaviour. The lower phase angle measured at the low frequencies also confirms the elastic response of the emulsions to the applied shear stress. This is so because at the lower frequencies the emulsion maintains their gel-like network.

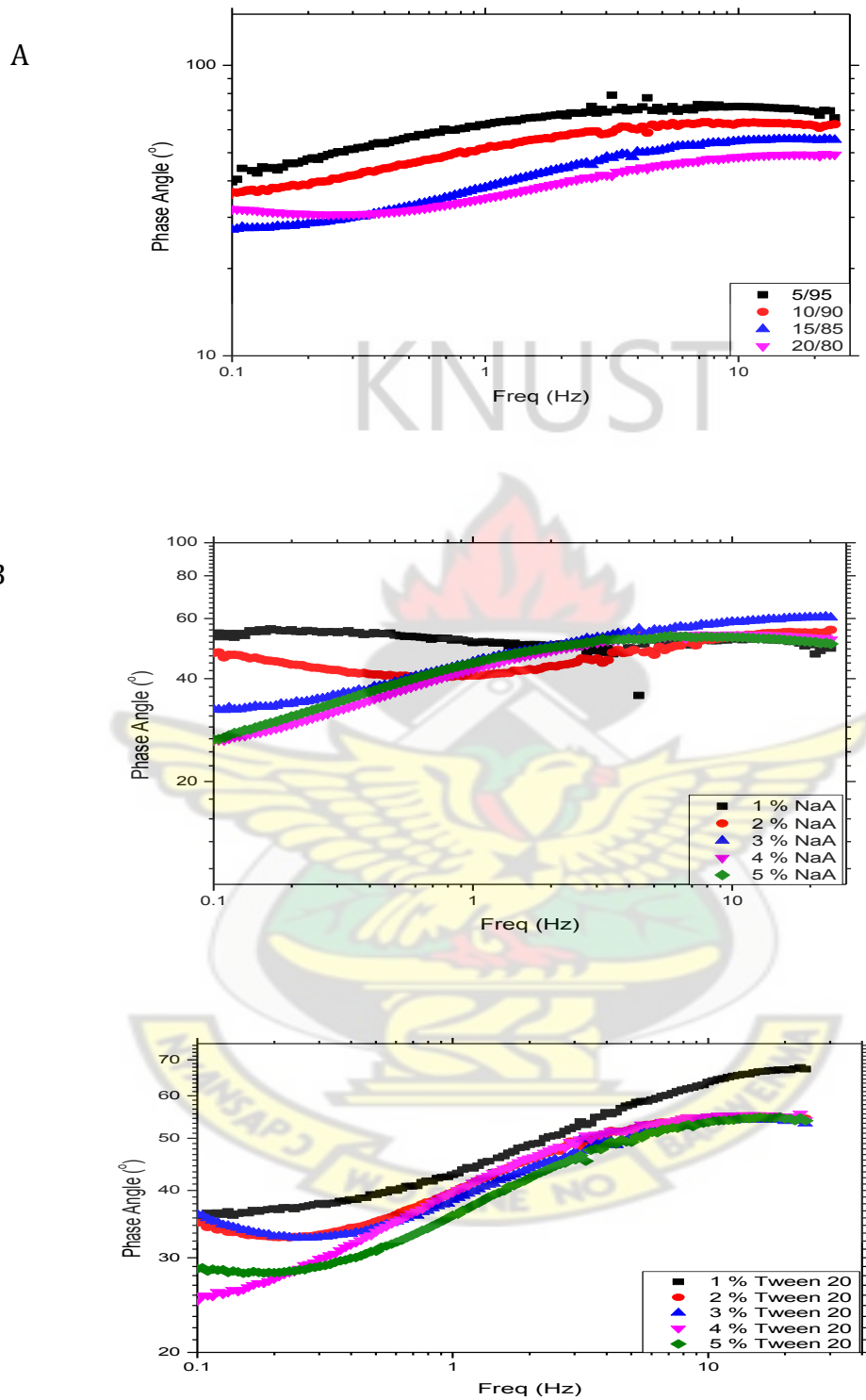


Figure 5-10: The change in phase angle with the frequency sweep at (A) increasing fat content at 3% Tween 20 and sodium alginate content (B) increasing sodium alginate concentration at 3% Tween 20 in 15/85 fat/water content (C) increasing Tween 20 concentration at 3% sodium alginate in 15/85 fat/water content.

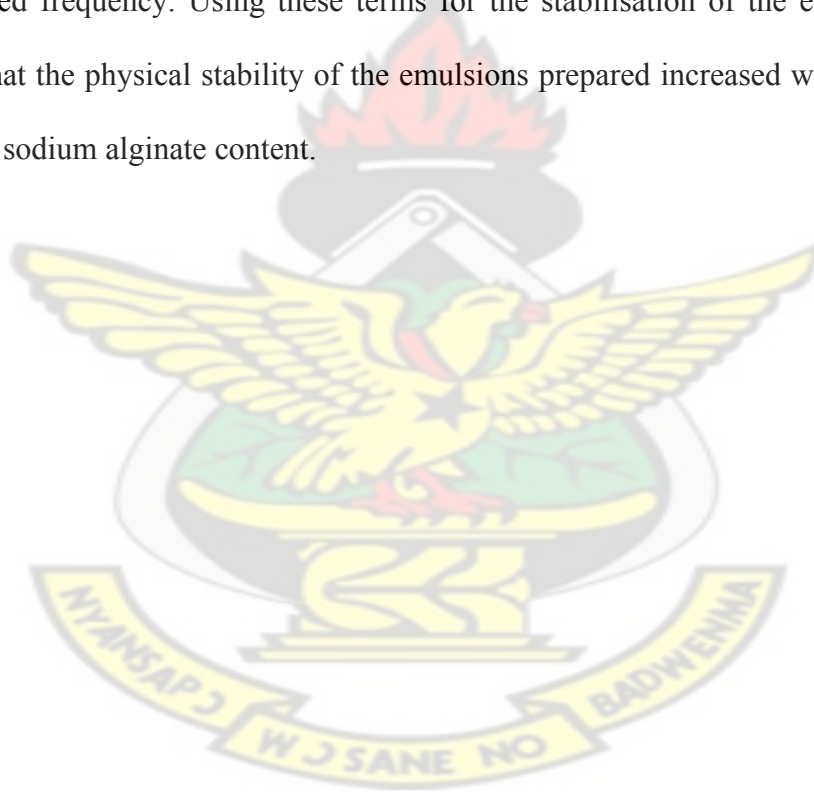
5.6 Conclusion

Homogenization of the melted fat in the aqueous phase gave well-distributed fat particles resulting in a creamy emulsion. The dispersal of fat particles in the continuous aqueous phase was seen in the micrographs obtained using the light microscope. The dispersed fat particles showed a fast instability against aggregation, with the emulsion separating into upper fat layer and a clear lower water layer. Addition of a surfactant (Tween 20) produced emulsions with evenly distributed dispersed fat particles in the continuous aqueous phase which was stable and lasted for about 3 hours after which the emulsions began to break down into two layers due to the de-adsorption of the surfactant molecules. The first was a creamy upper layer, which was ascribed to the interconnectivity of the fat particles, and the second, an opaque aqueous lower layer.

The mixed sodium alginate and Tween 20 emulsifier system gave a stabilised emulsion depending on the fat/water ratio. The emulsions formed showed the size of the particles ranged from 120 nm to 168 nm immediately after emulsification. There was increase in particle size to some extent depending on the fat content as well as the sodium alginate concentration after days of preparation. There was also phase separation for the emulsions produced from 5/95 fat/water ratio and to some extent emulsions produced from the 10/90 fat/water combinations and this phenomenon was linked with the increase in particle size after the 30 days period.

Assessing the stabilisation of the physical properties of the emulsion in the long term, the emulsions were found to show viscoelastic properties where by all emulsion systems

exhibited a profile of $G' > G''$ at the lower frequencies and gradually gave $G'' > G'$ at the higher frequencies and both parameters were found to be dependent on the change in frequency. Considering the dependence of the viscoelastic parameters on the frequency, it can be said that the emulsion system consists of weakly gel network. Since emulsions are categorized as physically unstable when $G'' > G'$ and both parameters depended on the frequency, by this criteria the emulsions produced can be said to exhibit properties of both a concentrated emulsion and dilute emulsion and both characteristics are dependent on the applied frequency. Using these terms for the stabilisation of the emulsion, it is concluded that the physical stability of the emulsions prepared increased with increasing solid fat and sodium alginate content.



CHAPTER 6

Encapsulation of Sudan Orange Dye in Fat Particles in the Fat-in-Water Emulsions

The level of interest in the use of oil-in-water emulsions for encapsulation of poorly water-soluble food and pharmaceutical ingredients as delivery system has increased over the years. Due to their compartmentalized hydrophobic and hydrophilic regions, they have a potential to encapsulate a polar, non-polar and sometimes both polar and non-polar bioactive ingredient for an effective delivery. They also possess the ability to control the chemical stability of the encapsulated active ingredient and to change their rheological properties to suit their specific application. Finally as a delivery system, the emulsion system serves the purpose to protect the active component against any form of chemical degradation.

Currently, several researches are looking at the use of crystallized lipids in emulsions enhance the release control and the stabilisation of the incorporated active ingredients. However, the ability of a solid fat internal phase to effectively encapsulate water insoluble compound depends on the crystallisation pattern of the fat matrix, the stability of the fat-in-water emulsion as well as the physical properties of the active compound itself. In this chapter, the efficiency of encapsulation of poorly water soluble dye in solid fat particles-in-water emulsion is investigated. The physical properties of the solid fat matrix as well as the dye compound are discussed and the method of formulation of the encapsulated product is also discussed. The physical properties of the encapsulated product is analysed and discussed inference to some selected properties including their particles size distribution, the crystallinity of the particles produced and their thermal

properties. The efficiency of the encapsulation process is assessed and discussed against parameters such as the loading capacity, release rate and the rate of leaching of the internal phase.

Since the emulsion stability was strongly affected by the volume phase of the fat/water ratios, (as discussed in the previous chapters), the encapsulated particles were prepared from the Allanblackia seed fat in water (15/85). The emulsions produced in the presence of the dye-loaded particles were found to be stable as the presence of the dye did not affect the emulsion stability. No effort was made to increase the encapsulation efficiency. This work is to only investigate and assess the importance of solid fat crystals in fat-in-water emulsion in delivery systems.

Sudan orange dye is a water insoluble compound (fat soluble) and has been used extensively in the cosmetics, pharmaceuticals and the food industries for the colouring of solvents, oils and other food products.

6.1 Formulation of Encapsulated Fat-in-Water Emulsion Product

6.1.1 Extraction and Characterisation of the Vegetable Fat used as Matrix in the Encapsulation Process

A naturally occurring vegetable fat was obtained from the seeds of Allanblackia fruits by the press extraction as described in section 3.1. The fat contains about 58 % saturated fat and 42 % unsaturated fat. It is observed to melt at around 36 °C and crystalizes at around 16 °C. The high stearic acid content (56.93 %) of the Allanblackia fat gives it the advantage to be used in food and food products. In addition the presence of a β'

polymorphs in its crystallisation process also gives it an added advantage of spreadability and smooth property which is an important characteristic of a food grade emulsion.

6.1.2 Preparation of the Encapsulated Particles

The method of emulsification is described in section 3.2.5.1. The encapsulated sudan orange dye particles (ESODP) were prepared by adding about 0.2 g of the dye compound to an already melted Allanblackia seed fat at 65 °C and the emulsion produced using the simple homogenization technique described in the previous sections. A yellowish creamy substance was obtained as shown in Figure 6-1 and observed for 24 hours to assess its stability against emulsion droplets breakdown. There was no observable separation of layers after the period and hence it was concluded that a stable product was formed.

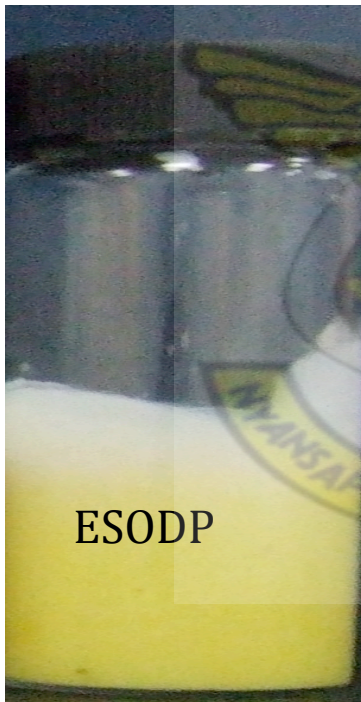


Figure 6-1: Encapsulated Sudan Orange Dye Particles (ESODP) in the crystallized fat particles-in-water emulsion system prepared from 15/85 Fat/water content with 3% Tween 20 and 3% sodium alginate.

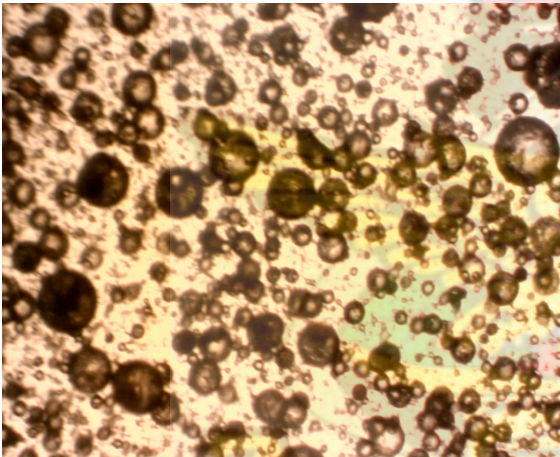
6.2 Characterization of the Encapsulated Sudan Orange Dye Particles (ESODP)

6.2.1 Particle Size and Size Distribution

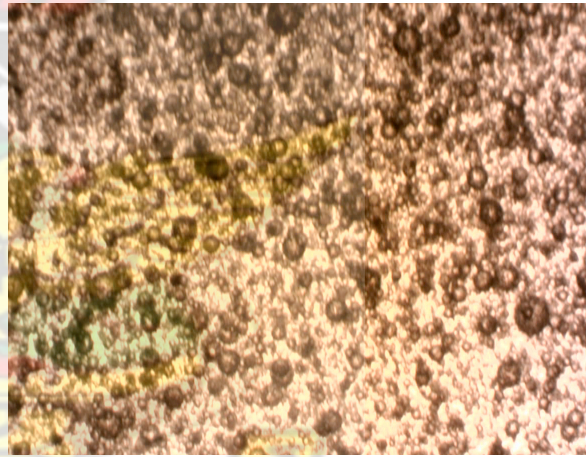
This study investigated the consequence of dye loading on the type and size distribution of the encapsulated particles. Particle size, and size dispersal are essential physical parameters for particulate delivery systems. The particle size was determined by the dynamic light scattering (DLS). The characterisation of the particle size distributions is based on the average size. The distribution of the dye within the solid fat particles was investigated with the light microscope. Both the DLS and the light microscopic analysis showed that the dye-free and dye-loaded particles contained spherical non-aggregated particles. From the results, it was observed that the dye showed a substantial impact on the particle size with mean sizes ranging from around 246.3 to 252.2 nm as compared to that of dye-free emulsion particle (136.8 to 163.2). The increase in size of the encapsulated particles is due to the presence of the dye, which is non-polar and has the ability to be incorporated into the solid fat network that is due to the occurrence of molecular diffusion of the water insoluble dye throughout the oil phase. This results in the overall size increase of the crystals formed in the emulsion particles. The encapsulated system also showed a wide particle dispersal as demonstrated by the polydispersity index (PDI) value of 0.30 and 0.31. After the homogenisation process, the emulsion was taken from the heat source and left to cool. The cooling process leads to the crystallisation of the dispersed fat droplets which was characterised by nucleation and a subsequent crystal growth in the emulsion system. Since the melting point of Sudan orange dye is higher (144 °C) than that of the vegetable fat matrix, the dye will experience supercooling at a much greater degree in the cooling process thereby forming

an initial nuclei upon which there is the occurrence of the crystal growth within the droplets. The formation of the stable nuclei from the melt leads to the growth of the crystals [75, 214]. As the crystals exhibit different faces, each face grows at distinctive rates, and this may to some extent account for the wide variety of different particle sizes formed. Also once the nuclei formed there is the possibility of mass transfer of the liquid fat molecules to the solid-liquid interface hence the ability to encapsulate the solid dye particles. The light microscope image Figure 6-2 showed no significant aggregation or flocculation and the particles generally spherical in shape with varying size distribution.

A



B



C



D

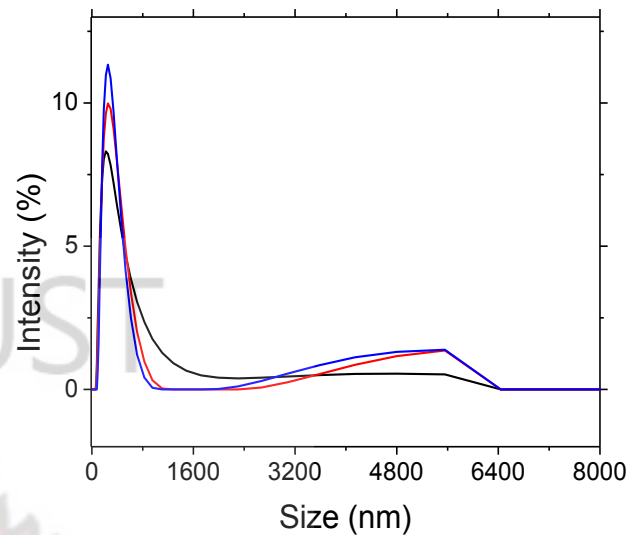


Figure 6-2: Light microscope images of (A) Encapsulated emulsion particles (B) fat-in-water emulsion particles (C) Magnified encapsulated dye particles in the fat matrix (D) particle size distribution from the DLS

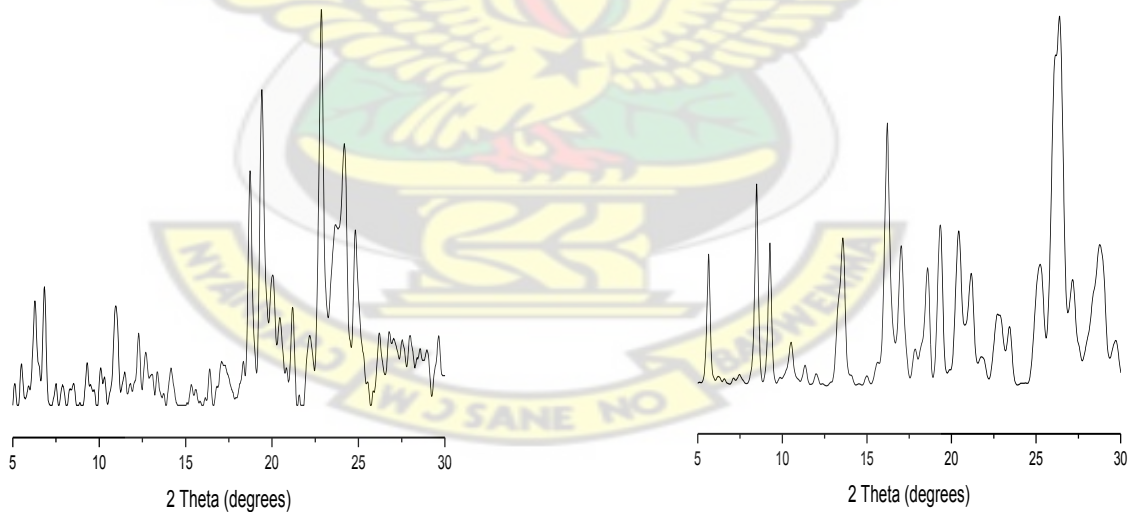
6.2.2 X-ray Diffraction Analysis

In order to examine the shielding ability of the solid fat matrix and the packing structure of the encapsulated particles, X-ray diffraction analysis was performed. The diffraction pattern and data obtained are shown in Figure 6-3. The diffraction obtained is compared with that for the sudan orange dye (raw material) and the Allanblackia fat. Generally Sudan Orange dye shows a cluster of peaks at 2θ of $25^\circ - 30^\circ$ but this was missing in the diffraction pattern of the encapsulated particles. The intensity of the signals at 2θ of $5^\circ - 15^\circ$ found in the diffraction of the Sudan Orange material showed a reduction in that of the encapsulated particles. On the other hand there was the presence of highly intense signal at 2θ of $20 - 25^\circ$ in the diffraction pattern of the encapsulated particles, which correspond to the signals obtained from the Allanblackia seed fat used as matrix. These

signals found in the fats have d-spacing values of 5.4 Å, 4.6 Å and 3.6 Å indicating the presence of β polymorphs in the fat. The absence and/or low signal diffractions of the diffraction pattern of the encapsulated dye shows the amorphousness of the material after the encapsulation process and this can influence the pattern of the encapsulated compound [117]. The shift in peak positions and the subsequent reduction in the intensity may be as a result of the destruction of the packing structure of dye. The crystallinity of the dye compound may also be affected by the presence of the alginate molecules in the emulsion system as polymer chains such as the alginate molecules with alternating sequence of inelastic and elastic units may exhibit liquid crystallinity [215].

A

B



C

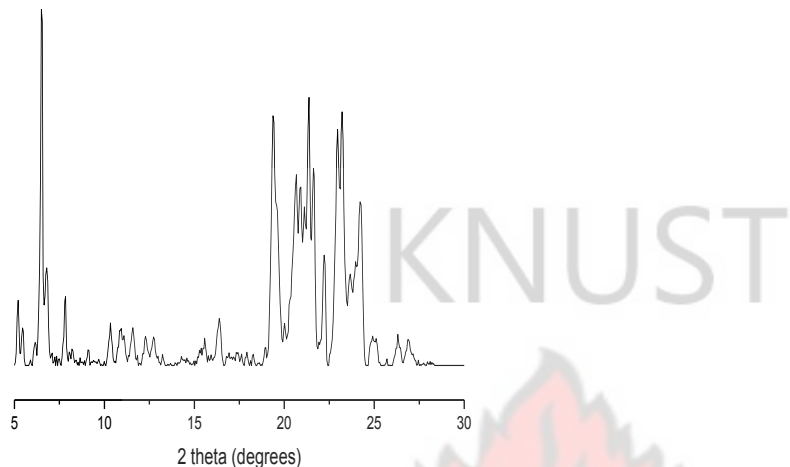
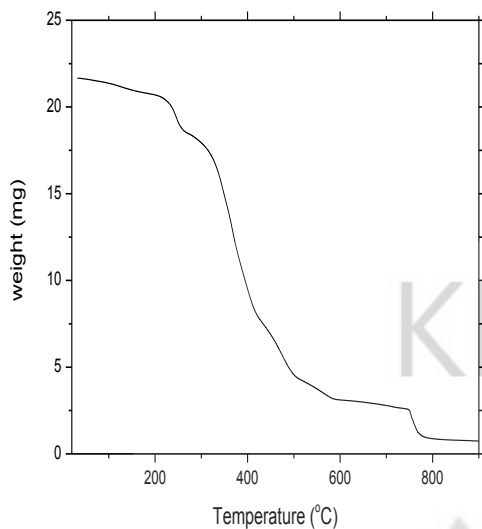


Figure 6-3: Diffraction patterns of (A) Encapsulated particles (B) Raw sudan orange dye particles and (C) Allanblackia fat crystals

6.2.3 Thermal Properties for Encapsulated Particles

Characterization of the thermal behavior of the encapsulated particles was carried out to estimate the effect of the emulsion ingredients on the physico-chemical properties of the emulsion system containing the encapsulated particles. This is important for their use in the delivery of active compounds in the food and pharmaceutical industries. The thermal properties were determined by the thermogravimetric analysis (TGA), and differential scanning calorimetry (DSC) and results shown in Figure 6-4.

A



B

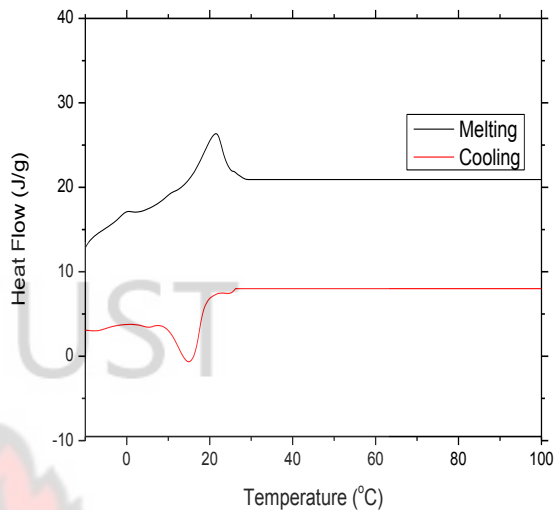


Figure 6-4: (A) Thermal decomposition curves of the encapsulated particles obtained from the thermogravimetric Analysis (TGA) and (B) Melting and Cooling profile of the encapsulated particles obtained from the differential scanning calorimetry (DSC).

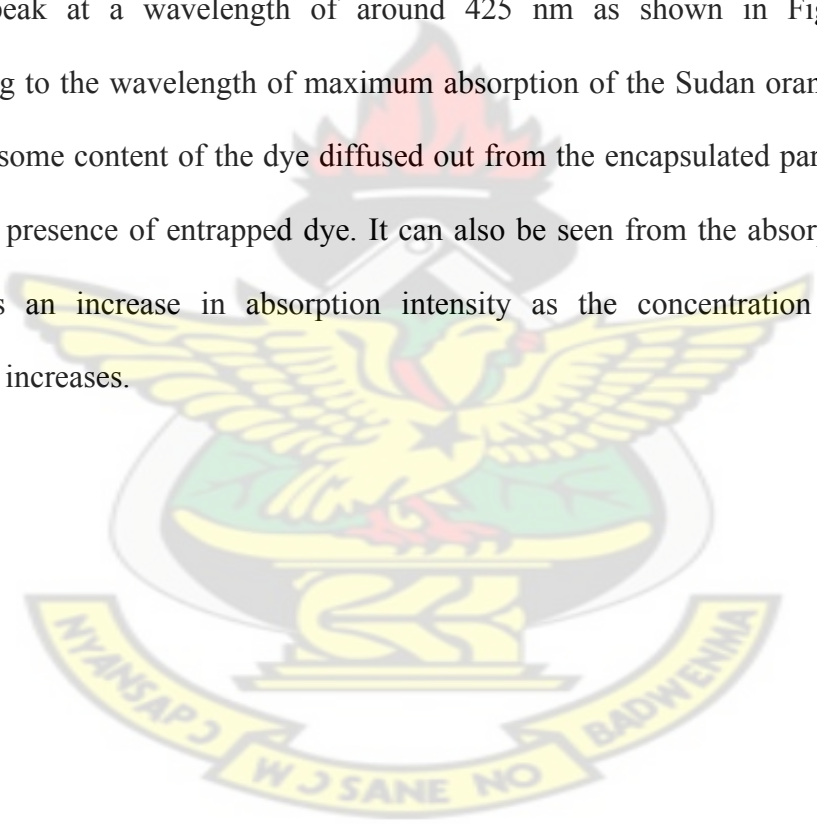
The use of thermogravimetric analysis was to investigate the variation in weight of a material as a with temperature change. This was first investigated to assess the effect of change in temperature on the encapsulated particles in the emulsion system. Figure 6-4 shows that the weight of the encapsulated emulsion decreases with increasing temperature from 100 to 800°C. It was observed that the encapsulated emulsion showed a multiple step degradation process as indicated in Figure 6-4A. This weight loss reflects the degradation of each of the components present in the emulsion system. The DSC gave the melting and cooling pattern of the encapsulated particles. Figure 6-4B shows the melting and cooling profiles for the encapsulated emulsion system. The results shows a major melting and crystallisation peaks at 15 – 26 °C and 15 – 22°C respectively. The

melting and cooling profiles show the encapsulated particles are crystalline at room temperature with its corresponding crystallisation temperature at 26 °C.

During the cooling of the emulsions, the dye crystallizes out first to produce the nucleus of the crystallized particles. This step is nucleation and it initiates the crystallisation process after which there is the occurrence of the crystal growth, therefore the high melting point of the encapsulated compound has a great effect on the over crystallisation of the encapsulated emulsion system. Even though the dye compound has a high melting point (146 °C), this did not considerably influence the melting point of the particles because they are completely soluble in the fat and so the dye dissolves as soon as the liquid fat is formed. This characteristic shows the dissolving property of the liquid fat for the poorly water soluble compound. The fat matrix crystallizes at 35 °C but this was reduced after it has been used in the emulsion system. The reduction in the melting point of the encapsulated fat particles may be as a result of the fact that small amounts of the fat is used in the preparation of the emulsion and the encapsulation, this therefore leads to a reduction in the crystal interactions. The lower the crystal interactions the lesser the energy required to overcome the crystal interaction for the melting to occur. The reduction can also be as a result of the presence of the emulsifier especially the presence of the Tween 20 surfactant which is liquid at room temperature can dilute the fat material hence causing a reduction in the melting point. On the other hand there is an observed increase in the crystallisation temperature, this is attributed to the high melting dye, which experiences supercooling, and begins to crystallize out early and therefore affecting the overall crystallisation of the encapsulated particles.

6.3 Encapsulation Efficiency

The dye load and the efficiency of the encapsulation process are important indicators to evaluate the delivery properties and advantages of the emulsion system for delivery products. The success of the encapsulation of the dye in the solid fat crystals was also confirmed by UV–vis spectrophotometric analysis for the loading capacity and their release rate pattern. The emulsion particles showed no absorption bands at wavelengths ranging from 300 to 500 nm, while the dye-loaded emulsion particles gave a maximum absorption peak at a wavelength of around 425 nm as shown in Figure 6-5 A, corresponding to the wavelength of maximum absorption of the Sudan orange dye. This implied that some content of the dye diffused out from the encapsulated particles, which indicates the presence of entrapped dye. It can also be seen from the absorption spectra that there is an increase in absorption intensity as the concentration of the dye encapsulated increases.



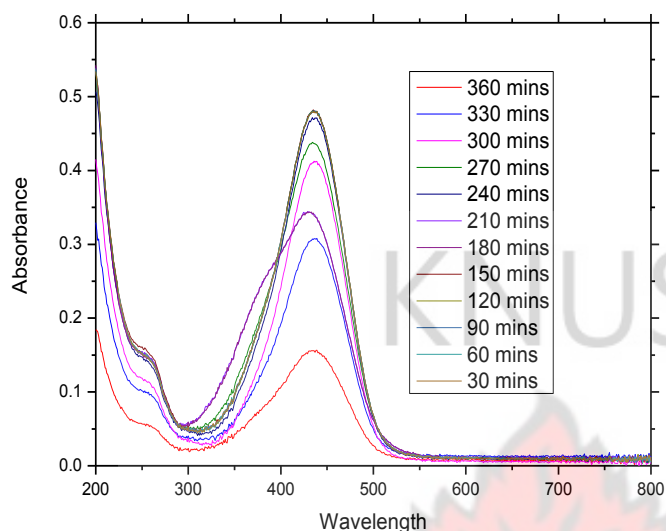


Figure 6-5: UV-vis absorption spectra of supernatant obtained from immersing encapsulated particles in water at different time intervals.

The whole purpose of the dye encapsulation is to study the ability of the fat matrix to protect the encapsulated dye from environmental stress and chemical degradation. Even though, the method used and the ingredients for the emulsion production usually may lead to a successful encapsulation, the quality of the end product in terms of their appearance and taste are also important in measuring of the success of the encapsulation process and its use as a delivery system. For this reason, the release rate and the rate of leaching were also investigated to determine the possible effect of the continuous aqueous phase on the encapsulated dye.

These measurements were used to investigate the efficiency of encapsulation. In order to determine the release rate, the encapsulated particles were soaked in water at different intervals and the supernatant filtered and their absorbance measured. It was observed that there was an initial (first 180 min) fast release of the dye into the water after which there was a decline in the amount of dye released with increasing time (210 – 360 mins). This is shown in Figure 6-5. The initial burst in release may be as a result of the fast surface desorption of the dye molecules, which were not completely embedded in the particles in the crystallized structure. However, as the same particles are soaked in different portions of the deionized water, there was a decline in the release even as the time increases. This may be as result of the fact that the rest of the dye was entrapped within the fat structure, which prevented the dye from diffusing into the aqueous phase.

Furthermore the efficiency of the encapsulation process was confirmed by the occurrence of leaching of the entrapped dye substance. The leaching studies were conducted to investigate any possible leakages of the internal phase into the continuous aqueous phase with time. The results showed that there was a leakage of about 36 % after about 4 hours. The percentage leaching was obtained as the weight loss after drying the particles over a period of time. The loss of weight is attributed to the presence of some of the dye particles, which may be loosely settled at the particle surface, and also the loss of some amount of moisture associated within the alginate layer. The loosely adhered dye particles and the alginate moisture makes up the 36 % of the total weight of the encapsulated particles at 240 mins after which there was a decline in leaching. Only the dye molecule found on the surface of the particles and those that were found in the alginate layer could come out because the dye found in the internal phase (corresponding

to about 64 %) is protected by the strong physical structure of the fat matrix.

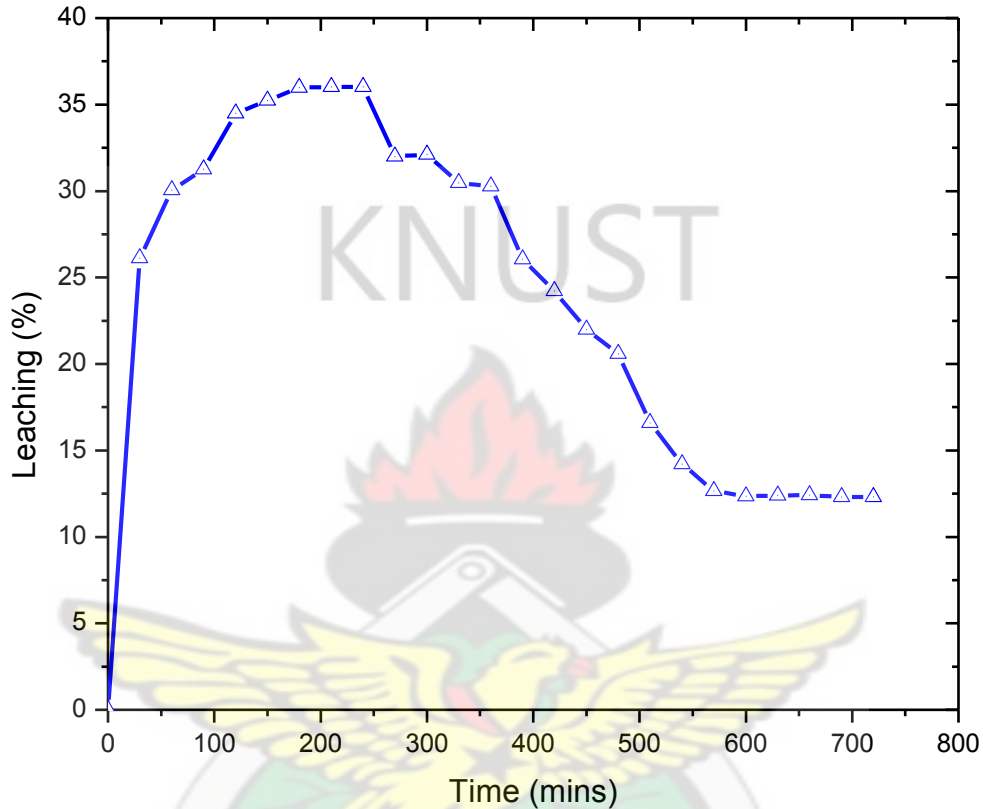


Figure 6-6: A plot of percent leaching of the dye from the encapsulated particles at different time intervals.

6.4 Conclusion

The formulation of encapsulated solidified fat particles and the efficiency of encapsulation of the solid fat particles-in-water emulsion for a poorly water-soluble compound were studied. A sudan orange dye was encapsulated in a fat-in-water emulsion by an emulsification method. The experimental results indicated that the solid fat could be used as a matrix for the development of a stable oil-in-water emulsion for its

application in the delivery of bioactive compounds. Results obtained for the particle size distribution analysis gave high particle sizes ranging from 246 to 250 nm. The encapsulated particles were smooth and spherical in shape with varying size distribution, which was as a result of the crystallisation mechanism of both the fat matrix and the sudan orange dye internal phase which are all solid substances at room temperature. The XRD data obtained showed a reduction in the crystallinity of both the fat matrix and the dye substance as a result of the presence of the alginate polymer, the aqueous phase and the Tween 20 surfactant. This was confirmed in the melting and cooling profile obtained from the DSC analysis. The results from the UV-vis analysis of the dye loading capacity showed a successful entrapment of the dye in the fat matrix. The spectra obtained showed an increase in the absorption intensity as the dye concentration increases. The rate of release of the dye and the leaching capacity showed effective encapsulation process. The study gave a possible leakage of 36 % of the dye substance at the maximum incubation time. The reductions in the leakage of the dye suggest the encapsulated particles can be stored for longer periods, which is an advantage of improved stability during storage and transportation. It is therefore concluded that fat crystal are capable of encapsulating bioactive substances for effective and sustained delivery mechanism.

CHAPTER 7

Conclusions and Recommendations

This thesis described the effects of solid fat particles and mixtures of sodium alginate and Tween 20 surfactant on the stabilisation mechanism of dispersed fat particles in water continuous aqueous segment in the emulsion. The focus of this work was as follows:

- To characterize the chemical constituents of two vegetable fats as well as to determine the effect of these chemical constituents on their thermal behaviour.
- To develop an oil-in-water emulsion using vegetable fat as the dispersed phase and stabilised by both a surfactant and a thickener
- To study the consequence of the mixture of surface active agent and thickener on the stabilisation mechanism of emulsions produced,
- Investigate the flow properties of the emulsion produced, and to encapsulate an active component and determine the efficiency of the encapsulation.

The conclusions drawn from the work and the recommendations made are as follows:

7.1 Conclusion

7.1.1 Chemical Constituents and Thermal Properties of Shea Butter and Allanblackia Seed Fat

The Allanblackia seed fat and the shea butter fat were found to contain about 58 % saturated, 42 % unsaturated fatty acids and 51 % saturated and 49 % unsaturated fatty acids respectively. Higher saturated fatty acid content accounts for the higher melting

point of the Allanblackia seed fat as compared to that of the Shea nut fat. The high melting point of the Allanblackia fat gives it the advantage of rigidity, which makes it convenient in terms of the handling and processing. Both the Allanblackia seed fat and shea nut fat showed polymorphic transformation in their crystallisation processes and this is as a result of the presence of TAGs with high melting temperatures. Allanblackia fat showed the formation of β' polymorphs in their crystallized fat. The β' polymorphic transformation gives the Allanblackia seed fat a good functionality and desirable plastic fats properties. The magnitude and position of the crystallisation exotherms of the Allanblackia and the shea nut fat were affected by rate of cooling. Additionally the crystallisation mechanism according to the isothermal crystallisation kinetics and the Avrami model, of both shea nut fat and the Allanblackia seed fat showed a two-step crystallisation mechanism.

7.1.2 Formulation and Stabilisation of Fat Particles-in-Water Emulsions

The stabilisation of the fat particles-in-water using the combined mixture of sodium alginate and Tween 20 emulsifier system was found to be dependent on the amount of the fat dispersed. At high concentrations the dispersed fat emulsions were stable against creaming while lower amounts of the fat showed instability against creaming. This implies that at the small fat content, the number of fat particle units produced within the emulsion system was small as compared with the total volume of the emulsion. These particles as generated were widely spread and spaced out to fill up the total volume of the emulsion system. The particles are in constant motion and since they are less dense as compared with the aqueous phase, they travel up faster with no or little obstruction in the aqueous phase. They settle on top of the aqueous phase and form aggregation leading to

the creamy upper layer. On the other hand high amount of fat leads to reduced water system used and huge number of fat units are distributed in the continuous phase. At high fat content, particles are closely packed and with the presence of the sodium alginate to prevent particles aggregation induces the formation of interconnecting fat particles, which results in the forming a network among the dispersed particles.

Again, sodium alginate and the Tween 20 emulsifiers gave a synergistic stabilisation influence to the emulsions. Long lasting physical stabilisation was seen to be dependent on both fat and sodium alginate content. Increase in the fat content, increased the fat particle connectivity which introduces some level of rigidity to the emulsions. The rigid network dictates the viscoelastic responds of the emulsion system. When sodium alginate was increased it increased the gel-like network in the emulsions, which increased the storage response leading to a more stable emulsion.

7.1.3 Encapsulation of Sudan Orange Dye in the Fat particles-in-Water Emulsion

The sudan orange dye was encapsulated in a fat-in-water emulsion by an emulsification method. This gave high particle sizes of 246 - 250 nm. Encapsulated particles were smooth and spherical in shape with varying size distribution, which was as a result of the crystallisation mechanism of both the fat matrix and the sudan orange dye internal phase. The results from the UV-vis analysis for the dye loading capacity showed a successful entrapment of the dye in the fat matrix. The spectra obtained showed that there was increase in the absorption intensity as the dye concentration increases. The rate of release of the dye and the leaching capacity showed effective encapsulation process. The study gave a maximum leakage of 36 % of the dye after which the rate of leakage of the dye reduced as incubation time increased. The reductions in the leakage of the dye suggest

the encapsulated particles can be stored for longer periods, which is an advantage of improved stability during storage and transportation.

7.1.4 General Conclusions

The research has shown that the properties of both *Allanblackia* seed fat and the shea nut fat depends on their fatty acids constituents and their crystallisation patterns depends on the cooling rate program used. It also shown that there is the occurrence of polymorphic transformations during their crystallisation processes.

The study further showed that stable fat particles-in-water emulsions could be formulated by using simple homogenization technique in the presence mixtures of a surfactant and rheological modifiers. It was found that the stability of the dispersed fat particles depended on the amount of fat used, since the stability increased with increasing fat content. The presence of the sodium alginate introduced a gel-like network, which entrapped the fat particles thereby restricting their movement in the emulsion system. The inhibited movement of the fat particles prevents particle-particle collision and hence improved stability against creaming.

Additionally, sudan orange dye, a water insoluble dye was effectively encapsulated within the dispersed fat particles with results from the UV-vis analysis showing a successful entrapment of the dye in the fat matrix. The release rate also showed that about 36 % of the dye was released into water after which the rate of release reduced even at long incubation times. The reductions in the leakage of the dye suggest the encapsulated particles can be stored for longer periods, which is an advantage of improved stability during storage and transportation.

7.2 Recommendations

1. Findings from this study provides basic information on the thermal behaviour of both shea nut fat and Allanblackia seed fat, and this can be used as a starting point for further studies on the variation in their thermal behavior of different varieties of shea nut fat and Allanblackia seed fat.
2. The research attempted to study the consequence of highly saturated vegetable fat used to formulate structured oil-in-water emulsion as their purpose in the food, pharmaceutical and cosmetics industries. For the long-term application of such an emulsion system in the various applications, it will be interesting to investigate the stability of the emulsion against oxidation since the presence of the alginate may influence the occurrence of oxidation in the emulsion.
3. In this work, the influence of the size of dispersed fat units on the stabilisation process in the emulsion was investigated. Nonetheless the sodium alginate works by increasing the viscosity of the water phase, which leads to a decline in the speed of the homogenizer, hence the possible production of larger particles. Therefore it will be interesting for further work to be done using different rheological modifiers which will not have a significant effect on the homogenization process.

References

1. Patidar K, Kshirsagar M, Saini V, Joshi P, Soni M: **Solid Dispersion Technology: A Boon for Poor Water Soluble Drugs.** *Indian J Nov Drug Deliv* 2011, **3**:83–90.
2. Rahman A, Hussain A, Hussain S, Mirza MA: **Role of Excipients in Successful Development of Self-Emulsifying / Microemulsifying Drug delivery system (SEDDS / SMEDDS).** *Drug Dev Ind Pharm* 2013, **39**(January 2012):1–19.
3. McClements DJ: **Crystals and Crystallization in Oil-in-Water Emulsions: Implications for Emulsion-based Delivery Systems.** *Adv Colloid Interface Sci* 2012, **174**:1–30.
4. Ting Y, Xia Q, Li S, Ho C-T, Huang Q: **Design of High-loading and High-stability Viscoelastic Emulsions for Polymethoxyflavones.** *Food Res Int* 2013, **54**:633–640.
5. Tadros TF: *Emulsion Formation , Stability , and Rheology.* First Edit. Wiley-VCH Verlag GmbH & Co. KGaA.; 2013:1–75.
6. Tadros T: *Emulsion Science and Technology: A General Introduction.* WILEY-VCH Verlag GmbH & Co. KGaA, Weinheim ISBN:; 2009:1–56.
7. Rosen MJ: *Surfactants and Interfacial Phenomena.* Third Edit. John Wiley & Sons, Inc., Hoboken, New Jersey. Published; 2004:1–455.
8. Pichot R, Spyropoulos F, Norton IT: **O/W Emulsions Stabilised by Both Low Molecular Weight Surfactants and Colloidal Particles: The Effect of Surfactant Type and Concentration.** *J Colloid Interface Sci* 2010, **352**:128–35.
9. Pallandre S, Decker E a, McClements DJ: **Improvement of Stability of Oil-in-Water Emulsions Containing Caseinate-Coated Droplets by Addition of Sodium Alginate.** *J Food Sci* 2007, **72**:E518–24.
10. Johansson I, Svensson M: **Surfactants Based on Fatty Acids and Other Natural Hydrophobes.** *Curr Opin Colloid Interface Sci* 2001, **6**:178–188.
11. Weiss J, Decker E a., McClements DJ, Kristbergsson K, Helgason T, Awad T: **Solid Lipid Nanoparticles as Delivery Systems for Bioactive Food Components.** *Food Biophys* 2008, **3**:146–154.
12. Strickley R: **Solubilizing Excipients in Oral and Injectable Formulations.** *Pharm Res* 2004, **21**.
13. Müller RH, Mäder K, Gohla S: **Solid lipid nanoparticles (SLN) for controlled drug delivery - a review of the state of the art.** *Eur J Pharm Biopharm* 2000, **50**:161–77.

14. Rousseau A: **Fat Crystals and Emulsion Stability - A Review.** *Food Res Int* 2000, **33**:3–14.
15. Hasenhuettl GL: **Synthesis and Commercial Preparation of Food Emulsifiers.** In *Food Emuls Their Appl.* Second Edi. Edited by Hasenhuettl GL, Hartel RW. Springer New York; 2008:11–37.
16. McClements DJ, Li Y: **Structured Emulsion-based Delivery Systems: Controlling the Digestion and Release of Lipophilic Food Components.** *Adv Colloid Interface Sci* 2010, **159**:213–28.
17. Hu FB, Stampfer MJ, Manson JE, Ascherio A, Colditz G a, Speizer FE, Hennekens CH, Willett WC: **Dietary Saturated Fats and their Food Sources in Relation to the Risk of Coronary Heart Disease in Women.** *Am J Clin Nutr* 1999, **70**:1001–8.
18. Thanasukarn P, Pongsawatmanit R, McClements DJ: **Impact of Fat and Water Crystallization on the Stability of Hydrogenated Palm Oil-in-Water Emulsions Stabilized by a Nonionic Surfactant.** *J Agric Food Chem* 2006, **54**:3591–7.
19. Fuller GT, Considine T, Golding M, Matia-Merino L, MacGibbon A, Gillies G: **Aggregation Behavior of Partially Crystalline Oil-in-Water Emulsions: Part I – Characterization Under Steady Shear.** *Food Hydrocoll* 2014.
20. Choi C-H, Jung J-H, Rhee YW, Kim D-P, Shim S-E, Lee C-S: **Generation of Monodisperse Alginate Microbeads and in situ Encapsulation of Cell in Microfluidic Device.** *Biomed Microdevices* 2007, **9**:855–62.
21. Zhang FJ, Cheng GX, Gao Z, Li CP: **Preparation of Porous Calcium Alginate Membranes/Microspheres via an Emulsion Templating Method.** *Macromol Mater Eng* 2006, **291**:485–492.
22. Xie M, Olderøy MØ, Andreassen J-P, Selbach SM, Strand BL, Sikorski P: **Alginate-controlled Formation of Nanoscale Calcium Carbonate and Hydroxyapatite Mineral Phase within Hydrogel Networks.** *Acta Biomater* 2010, **6**:3665–75.
23. Dang TD, Joo SW: **Preparation of Tadpole-shaped Calcium Alginate Microparticles with Sphericity Control.** *Colloids Surf B Biointerfaces* 2013, **102**:766–71.
24. Meier M a. R, Metzger JO, Schubert US: **Plant Oil Renewable Resources as Green Alternatives in Polymer Science.** *Chem Soc Rev* 2007, **36**:1788.
25. Hill K: **Fats and Oils as Oleochemical Raw Materials.** *Pure Appl Chem* 2000, **72**:1255–1264.

26. Lu Y, Larock R: **Novel Polymeric Materials from Vegetable Oils and Vinyl Monomers: Preparation, Properties, and Applications.** *ChemSusChem* 2009, **2**:136–47.
27. Drewnowski A, Popkin BM: **The Nutrition Transition : New Trends in the Global Diet.** *Nutr Rev* 1997, **55**:31–43.
28. Aparicio R, Aparicio-Ruiz R: **Authentication of Vegetable Oils by Chromatographic Techniques.** *J Chromatogr A* 2000, **881**:93–104.
29. Willett W, Sacks F: **Mediterranean Diet Pyramid: A Cultural Model for Healthy Eating.** *Am J Clin Nutr* 1995, **61**(suppl):1402S–1406S.
30. Marangoni AG, Acevedo N, Maleky F, Co E, Peyronel F, Mazzanti G, Quinn B, Pink D: **Structure and Functionality of Edible Fats.** *Soft Matter* 2012, **8**:1275–1300.
31. Ruiz-Samblás C, Marini F, Cuadros-Rodríguez L, González-Casado A: **Quantification of Blending of Olive Oils and Edible Vegetable Oils by Triacylglycerol Fingerprint Gas Chromatography and Chemometric Tools.** *J Chromatogr B Analyt Technol Biomed Life Sci* 2012, **910**:71–7.
32. Sanders TA: **Polyunsaturated Fatty Acids in the Food Chain in Europe.** *Am J Clin Nutr* 2000, **71**(1 Suppl):176S–8S.
33. FAO: *Fats and Fatty Acids in Human Nutrition.* Rome; 2008:9–36.
34. Ramos MJ, Fernández CM, Casas A, Rodríguez L, Pérez A: **Influence of Fatty Acid Composition of Raw Materials on Biodiesel Properties.** *Bioresour Technol* 2009, **100**:261–8.
35. Miyake Y, Yokomizo K, Matsuzaki N: **Rapid Determination of Iodine Value by ¹H Nuclear Magnetic Resonance Spectroscopy.** *J Am Oil ...* 1998, **75**:15–19.
36. Galià M, de Espinosa LM, Ronda JC, Lligadas G, Cádiz V: **Vegetable Oil-based Thermosetting Polymers.** *Eur J Lipid Sci Technol* 2010, **112**:87–96.
37. Xia Y, Larock RC: **Vegetable Oil-based Polymeric Materials: Synthesis, Properties, and Applications.** *Green Chem* 2010, **12**:1893.
38. Andjelkovic DD, Valverde M, Henna P, Li F, Larock RC: **Novel Thermosets Prepared by Cationic Copolymerization of Various Vegetable Oils—Synthesis and their Structure–Property Relationships.** *Polymer (Guildf)* 2005, **46**:9674–9685.
39. Park S-J, Jin F-L, Lee J-R: **Synthesis and Thermal Properties of Epoxidized Vegetable Oil.** *Macromol Rapid Commun* 2004, **25**:724–727.

40. Zlatanić A, Lava C, Zhang W, Petrovic SZ: **Effect of Structure on Properties of Polyols and Polyurethanes Based on Different Vegetable Oils.** *J Polym Sci Part B Polym Phys* 2004, **42**:809–819.
41. McClements DJ, Decker EA: **Lipid Oxidation in Oil-in-Water Emulsions : Impact of Molecular Environment on Chemical.** *J Food Sci* 2000, **65**:1270–1282.
42. Nikovska K: **Study of Olive Oil-in-Water Emulsions with Protein Emulsifiers.** *Emirates J Food Agric* 2012, **24**:17–24.
43. Mark J: *Physical Properties of Polymers Handbook.* American Institute of Physics, Woodbury, New York; 2007:379–398.
44. Sato K: **Crystallization Behaviour of Fats and Lipids - A Review.** *Chem Eng Sci* 2001, **56**:2255–2265.
45. Che Man YB, Tan CP: **Comparative Differential Scanning Calorimetric Analysis of Vegetable Oils: II. Effects of Cooling Rate Variation.** *Phytochem Anal* 2002, **13**:142–51.
46. Tan CP, Man YBC: **Differential Scanning Calorimetric Analysis of Edible Oils : Comparison of Thermal Properties and Chemical Composition.** *J Am Oil Chem Soc* 2000, **77**:143–155.
47. Zhang X, Li L, Xie H, Liang Z, Su J, Liu G, Li B: **Comparative Analysis of Thermal Behavior, Isothermal Crystallization Kinetics and Polymorphism of Palm Oil Fractions.** *Molecules* 2013, **18**:1036–52.
48. Walker R, Bosin W: **Comparison of SFI, DSC and NMR Methods for Determining Solid-liquid Ratios in Fats.** *J Am Oil Chem Soc* 1971:50–53.
49. Vittadini E, Lee J, Frega N: **DSC Determination of Thermally Oxidized Olive Oil.** *J Am Oil Chem* 2003, **80**:533–537.
50. Alakali JS, Eze SO, Ngadi MO: **Influence of Variety and Processing Methods on Specific Heat Capacity of Crude Palm Oil.** *Int J Chem Eng Appl* 2012, **3**:300–302.
51. **Thermogravimetric Analysis (TGA) A Beginner ' s Guide** [www.perkinelmer.com]
52. Santos JCO, Santos IMG, Conceição MM, Porto SL, Trindade MFS, Souza AG, Prasad S, Jr VJF, Araújo AS: **Thermoanalytical , Kinetics and Rheological Parameters of Commercial Edible Vegetables Oils.** *J Therm Anal Color* 2004, **75**:419–428.

53. Vittadini E, Lee JH, Frega NG, Min DB, Vodovotz Y: **DSC Determination of Thermally Oxidized Olive Oil.** *J Am Oil Chem Soc* 2003, **80**:533–537.
54. Tan S, Abraham T, Ference D, Macosko CW: **Rigid Polyurethane Foams from a Soybean Oil-Based Polyol.** *Polymer (Guildf)* 2011, **52**:2840–2846.
55. Hatakeyama T, Quinn FX: *Thermal Analysis: Fundamentals and Applications to Polymer Science, 2nd Edn.* second edi. John Wiley & Sons, Ltd. Chicchester, West Sussex, England; 1999:1–175.
56. Márquez AL, Pérez MP, Wagner JR: **Solid Fat Content Estimation by Differential Scanning Calorimetry: Prior Treatment and Proposed Correction.** *J Am Oil Chem Soc* 2012, **90**:467–473.
57. Renata B, Nassu T, Aparecida L, Gonçalves G: **Determination of Melting Point of Vegetable Oils and Fats by Differential Scanning Calorimetry (DSC) Technique.** *Grasas y ...* 1999, **50**:16–21.
58. Kong Y, Hay J: **The Measurement of the Crystallinity of Polymers by DSC.** *Polymer (Guildf)* 2002, **43**:3873–3878.
59. Lopez C, Bourgaux C, Lesieur P, Bernadou S, Keller G, Ollivon M: **Thermal and Structural Behavior of Milk Fat.** *J Colloid Interface Sci* 2002, **254**:64–78.
60. Bootello M a, Hartel RW, Levin M, Martínez-Blanes JM, Real C, Garcés R, Martínez-Force E, Salas JJ: **Studies of Isothermal Crystallisation Kinetics of Sunflower Hard Stearin-based Confectionery Fats.** *Food Chem* 2013, **139**:184–95.
61. Bootello M a., Garcés R, Martínez-Force E, Salas JJ: **Dry Fractionation and Crystallization Kinetics of High-Oleic High-Stearic Sunflower Oil.** *J Am Oil Chem Soc* 2011, **88**:1511–1519.
62. Foubert I, Fredrick E, Vereecken J, Sichiën M, Dewettinck K: **Stop-and-Return DSC Method to Study Fat Crystallization.** *Thermochim Acta* 2008, **471**:7–13.
63. Foubert I, Vanrolleghem P a, Dewettinck K: **A Differential Scanning Calorimetry Method to Determine the Isothermal Crystallization Kinetics of Cocoa Butter.** *Thermochim Acta* 2003, **400**:131–142.
64. Himawan C, Starov VM, Stapley AGF: **Thermodynamic and Kinetic Aspects of Fat Crystallization.** *Adv Colloid Interface Sci* 2006, **122**:3–33.
65. Chapagain BP, Wiesman Z: **MALDI-TOF / MS Fingerprinting of Triacylglycerols (TAGs) in Olive Oils Produced in the Israeli Negev Desert.** *J Agric Food Chem* 2009, **57**:1135–1142.

66. Lay JO, Liyanage R, Durham B, Brooks J: **Rapid Characterization of Edible Oils by Direct Matrix-Assisted Laser Desorption/Ionization Time-of-Flight Mass Spectrometry Analysis Using Triacylglycerols.** *Rapid Commun Mass Spectrom* 2006, **20**:952–8.
67. Teles M, Gerbaud V, Roux GAC Le: **Modeling and Simulation of Melting Curves and Chemical Interesterification of Binary Blends of Vegetable Oils.** *Chem Eng Sci* 2013, **87**:14–22.
68. Gunstone FD: *Vegetable Oils in Food Technology: Composition, Properties and Uses.* Paris: Blackwell Publishing Ltd; 2002:1–275.
69. Hartel RW: **Advances in Food Crystallization.** *Annu Rev Food Sci Technol* 2013, **4**:277–92.
70. Revalor E, Hammadi Z, Astier J, Grossier R, Garcia E, Hoff C: **Usual and Unusual Crystallization from Solution.** 2010, **312**:939–946.
71. Smith KW, Bhaggan K, Talbot G, Malssen KF Van: **Crystallization of Fats : Influence of Minor Components and Additives.** *J Am Oil Chem Soc* 2011, **88**:1085–1101.
72. Saadi S, Azis A, Mohd H, Sahri M, Chern H, Mohammed S: **Application of Differential Scanning Calorimetry (DSC), HPLC and pNMR for Interpretation Primary Crystallisation Caused by Combined Low and High Melting TAGs.** *Food Chem* 2012, **132**:603–612.
73. Sato K, García LB, Calvet T, Àngel M, Diarte C: **Highlight Article External factors affecting polymorphic crystallization of lipids.** 2013:1224–1238.
74. Sato K, Ueno S: **Crystallization , Transformation and Microstructures of Polymorphic Fats in Colloidal Dispersion States.** *Curr Opin Colloid Interface Sci* 2011, **16**:384–390.
75. Marangoni AG: **The Nature of Fractality in Fat Crystal Networks.** *Trends Food Sci Technol* 2002, **13**:37–47.
76. Bayés-García L, Calvet T, Cuevas-Diarte MÀ, Ueno S, Sato K: **In Situ Synchrotron Radiation X-ray Diffraction Study of Crystallization Kinetics of Polymorphs of 1,3-dioleoyl-2-palmitoyl glycerol (OPO).** *CrystEngComm* 2011, **13**:3592.
77. Bail S, Krist S, Masters E, Unterweger H, Buchbauer G: **Volatile compounds of shea butter samples made under different production conditions in western, central and eastern Africa.** *J Food Compos Anal* 2009, **22**:738–744.

78. Honfo FG, Akissoe N, Linnemann AR, Soumanou M, Van Boekel M a JS: **Nutritional composition of shea products and chemical properties of shea butter: a review.** *Crit Rev Food Sci Nutr* 2014, **54**:673–86.
79. Honfo FG, Linnemann AR, Akissoe NH, Soumanou MM, van Boekel M a JS: **Indigenous knowledge of shea processing and quality perception of shea products in Benin.** *Ecol Food Nutr* 2012, **51**:505–25.
80. Wilfred S, Adubofuor J, Oldham JH: **Optimum Conditions for Expression of oil from Allanblackia floribunda Seeds and Assessing the Quality and Stability of Oressed and Solvent Extracted Oil.** *African J Food Sci* 2010, **4**:563–570.
81. Adubofuor J, Sefah W, Oldham JH: **Nutrient Composition of Allanblackia Paviflora Seed Kernels and Oil Compared with some Plant Fats and Oils and Application of the Oil in Soap Preparation.** *J of Cereal and Oil Seeds* 2013, **4**:1–9.
82. Chiralt A: *Food Emulsions. Volume II;* .
83. Chen J, Vogel R, Werner S, Heinrich G, Clausse D, Dutschk V: **Influence of the Particle Type on the Rheological Behavior of Pickering Emulsions.** *Colloids Surfaces A Physicochem Eng Asp* 2011, **382**:238–245.
84. Engels T, Foster T, von Rybinski W: **The Influence of Coemulsifier Type on the Stability of Oil-in-Water Emulsions.** *Colloids Surfaces A Physicochem Eng Asp* 1995, **99**:141–149.
85. Guzey D, Mcclements DJ: **Formation , Stability and Properties of Multilayer Emulsions for Application in the Food Industry.** *Adv Colloid Interface Sci* 2007, **130**:227–248.
86. Payet L, Terentjev EM, June R V, Re V, Recei M, August V: **Emulsification and Stabilization Mechanisms of O / W Emulsions in the Presence of Chitosan.** *Langmuir* 2008, **24**:12247–12252.
87. Herrera ML: **Methods for Stability Studies.** In *Anal Tech Stud Phys Prop Lipid Emuls.* Edited by Herera ML. SpringerBriefs in Food, Health, and Nutrition 3; 2012:15–60.
88. Fredrick E, Walstra P, Dewettinck K: **Factors Governing Partial Coalescence in Oil-in-Water Emulsions.** *Adv Colloid Interface Sci* 2010, **153**:30–42.
89. Alvarado V, Wang X, Moradi M: **Stability Proxies for Water-in-Oil Emulsions and Implications in Aqueous-based Enhanced Oil Recovery.** *Energies* 2011, **4**:1058–1086.

90. McClements DJ, Weiss J: **Lipid Emulsions**. In *Bailey's Ind Oil Fat Prod*. Sixth Edit. Edited by Shahidi F. John Wiley & Sons, Inc., Hoboken, New Jersey. Published; 2005:457–502.
91. Crowder TM, Rosati JA, Schroeter JD, Hickey AJ, Martonen TB: **Fundamental Effects of Particle Morphology on Lung Delivery : Predictions of Stokes ' Law and the Particular Relevance to Dry Powder Inhaler Formulation and Development**. *Pharm Res* 2002, **19**:239–245.
92. Onsaard E, Vittayanont M, Srigan S, McClements DJ: **Comparison of Properties of Oil-in-Water Emulsions Stabilized by Coconut Cream Proteins with those Stabilized by Whey Protein Isolate**. *Food Res Int* 2006, **39**:78–86.
93. Binks BP, Lumsdon SO: **Influence of Particle Wettability on the Type and Stability of Surfactant-Free Emulsions** †. *Langmuir* 2000, **16**:8622–8631.
94. Aben S, Holtze C, Tadros T, Schurtenberger P: **Rheological Investigations on the Creaming of Depletion-Flocculated Emulsions**. *Langmuir* 2012, **28**:7967–7975.
95. Diftis NG, Biliaderis CG, Kiosseoglou VD: **Rheological Properties and Stability of Model Salad Dressing Emulsions Prepared with a Dry-heated Soybean Protein Isolate–Dextran Mixture**. *Food Hydrocoll* 2005, **19**:1025–1031.
96. Krynke KK, Jerzy PS: **Predicting Viscosity of Emulsions in the Broad Range of Inner Phase Concentrations**. *Colloids Surfaces A Physicochem Eng Asp* 2004, **245**:81–92.
97. Xin X, Zhang H, Xu G, Tan Y, Zhang J, Lv X: **Influence of CTAB and SDS on the Properties of Oil-in-Water Nano-Emulsion with Paraffin and Span 20 / Tween 20**. *Colloids Surfaces A Physicochem Eng Asp* 2013, **418**:60–67.
98. Dos Santos RG, Bannwart AC, Briceño MI, Loh W: **Physico-chemical Properties of Heavy Crude Oil-in-Water Emulsions Stabilized by Mixtures of Ionic and Non-ionic Ethoxylated Nonylphenol Surfactants and Medium Chain Alcohols**. *Chem Eng Res Des* 2011, **89**:957–967.
99. Pongsawatmanit R, Harnsilawat T, McClements DJ: **Influence of Alginate , pH and Ultrasound Treatment on Palm Oil-in-Water Emulsions Stabilized by Lactoglobulin**. 2006, **287**:59–67.
100. Derkach SR: **Rheology of Emulsions**. *Adv Colloid Interface Sci* 2009, **151**:1–23.
101. Tzoumaki M V., Moschakis T, Kiosseoglou V, Biliaderis CG: **Oil-in-Water Emulsions Stabilized by Chitin Nanocrystal Particles**. *Food Hydrocoll* 2011, **25**:1521–1529.

102. Tadros TF: **Fundamental Principles of Emulsions Rheology and their Applications.** *Colloids Surfaces A Physicochem Eng Asp* 1994, **91**:39–55.
103. Zhu J, Hayward RC: **Interfacial Tension of Evaporating Emulsion Droplets Containing Amphiphilic Block Copolymers: Effects of Solvent and Polymer Composition.** *J Colloid Interface Sci* 2012, **365**:275–279.
104. Garti N: **Progress in Stabilization and Transport Phenomena of Double Emulsions in Food Applications.** *Leb u-Technol* 1997, **30**:222–235.
105. Aben S, Holtze C, Tadros T, Schurtenberger P: **Rheological Investigations on the Creaming of Depletion-Flocculated Emulsions.** 2012.
106. Kim H, Bot A, Vries ICM De, Golding M, Pelan EG: **Effects of Emulsifiers on Vegetable-fat Based Aerated Emulsions with Interfacial Rheological Contributions.** *FRIN* 2013, **53**:342–351.
107. Koocheki A, Kadkhodae R, Ali S, Shahidi F, Reza A: **Influence of Alyssum Homolocarpum Seed Gum on the Stability and Flow Properties of O / W Emulsion Prepared by High Intensity Ultrasound.** *Food Hydrocoll* 2009, **23**:2416–2424.
108. Tan Y, Xu K, Niu C, Liu C, Li Y, Wang P, Binks BP: **Triglyceride–Water Emulsions Stabilised by Starch-based Nanoparticles.** *Food Hydrocoll* 2014, **36**:70–75.
109. Jiao J, Burgess DJ: **Rheology and Stability of Water-in-Oil-in-Water Multiple Emulsions Containing Span 83 and Tween 80.** *AAPS PhamSci* 2003, **5**:1–12.
110. Dickinson E, Golding M, Povey MJW: **Creaming and Flocculation of Oil-in-Water Emulsions Containing Sodium Caseinate.** *J Colloid Interface Sci* 1997, **185**:515–529.
111. Rahn-chique K, Puertas AM, Romero-cano MS, Rojas C: **Nanoemulsion Stability : Experimental Evaluation of the Flocculation Rate from Turbidity Measurements.** *Adv Colloid Interface Sci* 2012:1–48.
112. Boode K, Walstra P: **Partial Coalescence in Oil-in-Water Emulsions 1. Nature of the Aggregation.** *Colloids Surfaces A Physicochem Eng Asp* 1993, **81**:121–137.
113. Boode K, Bisperink C, Walstra P: **Destabilization of O / W Emulsions Containing Fat Crystals by Temperature Cycling.** *Colloids and surfaces1991* 1991, **61**:66–74.
114. Pichot R, Spyropoulos F, Norton IT: **Mixed-emulsifier Stabilised Emulsions: Investigation of the Effect of Monoolein and Hydrophilic Silica Particle Mixtures on the Stability Against Coalescence.** *J Colloid Interface Sci* 2009, **329**:284–91.

115. Rousseau D: **Fat Crystals and Emulsion Stability - A Review.** *Food Res Int* 2000, **33**:3–14.
116. Frascch-Melnik S, Norton IT, Spyropoulos F: **Fat-crystal Stabilised W/O Emulsions for Controlled Salt Release.** *J Food Eng* 2010, **98**:437–442.
117. Sagiri SS, Sethy J, Pal K, Banerjee I, Pramanik K, Maiti TK: **Encapsulation of Vegetable Organogels for Controlled Delivery Applications.** *Des Monomers Polym* 2012:37–41.
118. Nedovic V, Kalusevic A, Manojlovic V, Levic S: **An Overview of Encapsulation Technologies for Food Applications.** *Ital Oral Surg* 2011, **1**:1806–1815.
119. Whitby CP, Fornasiero D, Ralston J: **Effect of Adding Anionic Surfactant on the Stability of Pickering Emulsions.** *J Colloid Interface Sci* 2009, **329**:173–181.
120. Xu JH, Li SW, Tan J, Wang YJ, Luo GS: **Controllable Preparation of Monodisperse O/W and W/O Emulsions in the Same Microfluidic Device.** *Langmuir* 2006, **22**:2004–2007.
121. Dickinson E, Golding M, Povey MJW: **Creaming and Flocculation of Oil-Water Emulsions Containing Sodium Caseinate.** *J Colloid Interface Sci* 1997, **185**:515–529.
122. Relkin P, Sourdret S: **Factors Affecting Fat Droplet Aggregation in Whipped Frozen Protein-Stabilized Emulsions.** *Food Hydrocoll* 2005, **19**:503–511.
123. Comas D., Wagner JR, Tomas M.: **Creaming Stability of Oil in Water (O / W) Emulsions : Influence of pH on Soybean Protein – Lecithin Interaction.** *Food Hydrocoll* 2006, **20**:990–996.
124. Frascch-Melnik S, Spyropoulos F, Norton IT: **W1/O/W2 Double Emulsions Stabilised by Fat Crystals-Formulation, Stability and Salt Release.** *J Colloid Interface Sci* 2010, **350**:178–85.
125. Surh J, Vladislavljevi Cacute GT, Mun S, McClements DJ: **Preparation and Characterization of Water/Oil and Water/Oil/Water Emulsions Containing Biopolymer-Gelled Water Droplets.** *J Agric Food Chem* 2007, **55**:175–84.
126. Infante MR, Pérez L, Morán MC, Pons R, Mitjans M, Vinardell MP, Garcia MT, Pinazo A: **Biocompatible Surfactants from Renewable Hydrophiles.** *Eur J Lipid Sci Technol* 2010, **112**:110–121.
127. Alam S, Kalita H, Kudina O, Popadyuk A, chisholm BJ, Voronov A: **Soy-Based Surface Active Copolymers As a Safer Replacement for Low Molecular Weight Surfactants.** *ACS Sustain Chem Engineering* 2013, **1**:19–22.

128. Yangxin YU, Jin Z, Bayly AE: **Development of Surfactants and Builders in Detergent Formulations.** *Chinese J Chem Eng* 2008, **16**:517–527.
129. Hasenhuettl GL: **Synthesis and Commercial Preparation of Food Emulsifiers.** 2008:11–38.
130. Schramm L, Stasiuk E, Marangoni D: **2 Surfactants and their applications.** *Annu Reports Progr Chem* 2003, **99**:3–48.
131. Chu Z, Feng Y: **Vegetable-Derived Long-Chain Surfactants Synthesized via a “Green” Route.** *ACS Sustain Chem Engineering* 2013, **1**:75–79.
132. Maag H: **Fatty Acid Derivatives: Important Surfactants for Household, Cosmetic and Industrial Purposes.** *J Am Oil Chem Soc* 1984, **61**:259–267.
133. Rahate AR, Nagarkar JM: **Emulsification of Vegetable Oils using a Blend of Nonionic Surfactants for Cosmetic Applications.** *J Dispers Sci Technol* 2007, **28**:1077–1080.
134. Raths H-C, Weuthen M, Elsner M: **Gemini Surfactants.** 2004:1–14.
135. Li W, Yu L, Liu G, Tan J, Liu S, Sun D: **Oil-in-Water Emulsions Stabilized by Laponite Particles Modified with Short-Chain Aliphatic Amines.** *Colloids Surfaces A Physicochem Eng Asp* 2012, **400**:44–51.
136. Torres LG, Iturbe R, Snowden MJ, Chowdhry BZ, Leharne S a.: **Preparation of O/W Emulsions Etabilized by Solid Particles and Their Characterization by Oscillatory Rheology.** *Colloids Surfaces A Physicochem Eng Asp* 2007, **302**:439–448.
137. Zinoviadou KG, Scholten E, Moschakis T, Biliaderis CG: **Engineering Interfacial Properties by Anionic Surfactant – Chitosan Complexes to Improve Stability of Oil-in-Water Emulsions.** *Food Funct* 2012, **3**:312–319.
138. Binks BP: **Particles as Surfactants—Similarities and Differences.** *Curr Opin Colloid Interface Sci* 2002, **7**:21–41.
139. Manosroi A, Wongtrakul P, Manosroi J, Sakai H, Sugawara F, Yuasa M, Abe M: **Characterization of Vesicles Prepared with Various Non-ionic Surfactants Mixed with Cholesterol.** *Colloids Surfaces B Biointerfaces* 2003, **30**:129–138.
140. Shrestha A: **Effect of Span 80-Tween 80 Mixture Compositions on The Stability of Sunflower Oil-Based Emulsions.** 2011:3–10.
141. Ching AL, Liew C V, Heng PWS, Chan LW: **Impact of Cross-linker on Alginate Matrix Integrity and Drug Release.** *Int J Pharm* 2008, **355**:259–268.

142. Tafaghodi M, Tabasi SAS, Jaafari MR: **Formulation , Characterization and Release Studies of Alginate Microspheres Encapsulated with Tetanus Toxoid.** *J Biomater Sci Polym Ed* 2006, **17**:909–924.
143. Hambleton A, Debeaufort F, Bonnotte A, Voilley A: **Influence of Alginate Emulsion-based Films Structure on its Barrier Properties and on the Protection of Microencapsulated Aroma Compound.** *Food Hydrocoll* 2009, **23**:2116–2124.
144. Sosa-Herrera MG, Lozano-Esquivel IE, Ponce de León-Ramírez YR, Martínez-Padilla LP: **Effect of Added Calcium Chloride on the Physicochemical and Rheological Properties of Aqueous Mixtures of Sodium Caseinate/Sodium Alginate and Respective Oil-in-Water Emulsions.** *Food Hydrocoll* 2012, **29**:175–184.
145. Reis CP, Neufeld RJ, Vilela S, Ribeiro AJ, Veiga F: **Review and Current Status of Emulsion/Dispersion Technology using an Internal Gelation Process for the Design of Alginate Particles.** *J Microencapsul* 2006, **23**:245–57.
146. Sakai S, Ito S, Kawakami K: **Calcium Alginate Microcapsules with Spherical Liquid Cores Templated by Gelatin Microparticles for Mass Production of Multicellular Spheroids.** *Acta Biomater* 2010, **6**:3132–7.
147. Silva CM, Ribeiro AJ, Figueiredo IV, Gonçalves AR, Veiga F: **Alginate Microspheres Prepared by Internal Gelation: Development and Effect on Insulin Stability.** *Int J Pharm* 2006, **311**:1–10.
148. Koocheiki A, Kadkhodae R, Mortazavi SA, Shahidi F, Taherian AR: **Influence of Alyssum Homolcarpum Seed Gum on the Stability and Flow Properties of O/W Emulsion Prepared by High Intensity Ultrasound.** *Food Hydrocoll* 2009, **23**:2416–2424.
149. Muthuprasanna P, Surya K, Sobhita P, Satish IA, Chandiran IS, Arunachalam G, Shalini S: **Basics and Potential Applications of Surfactants - A Review.** 2009, **1**:1354–1365.
150. Hanasukarn P, Pongsawatmanit R, McClements DJ: **Impact of Fat and Water Crystallization on the Stability of Hydrogenated Palm Oil-in-Water Emulsions Stabilized by a Nonionic Surfactant.** *J Agric Food Chem* 2006, **54**:3591–3597.
151. Eduardo A, Barratt G, Chéron M, Egito EST: **Development of Oil-in-Water Microemulsions for the Oral Delivery of Amphotericin B.** *Int J Pharm* 2013, **454**:641–648.
152. Palanuwech J, Coupland JN: **Effect of Surfactant Type on the Stability of oil in Water Emulsions to Dispersed Phase Crystallization.** *Colloids Surfaces A Physicochem Eng Asp* 2003, **223**:251–262.

153. Hsu J-P, Nacu A: **Behavior of Soybean Oil-in-Water Emulsion Stabilized by Nonionic Surfactant.** *J Colloid Interface Sci* 2003, **259**:374–81.
154. Devani MJ, Ashford M, Craig DQM: **The Development and Characterisation of Triglyceride-based “Spontaneous” Multiple Emulsions.** *Int J Pharm* 2005, **300**:76–88.
155. Nedovic V, Kalusevic A, Manojlovic V, Levic S: **An Overview of Encapsulation Technologies for Food Applications.** *Procedia Food Sci* 2011, **1**:1806–1815.
156. Zuidam NJ, Shimoni E: **Overview of Microencapsulates for Use in Food Products or Processes and Methods to Make Them.** In *Encapsulation Technol Act Food Ingredients Food Process*. Edited by Zuidam NJ, Nedovic VA. Springer Science +Business Media, LLC; 2010:3–30.
157. Vos P De, Faas MM, Spasojevic M, Sikkema J: **Encapsulation for Preservation of Functionality and Targeted Delivery of Bioactive Food Components.** *Int Dairy J* 2010, **20**:292–302.
158. Fang Z, Bhandari B: **Encapsulation of Polyphenols - A Review.** *Trends Food Sci Technol* 2010, **21**:510–523.
159. Yoksan R, Jirawutthiwongchai J, Arpo K: **Encapsulation of Ascorbyl Palmitate in Chitosan Nanoparticles by Oil-in-Water Emulsion and Ionic Gelation Processes.** *Colloids Surf B Biointerfaces* 2010, **76**:292–7.
160. Choi M-J, Ruktanonchai U, Min S-G, Chun J-Y, Soottitantawat A: **Physical Characteristics of Fish Oil Encapsulated by β -cyclodextrin using an Aggregation Method or Polycaprolactone using an Emulsion-Diffusion Method.** *Food Chem* 2010, **119**:1694–1703.
161. Pool H, Mendoza S, Xiao H, McClements DJ: **Encapsulation and Release of Hydrophobic Bioactive Components in Nanoemulsion-based Delivery Systems: Impact of Physical Form on Quercetin Bioaccessibility.** *Food Funct* 2013, **4**:162–74.
162. Kumari A, Yadav SK, Yadav SC: **Biodegradable Polymeric Nanoparticles Based Drug Delivery Systems.** *Colloids Surf B Biointerfaces* 2010, **75**:1–18.
163. Khan UN, Bharathi NP, Sheikh S, Hashmi A.: **Development of Water-Borne Green Polymer Used as a Potential Nano Drug Vehicle and its In Vitro Release Studies.** *J Polym Environ* 2011, **19**:607–614.
164. Driscoll CMO, Griffin BT: **Biopharmaceutical Challenges Associated with Drugs with Low Aqueous Solubility — The Potential Impact of Lipid-based Formulations.** *Adv Drug Deliv Rev* 2008, **60**:617–624.

165. Munin A, Edwards-lévy F: **Encapsulation of Natural Polyphenolic Compounds; a Review.** *Pharmaceutics* 2011, **3**:793–829.
166. Bonnet M, Cansell M, Berkaoui A, Ropers MH, Anton M, Leal-Calderon F: **Release Rate Profiles of Magnesium from Multiple W/O/W Emulsions.** *Food Hydrocoll* 2009, **23**:92–101.
167. Borgogna M, Bellich B, Zorzini L, Lapasin R, Cesàro A: **Food Microencapsulation of Bioactive Compounds: Rheological and Thermal Characterisation of Non-conventional Gelling System.** *Food Chem* 2010, **122**:416–423.
168. De Vos P, Faas MM, Spasojevic M, Sikkema J: **Encapsulation for Preservation of Functionality and Targeted Delivery of Bioactive Food Components.** *Int Dairy J* 2010, **20**:292–302.
169. Zuidam NJ, Shimoni E: **Overview of Microencapsulates for Use in Food Products or Processes and Methods to Make Them.** In *Encapsulation Technol Act Food Ingredients Food Process*. Edited by Zuidam NJ, Nedovic V. Springer Science +Business Media, LLC; 2010:3–30.
170. Polavarapu S: **Microencapsulation of Fish Oil / Olive Oil Blends using Sugar Beet Pectin as an Encapsulant.** The University of Melbourne; 2011(June):1–105.
171. Li B, Jiang Y, Liu F, Chai Z, Li Y, Leng X: **Study of the Encapsulation Efficiency and Controlled Release Property of Whey Protein Isolate - Polysaccharide Complexes in W1/O/W2 Double Emulsions.** *Int J Food Eng* 2011, **7**:1–16.
172. McClements DJ, Decker E a, Weiss J: **Emulsion-based Delivery Systems for Llipophilic Bioactive Components.** *J Food Sci* 2007, **72**:R109–24.
173. Mun S, Choi Y, Rho S-J, Kang C-G, Park C-H, Kim Y-R: **Preparation and Characterization of Water / Oil / Water Emulsions Stabilized by Polyglycerol Polyricinoleate and Whey Protein Isolate.** *J Food Sci* 2010, **75**:E116–E125.
174. Soo S, Yeol M, Andrew E, Henson L, Popplewell LM, Julian D, Jun S: **Stabilization of Orange Oil-in-Water Emulsions : A New Role for Ester Gum as an Ostwald Ripening Inhibitor.** *Food Chem* 2011, **128**:1023–1028.
175. Rodrigues MA, Matos HA, Azevedo EG De: **Single-Step Co-Crystallization and Lipid Dispersion by Supercritical Enhanced Atomization.** *Cryst Growth Des* 2013, **13**:4940–4947.
176. Yeo Y, Park K: **Control of Encapsulation Efficiency and Initial Burst in Polymeric Microparticle Systems.** *Arch Pharm Res* 2004, **27**:1–12.

177. Mattu C, Li R, Ciardelli G: **Chitosan Nanoparticles as Therapeutic Protein Nanocarriers : the Effect of pH on Particle Formation and Encapsulation Efficiency.** *Polym Compos* 2013, **1**:1538–1545.
178. Nii T, Ishii F: **Encapsulation Efficiency of Water-Soluble and Insoluble Drugs in Liposomes Prepared by the Microencapsulation Vesicle Method.** *Int J Pharm* 2005, **298**:198–205.
179. Sanchez A, Gupta RK, Alonso MJ, Siber GR, Langer R: **Pulsed Controlled-Release System for Potential Use in Vaccine Delivery.** *Pharm Sci* 1996, **85**:547–552.
180. Cheow WS, Hadinoto K: **Enhancing Encapsulation Efficiency of Highly Water-soluble Antibiotic in Poly (lactic-co-glycolic acid) Nanoparticles : Modifications of Standard Nanoparticle Preparation Methods.** *Colloids Surfaces A Physicochem Eng Asp* 2010, **370**:79–86.
181. Mukerjee A, Vishwanatha JK: **Formulation , Characterization and Evaluation of Curcumin-loaded PLGA Nanospheres for Cancer Therapy.** *Anticancer Res* 2009, **29**:3867–3875.
182. Mattu C, Li R, Ciardelli G: **Chitosan Nanoparticles as Therapeutic Protein Nanocarriers : the Effect of pH on Particle Formation and Encapsulation Efficiency.** In *6th Confimes Polym Compos*; 2012:1538–1545.
183. Shah KA, Date AA, Joshi MD, Patravale VB: **Solid lipid nanoparticles (SLN) of tretinoin : Potential in topical delivery.** *Int J Pharm* 2007, **345**:163–171.
184. Freytag T, Dashevsky A, Tillman L, Hardee GE, Bodmeier R: **Improvement of the Encapsulation Efficiency of Oligonucleotide-Containing Biodegradable Microspheres.** *J Control release* 2000, **69**:197–207.
185. Lorenzo AT, Arnal ML, Albuerne J, Müller AJ: **DSC Isothermal Polymer Crystallization Kinetics Measurements and the use of the Avrami Equation to fit the data: Guidelines to Avoid Common Problems.** *Polym Test* 2007, **26**:222–231.
186. Graydon JW, Thorpe SJ, Kirk DW: **Determination of the Avrami Exponent for Solid State Transformations from Non-isothermal Differential Scanning Calorimetry.** *J Non Cryst Solids* 1994, **175**:31–43.
187. Pichot R: **Stability and Characterisation of Emulsions in the Presence of Colloidal Particles and Surfactants.** The University of Birmingham; 2010(November):10–180.
188. **Purdue University - Scanning Electron Microscope** [www.purdue.edu/ehps/rem/rs/sem.htm]

189. Pecora R: **Dynamic Light Scattering Measurement of Nanometer Particles in Liquids.** *J of Nanoparticle Res* 2000, **2**:123–131.
190. Instruments T: *ARES Rheometer, Rheometrics Series User Manual.* New Castle; 2003(June):10–200.
191. Atangana AR, van der Vlis E, Khasa DP, van Houten D, Beaulieu J, Hendrickx H: **Tree-to-tree Variation in Stearic and Oleic Acid Content in Seed Fat From *Allanblackia floribunda* from Wild Stands: Potential for Tree Breeding.** *Food Chem* 2011, **126**:1579–1585.
192. Enweremadu CC, Alamu OJ: **Development and Characterization of Biodiesel from Shea Nut Butter.** *Int Agrophysics* 2010, **24**:29–34.
193. Christopoulou E, Lazaraki M, Komaitis M, Kaselimis K: **Effectiveness of Determinations of Fatty Acids and Triglycerides for the Detection of Adulteration of Olive Oils with Vegetable Oils.** *Food Chem* 2004, **84**:463–474.
194. European Food Safety Authority: **Opinion of the Scientific Panel on Dietetic Products, Nutrition and Allergies on a Request from the Commission Related to the Safety of *Allanblackia* Seed Oil for use in Yellow Fat and Cream Based Spreads.** *EFSA J* 2007, **580**:1–10.
195. Honfo FG, Akissoe N, Linnemann AR, Soumanou M, Van Boekel M a JS: **Nutritional composition of shea products and chemical properties of shea butter: a review.** *Crit Rev Food Sci Nutr* 2014, **54**:673–86.
196. Knothe G, Kenar JA: **Determination of the Fatty Acid Profile by 1 H-NMR Spectroscopy.** *Eur J Lipid Sci Technol* 2004, **106**:88–96.
197. Miyake Y, Yokomizo K, Matsuzaki N: **Determination of Unsaturated Fatty Acid Composition by High-Resolution Nuclear Magnetic Resonance Spectroscopy.** *J Am Oil Chem Soc oil* 1998, **75**:7–10.
198. Guillen MD, Ruiz A: **Rapid Simultaneous Determination by Proton NMR of Unsaturation and Composition of Acyl Groups in Vegetable Oils.** *Eur J Lipid Sci Technol* 2003, **105**:688–696.
199. Conceicao MM, Candeia RA, Silva FC, Bezerra AF, Fernandes VJ, Souza AG: **Thermoanalytical Characterization of Castor Oil Biodiesel.** *Renew Sustain Energy Rev* 2007, **11**:964–975.
200. Vereecken J, Foubert I, Smith KW, Sassano GJ, Dewettinck K: **Crystallization of Model Fat Blends Containing Symmetric and Asymmetric Monounsaturated Triacylglycerols.** *Eur J Lipid Sci Technol* 2010, **112**:233–245.

201. Abd. Rashid N, Chiew Let C, Chong Seng C, Omar Z: **Crystallisation Kinetics of Palm Stearin, Palm Kernel Olein and their Blends.** *LWT - Food Sci Technol* 2012, **46**:571–573.
202. De Graef V, Foubert I, Smith KW, Cain FW, Dewettinck K: **Crystallization Behavior and Texture of Trans-containing and Trans-free Palm Oil Based Confectionery Fats.** *J Agric Food Chem* 2007, **55**:10258–65.
203. Campos R, Narine SS, Marangoni AG: **Effect of Cooling Rate on the Structure and Mechanical Properties of Milk Fat and Lbbard.** 2002, **35**:971–981.
204. Martini S, Herrera ML, Hartel RW: **Effect of Cooling Rate on Crystallization Behavior of Milk Fat Fraction / Sunflower Oil Blends.** *J Am Oil Chem Soc* 2002, **79**:1055–1062.
205. Foubert I, Vanrolleghem PA: **Modelling of the Crystallization Kinetics of Fats.** *Trends Food Sci Technol* 2003, **14**:79–92.
206. Smith KW, Bhaggan K, Talbot G, Malssen KF: **Crystallization of Fats: Influence of Minor Components and Additives.** *J Am Oil Chem Soc* 2011, **88**:1085–1101.
207. Neff WE, List GR, Mounts TL: **Physical Properties of Interesterified Fat Blends.** *J Am Oil Chem Soc* 1993, **70**:467–471.
208. Metin S, Hartel RW: **Thermal Analysis of Isothermal Crystallization Kinetics in Blends of Cocoa Butter with Milk Fat or Milk Fat Fractions.** *J Am Oil Chem Soc* 1998, **75**:1617–1624.
209. Bayés-García L, Calvet T, Àngel Cuevas-Diarte M, Ueno S, Sato K: **In Situ Observation of Transformation Pathways of Polymorphic forms of 1,3-dipalmitoyl-2-oleoyl glycerol (POP) Examined with Synchrotron Radiation X-ray Diffraction and DSC.** *CrystEngComm* 2013, **15**:302.
210. Acevedo NC, Block JM, Marangoni AG: **Unsaturated Emulsifier-Mediated Modification of the Mechanical Strength and Oil Binding Capacity of a Model Edible Fat Crystallized under Shear.** *Langmuir* 2012, **28**:16207–16217.
211. Acevedo NC, Block JM, Marangoni AG: **Unsaturated Emulsifier-Mediated Modification of the Mechanical Strength and Oil Binding Capacity of a Model Edible Fat Crystallized under Shear.** *Langmuir* 2012, **28**:16207–17.
212. Giap SGE, Nik WMNW, Ahmad MF, Amran A, Telipot M, Science M: **The Assessment of Rheological Model Reliability in Lubricating Behaviour of Vegetable Oils.** *Engineering e-Transaction* 2010, **4**:81–88.

213. Georgiadis N, Ritzoulis C, Sioura G, Kornezou P, Vasiliadou C, Tsiptsias C: **Contribution of Okra Extracts to the Stability and Rheology of Oil-in-Water Emulsions.** *Food Hydrocoll* 2011, **25**:991–999.
214. Harris L: **A Study of the Crystallisation Kinetics in PEEK and PEEK Composites.** University of Birmingham; 2011(September):12–88.
215. Bruno L, Kasapis S, Heng PWS: **Effect of Polymer Molecular Weight on the Structural Properties of Non Aqueous Ethyl Cellulose Gels Intended for Topical Drug Delivery.** *Carbohydr Polym* 2012, **88**:382–388.

KNUST



APPENDICES

KNUST



Appendix 1

PUBLICATIONS ARISING

- I. Badu M., Awudza J.A.M. Characterisation and Identification of the Triacylglycerols Content of Two Vegetable Oils and Fat using MALDI-TOF/TOF Mass Spectroscopic Technique. *Journal of Food Chemistry* (Manuscript No. FOODCHEM – D – 15-01401 Under Review).
- II. Badu M. Awudza J.A.M., Ricardo N., Yeates S. Determination of Chemical Constituents and Thermal Behaviour of Allanblackia Seed Fat. *European Journal of Lipid Science and Technology* (Submitted for Review)
- III. Badu M. Awudza J.A.M., Ricardo N., Yeates S. Determination of Chemical Constituents and Thermal Behaviour of shea butter (*Preparation*)
- IV. Badu M. Awudza J.A.M., Ricardo N., Yeates S. Formulation, Stabilisation and Characterisation of Fat Particles-in-Water Emulsions – Effect of Tween 20 and Sodium Alginate Mixtures (*Preparation*)

KNUST

